Potential Electricity Generation from Small Scale Solar Photovoltaic Systems -

Case Study 1: Solar Harvesting Potential from roofs of Invercargill Homes

And

Case Study 2: Model Validation using Existing Data from PV Generation on Selected New Zealand Schools

A thesis presented in partial fulfilment of the requirements for the degree of

MASTER OF CONSTRUCTION

School of Engineering and Advanced Technology

At Massey University, Albany,

New Zealand

SAMANANT SAKDISETH

2015

ABSTRACT

Solar energy is abundant, free and non-polluting. Solar energy can offset the consumption of fossil fuels, greenhouse gas emission reduction targets and contribute to meeting the fast-growing energy demands. The use of solar energy for electricity generation from photovoltaic (PV) panels has increased but is still not a widely utilised technology in New Zealand. This research approximated the potential solar energy that could be harvested from the rooftops of existing residential buildings in a case study city.

This research is divided into two work strands, each involving a case study. The first strand investigated if a model could be developed, using existing data sources to determine the solar harvesting potential from the rooftops of existing residential buildings. The second strand involved the validation of the solar PV prediction model proposed in the first strand of the research, to test the reliability of the modelling outcomes.

Invercargill City was selected as the study city for case study 1. Invercargill is the southernmost city in New Zealand so represents a worst case scenario. The method involved merging computer-simulation of solar energy produced from PV modelling and mapping incoming solar radiation data from north facing residential rooftop area. The work utilised New Zealand statistical census map of population and dwelling data, as well as digital aerial map to quantify the efficient roof surface area available for PV installations. The solar PV potential was calculated using existing formulas to investigate the contribution of roof area to the solar PV potential in buildings using roof area and population relationship.

The estimated solar PV potential was 82,947,315 kWh per year generated from the total solar efficient roof surface area of 740,504 m². This equates to approximately 60.8% of the residential electricity used in Invercargill's urban

area, based on the 7,700 kWh typical annual electricity consumptions per household. The result represents an immense opportunity to harvest sustainable energy from Invercargill's residential rooftops.

To verify the accuracy of the developed method for predicting the PV outputs, the model was applied to actual generation data from grid-connected solar photovoltaic (PV) systems that are installed in New Zealand schools under the Schoolgen programme (Case Study 2). A total of 66 Schoolgen PV rooftop models were incorporated in the analysis. At this stage, the actual system parameters including size, panel type and efficiency were included in the analysis. The performance prediction and analysis outcome showed the parameters and operating conditions that affect the amount of energy generated by the PV systems. This part of the research showed the area where the PV model can be improved.

The predicted generation from the model was found to be lower than the actual generation data. Schoolgen systems operating at over 0.75 performance ratio were found to be underestimated. This indicated that most Schoolgen PV systems were operating at higher capacities than predicted by the default value of system losses. The analysis demonstrated the effects of PV technology type, site orientation, direction and tilted angle of the panels on the ability to generate expected amount of potential capacity based on solar resource availability in different site scenarios. This in turn has provided more in depth analysis of the research and served to expand the area for improvements in the design of the model.

ACKNOWLEDGEMENT

I would like to express my sincere gratitude and appreciation to my chief supervisor, Professor Robyn Phipps, for her constant advice and guidance, with generous support and encouragement from the beginning through to the completion of this thesis.

I would also like to thank my co-supervisor, Professor Jasper Mbachu, for the time and effort discussing research topics and direction.

I am grateful to the love and support of my family. Their patience and kind understanding have truly contributed in making this study possible.

TABLE OF CONTENTS

LIST OF FIGURES

LIST OF TABLES

LIST OF EQUATIONS

ABBREVIATIONS

AC: Alternating Current electricity

BIPV: Building Integrated Photovoltaics

BOS: Balance of System

CAD: Computer Aided Design

COP: Coefficient of Performance

DC: Direct Current electricity

DEM: Digital Elevation Model

DHI: Diffuse Horizontal Irradiance

DNI: Direct Normal Irradiance

FIT: Feed-in Tariff

GIS: Geographic Information System

GHI: Global Horizontal Irradiance

GW: Gigawatts (10^9 Watts)

GWh: Gigawatt-hour

HEEP: Household Energy End-use Project

kW: Kilowatt (10^3 Watts)

kWh: Kilowatt-hour

kWp: Kilowatt-peak

LCOE: Levelized cost of electricity

LiDAR: Light Detection and Ranging technology

MJ: Megajoule (10^7 Joules)

MPP: Maximum Power Point

MPPT: Maximum Power Point Tracking

MWh: Megawatt-hour (10^7 Watt-hours)

OECD: The Organisation for Economic Co-operation and Development

PV: Photovoltaics

PJ: Petajoule (10^{15} Joules)

RPS: Renewable Portfolio Standards

SVF: Sky View Factor

UHI: Urban heat island

CHAPTER 1: INTRODUCTION

This chapter defines the purpose of the research and outlines the research problem that pertains to the goal of this study. The chapter sets out the research objectives and provides an outline for the thesis.

1.1 Purpose

The aim of this research was to test if existing geographical information system (GIS) data and statistical analysis could be combined to determine the solar efficient roof area of a topographically flat city in New Zealand. The purpose of this was to calculate the potential solar photovoltaic (PV) energy that could be harvested from residential rooftops within the study area.

Solar PV energy holds considerable potential of renewable opportunities to contribute to greenhouse gas mitigation and energy security, both of which are "a major undertaking" ((MED [Ministry of Economic Development], 2011, p.1) for the New Zealand Government. Distributed generation of electricity by rooftop solar PV offers a source of renewable energy supply for daytime energy use to reduce peak demand from the residential sector and help meet New Zealand energy strategy target of having 90% of electricity generated by renewable sources by 2025.

This research attempted to calculate the potential solar PV energy that exists on rooftops of residential buildings throughout a case-study city to explore the energy supply capacity from large-scale PV deployments. For this purpose, a methodology was developed to merge the capabilities of computer-simulation in PV modelling, and mapping incoming solar radiation data to quantify the solar efficient roof area. The solar PV potential was calculated using existing formulas to investigate the contribution of roof area to the solar PV potential in buildings. The outcome was then compared to the residential energy demand of the city.

To verify the accuracy of the developed method for predicting the PV outputs, the model was applied to actual generation data from grid-connected solar PV systems that have been installed in New Zealand schools under the Schoolgen programme. The research also focused on assessing energy generation to determine the impact of influencing factors on energy outputs. This aspect of analysis was undertaken to evaluate the performance of small-scale PV distributed generation in New Zealand and to identify the area where the PV model can be improved.

1.2 The Need for the Research

The potential contribution of a small-scale PV electricity generation is not well understood in New Zealand. The prospect of solar energy is promising but financial considerations are a very important driver of PV uptake (Ford et al., 2014). The relatively high upfront cost of installation and the economic uncertainty around financial return on PV investment have been the main barriers affecting the rate of PV uptake in New Zealand market (Ford et al., 2014).

The economic value of a PV investment remains questionable despite a drop in panel price (The Press, 2013). The value of energy produced by a PV system varies substantially in the presence of regulatory measures. The economic implication of a grid-connected system depends largely on the quantity of power output that is used on-site to offset the purchased energy, and the quantity that is injected to the grid (Wood et al., 2013). In order to determine the economics of a PV investment, the actual generation must be assessed in relation to the energy consumption patterns of the building. As the cost and performance data play a central role in the setting of policy support measures and investor decisions (IRENA [International Renewable Energy Agency], 2012), a lack of an effective system for estimating the power generation in term of costs and benefits represents a significant barrier that hinders the prospect of PV uptake in New Zealand.

The value of a PV system is largely determined by the amount of energy generation. Besides the solar radiation as a primary source of PV energy production, other system parameters (i.e. module efficiency and inclination angle) also have strong influences on energy output. In the case of a rooftop PV system, the available roof area suitable for a PV installation is crucial for energy distribution. This must be considered from the site-specific factors which include:

- Shading from trees and immediate urban surroundings
- Orientation of the rooftop and panel angle
- Building parameters (i.e. architectural features, roof configurations and other competing uses)
- "Solar quality" of the location (EECA [Energy Efficiency and Conservation Authority], 2001, p.11) i.e. local climatic condition, solar intensity and insolation level in the region
- Panel temperature (which depends on ambient temperature and insolation conditions)

Understanding the full potential of solar PV on the available roof area of a city has important implications on the opportunities to maximise the use of these technologies. There have been several related studies on the rooftop solar potentials carried out both internationally and in New Zealand. However, other researches on this topic have particular emphasis on differing contexts and scales of analysis that were not readily applicable in other locations given the variability of site-specific factors. So far, the solar harvesting potential in most regions remains unknown due to the limitation of roof area data and other input required for PV analysis.

In this research, the study aims to fill this gap of knowledge by focusing on an estimation of rooftop areas that are solar efficient and suitable for PV installations. Invercargill City was selected as a case study to develop a site-specific PV analysis model to overcome the lack of data for predicting rooftop PV potential of the city. Invercargill is the southernmost city in New Zealand with a flat topography. The external average temperature for Invercargill is below

the threshold for heating in other regions and was found to have the highest constant heating energy use (BRANZ, 2010). The housing stock in this area is the oldest with most houses being pre-1978 (BRANZ, 2010). The aging housing stock in colder climate has been identified as a major contributor to health problems in Invercargill because of cold and damp conditions (Davis, 2015). At the time this research was being conducted, the city has not received a site specific study on its PV potential. This presents an opportunity to incorporate the city's urban renewal strategy for improving housing quality while utilizing the existing buildings into the development of renewable electricity resources.

From the available roof area, total PV potential was calculated and compared to the total household energy demands. The research findings indicated how the potential contribution of solar PV can make towards electricity supply of the city. Thus provide for essential information to inform urban energy planning practices, and promote the city's transition towards sustainable energy from renewable distributed generation at a local level in New Zealand.

The accurate prediction of energy generation is crucial for the evaluation of the economic value of the system. To verify the accuracy of the developed method for predicting the PV outputs, the Schoolgen programme was selected as the second case study as it provided an available database of electricity generation produced from the PV systems of all Schoolgen schools (Schoolgen and NZ Power Company Genesis Energy, 2006-2015). This provides a valuable data source for the analysis of PV generation and performance under the actual state of operation. Understanding the energy output variations based on the resource of different sites is particularly helpful in identifying the strengths and weaknesses of each system. The analysis provides some indications of the system parameters and operating conditions that affect performance.

1.3 Research Objectives

1.3.1 Case Study 1 – Solar Harvesting Potential from Roofs of Invercargill Homes

This research is divided into two work strands, each involving a case study. The first strand investigated if a model could be developed, using existing data sources to determine the solar harvesting potential from the rooftops of existing residential buildings in Invercargill, Southland region, New Zealand. As this is a geographically flat city, with a relatively homogeneous housing typology. The research focused on using existing site-specific data of the New Zealand statistical census map of population and dwelling data, as well as digital aerial map to quantify the solar efficient roof area available for PV installations in a flat terrain city.

The study utilized the computer-simulation and PV modelling tools to estimate incoming solar radiation on rooftops. The solar PV potential was calculated using existing formulas based on roof area and population relationship. The study calculated PV potential for a sample set and extrapolated to the entire study area. The model can be customised and applied to other similar flat terrain city, as well as in the larger scale of analysis. To meet this research goal, research objectives were formulated.

<u>The research objectives for Case Study 1 are:</u>

- To develop a site-specific PV analysis model for predicting the solar harvesting potential from residential rooftops, and apply the model to Invercargill. Database information to be used includes:
    - The total roof surface area in the existing residential buildings of Invercargill City's urban development area.
    - The total solar efficient (north facing) roof area suitable for solar harvesting potential by roof-mounting solar energy system in the study area.
    - The total amount of solar PV potential of residential rooftops in the study area.

- To customize the model to predict the solar energy potential in other simple terrain settings.
- To analyse the current resource available in the public domain that could be utilized for predicting the solar harvesting potential of residential rooftops in other locations in New Zealand.

1.3.2 Case Study 2 – Model Validation using Existing Data from PV Generation on Selected New Zealand Schools

The second strand involved the validation of the solar PV prediction model proposed in the first strand of the research, to test the reliability of the modelling outcomes. This was undertaking using the methods developed to calculate the rooftop PV potential and estimated performance of existing photovoltaic installations. The research focus of this case study was to conduct the performance prediction for comparing the modelled estimate energy output with the actual generation data from the PV systems that have been installed in New Zealand schools under the Schoolgen programme. The energy generation of each Schoolgen system was evaluated and compared to assess the system parameters and operating conditions that affect PV performance.

<u>The research objectives for Case Study 2 are:</u>

- To measure the reliability of the PV potential model in calculating the energy generation of solar photovoltaic (PV) systems - based on the comparison of the modelled energy output potential against the actual energy generation data of Schoolgen PV systems.
- To provide a performance prediction and analysis of Schoolgen programme PV systems.
- To analyse the capabilities of the analysis tools used for predicting the amount of energy output of a PV system.
- To provide the background information about PV technologies and key factors that is relevant to grid-connected PV implementations in New Zealand schools.

1.4 Limitations of the Research

In this study, the lack of roof area data was a limiting factor. This study addressed the rooftop PV applications. As such the amount of roof area was required as an input data to determine the solar efficient roof area for calculating PV potential. Because no immediate information such as three-dimensional roof data or other high resolution data sources were currently available in the chosen study area, the sample sets of rooftop were required to be manually digitized for the analysis.

Among several factors, shadow casting effect is a major factor limiting the solar access of buildings (Levinson et al., 2009). Shading losses by trees and surrounding obstacles from neighbourhood elevating structures can limit the solar access of rooftop solar-energy system. Without the automated data, it was not possible to manually extract every existing vegetation and surrounding obstacles for shading losses. Due to the size of area, it was not feasible within the timeframe to quantify the shadow casting effects among buildings by manually digitizing three-dimensional model of the city. For this reason, a separate simulation for determining shading losses was outside the scope of this study. Due to the flat plain of Invercargill City, the decision was made to assume that the topographic influence as well as the shadow casting effects from trees and buildings in the study area were minimal. The average result was considered as the approach for this study.

1.5 Structure of the Thesis

The two case studies of the research were organised into seven chapters of the thesis, each chapter is constructed as follows:

Chapter 1 is the introduction which consists of the purpose, the need for the research, as well as the range of research objectives. The chapter highlights the research framework in dividing the thesis into two part of the work strands along with the structure of the thesis.

Chapter 2 provides the literature review of background information to introduce the key concepts embodied in the context of the research topic. The

chapter discusses the current issues surrounding the subject and reviews the existing methods used in the relevant field. The chapter highlights the findings and materials from the literatures to inform the conduction phases of the research.

Chapter 3 presents **Case Study 1 – Solar Harvesting Potential from Roof of Invercargill Homes.** This part of the work stream was to develop a site-specific PV analysis model for predicting solar harvesting potential of residential rooftops in Invercargill. The chapter provides the brief explanations of the study area and the methods developed for analysing the city's solar energy potential.

Chapter 4 outlines the results obtained from the previous chapter. The results presented here demonstrate the outcomes of various statistical analyses and data processing methods to meet the first case study's research objectives. The chapter includes the review of the methodology used in conducting the research. It also informs the direction to apply the developed model for future analysis.

Chapter 5 presents the model validation part of the research for **Part 2 – Model Validation using Existing Data from PV Generation on Selected New Zealand Schools**. The methods of model validation by comparing the modelled findings to Schoolgen PV generation data are presented in this chapter. This chapter also discusses the direction for analysing PV energy generation and a performance prediction of Schoolgen PV systems.

Chapter 6 outlines the results obtained from the model validation methods. The chapter also provides for a performance prediction and analysis of Schoolgen PV systems. The analyses results show some key indications from the research findings in relation to the second case study's research objectives.

Chapter 7 provides the summary and conclusions drawn from the findings of the research along with the recommendation for further studies.

The next chapter includes a review of existing literatures that pertain to the goal of this study. It covers the various approaches of solar radiation modelling and simulation tools used in past researches to predict the amount of solar energy available on rooftops for large-scale PV deployment. The main areas for modelling solar radiation, calculating rooftop area, and calculating solar potential from solar efficient roof area were discussed in this chapter to inform the methods for this study.

CHAPTER 2: LITERATURE REVIEW

The following literature review provides the background information to introduce the key concepts embodied in the context of the research topic. It discusses the issues surrounding the New Zealand energy supply system and the trend towards the use of renewable generation from solar energy to tackle the energy challenges. It explores the implementation of distributed generation of solar PV and key factors including solar radiation and the effects of technologies. Then, the literature review included here discusses the existing methods for quantifying rooftop PV potential using solar radiation modelling tools. The chapter highlights the material from the literatures to inform the conduction phases of the research.

2.1 Background

2.1.1 Trends in Renewable Electricity in the Global Context: A Key Strategy to Energy Crisis and Climate Change

The world faces a major challenge under the strain of fast-growing energy demands and declining of fossil fuel resources. The corresponding issues associated with volatile and increasing energy prices, inefficient use of energy, and the global impacts from conventional carbon-based energy production to greenhouse gas emission, make supplying this energy increasingly difficult. As the relevance of global warming and climate change requires a transition towards a low-carbon economy, the profound question looms over the world's energy concerns of how to ensure that our future energy needs are met under the balance between the three dimensions of the energy trilemma - reliability, affordability and sustainability (World Energy Council, 2014, December).

At the core of proposals to mitigating climate change and driving progress towards a low-carbon economy, renewable energy is featured to play a central role in several international frameworks for climate change energy policies and

agenda. Renewable energy comes from sources that are naturally replenished in a relatively short timeframe. Sunlight, wind, water and geothermal heat are all renewable energy sources (EECA [Energy Efficiency and Conservation Authority], 2014c). The significant supply potential by means of renewable energy is considered a key solution of alternative energy sources to replace conventional fuels in four distinct areas - electricity generation, hot water/space heating, transport fuels and rural (off-grid) energy services (REN21 [Renewable energy policy network for the 21st century], 2012). The benefits from emerging renewable energy technologies are gaining momentum for cleaner and more efficient energy solutions, attaining great significance in the opportunities for climate change mitigation from the renewable energy sector.

At the international level, countries are responding to the energy challenges by moving toward integration of renewables into electricity supply (Gipe, 2013). As governments step up efforts to transform the local energy industries, many are bringing renewable power generation into their energy portfolio through wide-ranging public policies and political leaderships. At least 118 countries had some type of renewable energy targets and support policies in place by 2012 as instruments to encourage increasing markets and outline goals to increase electricity generation from renewable resources (REN21, 2012). The policy mechanism such as feed-in-tariffs (FITs) and renewable portfolio standards (RPS) are the most commonly used support policies in this sector (REN21, 2012). Each has been designed to provide economic incentives for investments and encourage electricity producers to supply a minimum share of their electricity from designated renewable resources (U.S. Energy Information Administration, 2013). The closer integration of related policies in the economic sectors can be seen through improved business and financing models tailored to best fit the specific areas' resource base and local preferences.

Despite rapid expansion and the continuing upward trend of renewable energy growth, the current state of renewables uptake in all end-use sectors still remains relatively small in term of realizing the global emissions reduction target to stop

global warming (IEA [International Energy Agency], 2013a). As the world has consumed 80.6% fossil fuels, renewable energy sources only supplied 16.7% of global final energy consumption in 2010 - the figure at which the "modern renewable energy" (including hydropower, wind, solar, geothermal, biofuels, and modern biomass) made up an estimated 8.2% share of the total (REN21, 2012, p.21) (see Figure 2-1). This reflects the continued domination of fossil fuels in the energy mix and the alarmingly slow uptake of the low-carbon supply technologies. A lack of long-term policy certainties around technological, political and economic infrastructure to support the radical change remains the key issue leading to the consequences that have deteriorated the clean energy investment environment (World Energy Council, 2014, December; IEA, 2014).

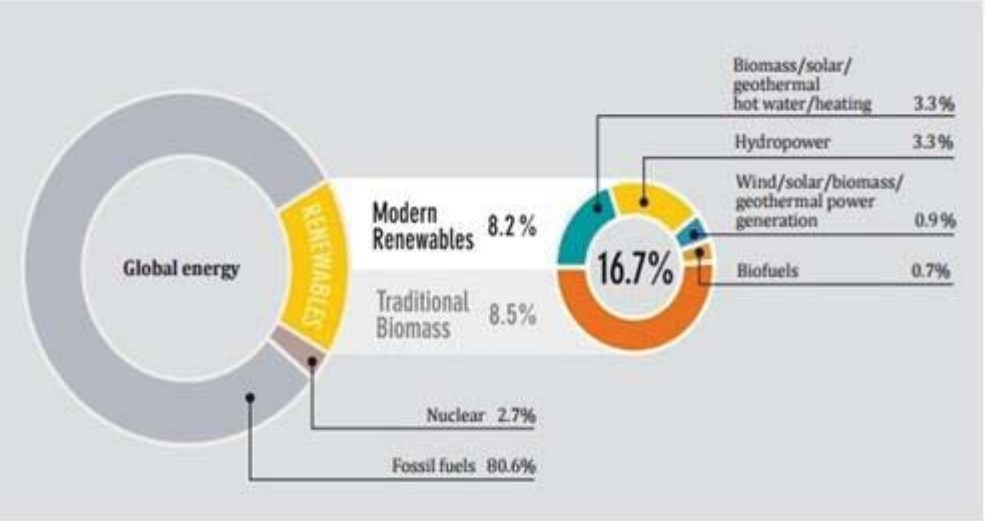

Figure 2-1: Renewable energy share of global final consumption in 2010 (Source: REN21, 2012, p.21)

In spite of these setbacks, renewable electricity production continues to progress. Growth was shifting beyond traditional market where installed cumulative capacity rose significantly in recent years making "renewable power generation technologies become fastest-growing power source" (IEA, 2014, p. 20). With rapid deployment of the renewable power-generating capacity added globally, the growth of renewable share in the world's electricity mix increased at a rapid rate from 16.7% in 2010 to 19% in 2012 and 22.1 % by the end of 2013 (REN21, 2014, p.25) (see Figure 2-2), and is estimated to rise to 25% in 2018

(IEA, 2013b). While hydropower remained the principle source of renewables in supplying global electricity, the share of non-hydro generation from variable sources such as wind and solar PV has grown more rapidly to dominate the renewable generating capacity in recent years (IEA, 2013b; REN21, 2014).

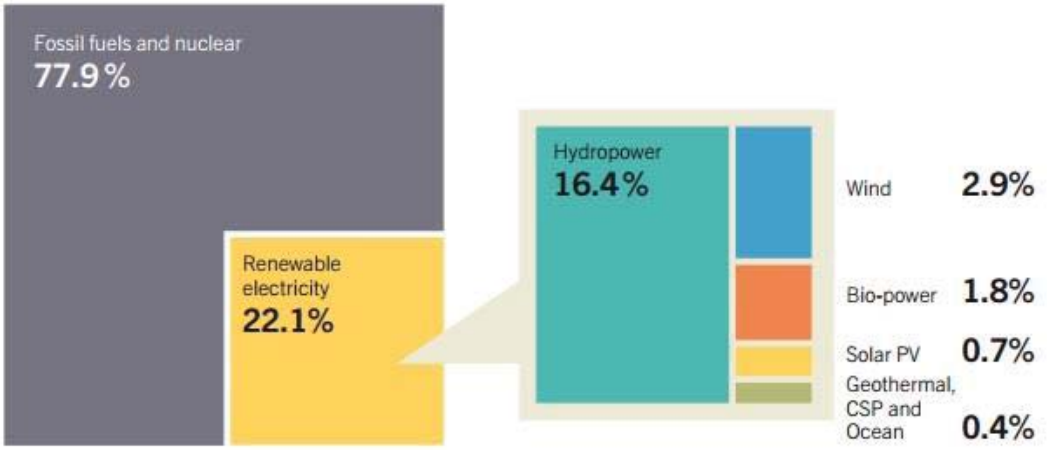

Figure 2-2: Renewable energy share of global final energy consumption in 2012 (Source: REN21, 2014, p.25)

Of all emerging renewable technologies, solar PV has experienced the highest annual growth rate of 74% in 2011 (REN21, 2012) (see Figure 2-3). The growth came primarily from European countries with the greatest increase seen in Germany by 46.7% increase in new added solar PV capacity (REN21, 2012). The significant additions in China, followed by Japan and United States have also played a substantial role in adding more than 39 GW to the total global solar PV capacity exceeding 139 GW in 2013 (REN21, 2014). There is also a continuation of the growth that can be seen in New Zealand market (Ford et al., 2014). The cumulative installed capacity of PV distributed generations in New Zealand has grown from about 7 MW at the end of 2013 to about 20 MW in 2015 (Miller et al., 2015). This trend is projected to double or even triple by 2018 from expanded installations of small-scale, distributed renewable generations where consumers generate their electricity on-site (REN21, 2014).

The community-owned and co-operative projects are also expected to increase from the industrial and commercial consumers installing and operating their own

renewable systems for the reliability of energy supply while reducing energy costs. As worldwide renewable generation capacity continues to rise, it is anticipated that solar power generators will become the largest source of renewables to produce the majority of the global electricity demand by 2060 (IEA, 2011 in Sills, 29 Aug. 2011). The global trend will be that solar PV will be a mainstream provider and changes the way the world is powered (EPIA [European Photovoltaic Industry Association], 2014).

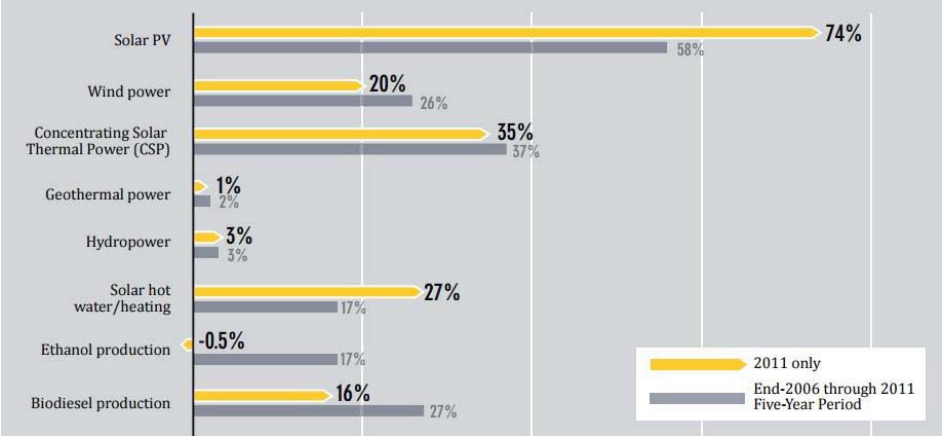

Figure 2-3: Average annual growth rates of renewable capacity 2006-2011 (Source: REN21, 2012, p.22)

2.1.2 New Zealand Electricity and Solar PV Potential

Renewables have already played a significant role in the New Zealand's electricity generation. In 2013, New Zealand generated 41,876 GWh of electricity, of which 75.1% came from renewable resources (MBIE [Ministry of Business Innovation & Employment], 2014b). However, despite the high percentage of renewable electricity contribution placing New Zealand the third highest among the OECD countries after Norway and Iceland, the overall New Zealand's emissions from the energy sector experienced the major growth of 32% between 1990 and 2013 averaging 1.2% growth per annum (MBIE, 2014a). Due to the emissions from electricity generation sector increased 24% from 2011 to 2012 as well as the domination of emissions from transport sector, "New Zealand is having one of the largest increases amongst Annex 1 countries in energy sector emissions since 1990" (MBIE, 2013, p. 4).

New Zealand's electricity emissions intensity is relatively low, by international standards, due to the high proportion of energy produced by hydro generation and geothermal (MBIE, 2014a). This provides a strong renewable base shown in 2013 when emissions from electricity generation fell 19% from the previous year after hydro generation returned to operate at normal levels. But the current technologies remain sensitive to rainfall, so that the lower-than-normal hydro production period resulted in a significant increase in emissions from the heavy use of coal and gas. Due to the risks and opportunities associated with the contribution of electricity future, the New Zealand Government is committed under the national policy statement by recognizing the benefits of renewable electricity generation as a matter of national significance - to achieve the target of 90% of electricity to be derived from renewable energy sources by 2025 (New Zealand Government, 2011).

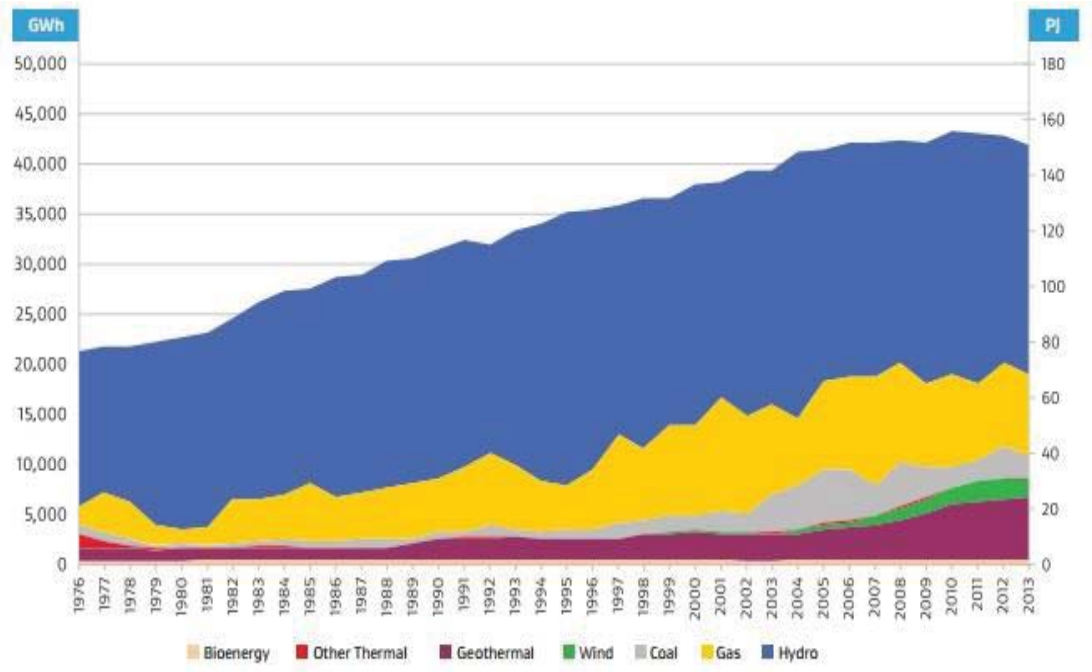

Figure 2-4: New Zealand annual electricity generation by fuel type (Source: MBIE, 2014b, p.56)

Despite New Zealand's diverse portfolio of renewable energy resources, solar radiation in New Zealand is an abundant energy source with high potential that can be harnessed in many geographic areas. Modern technologies of PV panel can produce clean energy in silent, unobtrusive environments with no pollution.

Among all other New Zealand's extensive renewable opportunities, solar energy is proving to be an effective source given its abundance and "practically inexhaustible energy available" (EECA, 2001, p.1). Solar radiation can be distributed using the solar thermal technologies to heat water. A well-designed and installed solar water heating system could potentially meet 50-75% of residential hot water energy demands (EECA, 2014a), and displacing around 2,200 - 2,500 kWh of annual household electricity (EECA, 2001).

The solar photovoltaic (PV) system converts sunlight into electricity directly through arrays of solar PV panels typically mounted on roofs. A well-located standard domestic PV system of 1kWp could generate between 2.5kWh – 5kWh of electricity per day or 880-1,750 kWh per year (EECA, 2014b). As New Zealand residential energy use was 62.8 PJ in 2007, which was accounted for 13% of the country's total energy consumption (BRANZ, 2010). The Household Energy End-Use Project (HEEP) studies identified that average household energy use (all fuel) is 11,410 kWh per year, of which 34% is dominated by space heating and 29% by hot water (BRANZ, 2010). Electricity use accounts for 69% of total residential fuel use (BRANZ, 2010). From these figures, it was calculated that approximately 1.7 tonnes of CO2/year are emitted from a New Zealand household, which equals to 2,600,000 tonnes of CO2/year emissions from the total New Zealand housing stock (NZ HEW, 2008).

According to EECA (2001, p.10), "the total household rooftop area in New Zealand is exposed to primary solar energy that is equivalent to about twice the total national energy consumed". For instance, an average 150m² rooftop can potentially contribute to a household's total energy requirements (EECA, 2001). Similarly, more recent research on the potential of rooftops (Byrd et al., 2013) in New Zealand also showed that the low density suburb with large roof areas are capable of producing surplus electricity. In this context, there exists the solar energy potential in rooftops that could be harvested for PV generated electricity to contribute towards reducing household emissions from the residential sector.

2.1.3 Current Status of PV Deployment in New Zealand

2.1.3.1 Residential Household Sector

Despite its widespread availability and environmental benefits, the solar resource in New Zealand is still underutilized. The use of solar photovoltaic (PV) panels to generate electricity remains a small proportion of total energy generated due to a lack of government subsidies and official supports for solar energy technologies to benefit large-scale implementations in New Zealand at present. Solar energy currently only contributes 0.1% to the New Zealand's overall renewable electricity generation (MBIE, 2014b). With only about 2% of New Zealand homes have solar water heating systems and 0.2% households have grid-connected PV systems (EECA, 2014c). Currently New Zealand has an installed PV capacity of about 2.7 watts per person (the rate increased from 1.9 watts installed capacity per person at the end of 2013) (Ford et al., 2014), compared to Germany at 440 watts per person and Australia at 139 watts per person in 2013.

Major barriers include relatively high initial cost of the system, expense of installations, limited understanding of the various technologies and information to quantify the potential capacity for determining economic return on investment (EECA, 2010; IRENA, 2013). The International Renewable Energy Agency (2013) also emphasizes that the lack of cost and performance data in the public domain represents a significant barrier to the accelerated deployment of renewables. Beyond these factors there are also regulations and a wide range of resource and building consent processes that are currently constrained the adoption of solar PV in term of small-scale distributed renewable electricity generations in New Zealand (EECA, 2010).

Nevertheless, solar PV deployment in New Zealand is growing slowly due to the rise in worldwide production and declining costs of the systems. The combination of lowering panel prices, rapid improvements in efficiency and the effects of rising power bill contributed to a large increase in demand as New Zealanders were looking to gain greater energy freedom by investing in solar PV

for generating their own electricity needs. While prior uptakes were built largely upon the off-grid systems for displacing diesel or petrol generators in the areas of uneconomic remote lines, the recent attention has been focused around the installations of grid-connected systems to the local electricity network (Watt, 2009). The uptake of this type showed an increase of nearly 50% of the total generation capacity of small-scale PV installations during 2012-2013 (MBIE, 2014b, p.50). The key benefit based on the generation in this range is the offset portions of the premises' daytime electricity use and the ability to add value by exporting excess power back to the utility grid. However, the ‘buy-back' rate offered from electricity retailer varies as each company has its own terms and conditions for buying excess electricity from distributed generation. In the absence of guidelines and regulations, this has become a critical issue adding to greater uncertainties for people looking to invest in solar PV.

2.1.3.2 Solar Electricity for New Zealand Schools

The continuing growth of energy demand and rising energy costs affect every sector in New Zealand, including schools. Schools, being occupied by the peak sun hours, are ripe for solar energy harvesting. Particularly at the primary level where there is a specific need to provide young children with a healthy environment of appropriate heating temperature and air quality. A large number (95%) of New Zealand primary schools are old uninsulated buildings, which experience long thermal losses in winter and a waste in large amount of their energy consumption (Swarbrik, 2012; Wang, 2015). The added financial pressure from a change in funding structure provides a higher incentive for schools to generate their own electricity towards energy savings, improving energy efficiency, and reducing costs.

The majority of energy consumption in schools mainly goes to space heating and light during school hours (King, 17 Feb. 2014). This matches with the optimum solar radiation hours for schools' advantage to tap into a free and abundant source of solar energy. Especially since the lower PV panel prices in recent years, making the solar technology become a more viable option for

renewable energy generation on site. With government policy initiatives through program funding, schools around the world are already gaining benefits from their solar PV installations. This includes Australian National Solar School Programme (NSSP) funding of over $217 million to 5,310 schools (almost 60% of all Australian schools) to install solar power systems and a range of energy efficiency measures (Australian Government, n.d.). In United States, 3,727 schools with solar installations has combined capacity of 490 MW and generating around 642,000 MWh of electricity every year (SEIA [Solar Energy Industries Association, 2015).

The rate of solar PV uptake in New Zealand schools is still slow compared to international levels. Despite the reduction in panel prices there are still significant upfront costs that are out of reach for most schools around the country (King, 17 Feb. 2014). There is no government funding, however, a community solar power initiative such as Solar Schools program has been launched to help getting solar PV into schools. The solar crowd funding mechanism offers the local communities to invest in the school's PV system while receiving returns on their investment through energy savings and selling excess to the grid (Nelson Environment Centre, 2014). The Green Party's Solar in Schools policy also launched to assist more schools in obtaining solar by investing $20 million into solar PV systems for schools around New Zealand (Green Party of Aotearoa New Zealand, 2014).

Another established community initiative is the Schoolgen programme developed as a key sustainability approach by Genesis Energy. Launched in 2006, the programme has provided 71 schools (as of the end of 2014) with either a 2 or 4 kW PV system at no cost to the schools (Schoolgen and NZ Power Company Genesis Energy, 2006-2015). This total capacity of more than 100 kW Schoolgen installations making it so far the largest distributed solar power station in New Zealand (Schoolgen and NZ Power Company Genesis Energy, 2006-2015). The programme provides for these schools to generate solar electricity. The real-time

generation data is displayed to provide for the educational resources about energy efficiency and potentials of renewable electricity generation in New Zealand.

2.2 Review of PV Technologies and Developments

2.2.1 Solar Photovoltaic System and Components

A solar PV generator is mainly an assembly of electrical connection of solar cells. It typically generates electricity by converting solar radiation into usable power by means of the PV cells which are electricity-producing devices made of semiconductor materials. When sunlight shines on a PV cell, the absorbed light is transferred to electrons in the atoms of the cell through the energy conversion process known as the photovoltaic effect. These electrons are then freed from their current positions in the cell and become parts of the electrical flow. Since the voltage and current of a single cell is low, these individual PV cells commonly known as solar cells are then assembled to connect together to create a PV "module" or "panel", which in turn can be combined and interconnected to a supporting frame or structure to form a solar array of different sizes and required power output for the system (Figure 2-5).

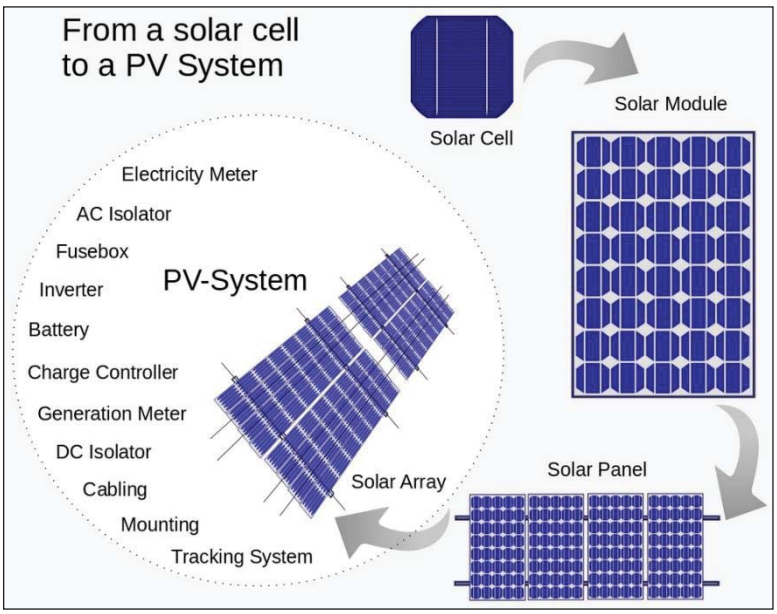

Figure 2-5: The possible components of a photovoltaic system (Source: Wikipedia, 2015a)

The major components of a PV system include an array of solar modules combining with the various system components that enable the PV-generated direct-current electricity (DC) to be properly applied to the condition of use by converting it to the compatible alternate-current electricity (AC) (Solar Energy Technologies Programme, 2005). These items are referred to as 'balance of the system' (BOS) which mainly comprises of one or more inverters, as well as other technical wiring, connection materials and additional options such as monitoring and tracking devices, depending on the installation type. While a grid-connected PV system requires a power conditioning unit and grid connection equipment, an off-grid system may include a battery storage solution and associated charging devices to provide dependable power to the system. (See Figure 2-6).

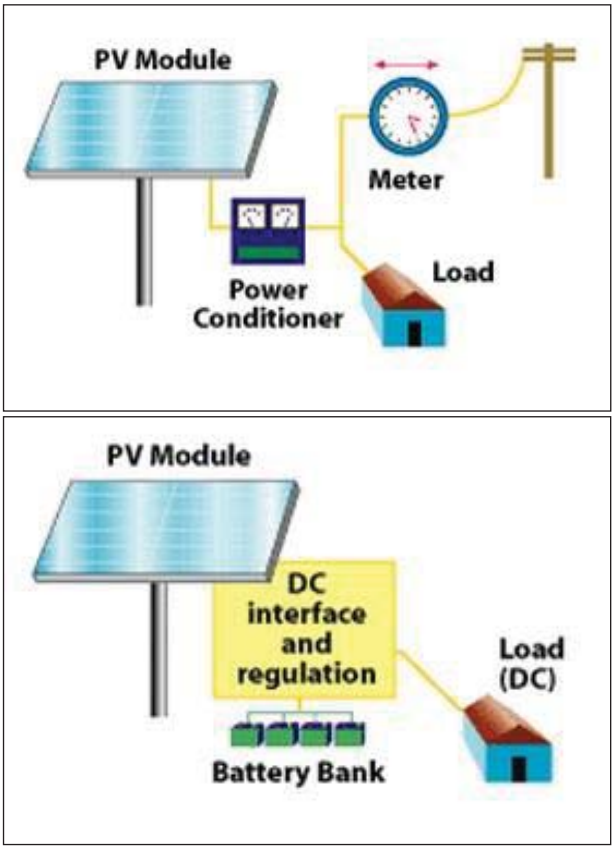

Figure 2-6: Illustrations of a typical grid-connected PV system with a power conditioning unit and connections to utility grid in comparison to a stand-alone off-grid system consisting of a battery system (Source: Solar Energy Technologies Programme, 2005)

2.2.2 PV Cell Technologies

The types of PV module vary by semiconducting characteristics of material and certain technology used in absorbing sunlight and the efficiency in energy conversion. Currently there are three main types of materials which can be classified into first, second and third generation of solar cells. The complete photovoltaic devices are made of different materials by various ways of structurally designs, composition and atomic arrangement, in order to produce solar cells that have optimal performance in accordance with the amount and choice of material used (Solar Energy Technologies Programme, 2005).

2.2.2.1 First Generation Cells - Crystalline Silicon (c-Si)

First generation cells are made of crystalline silicon (c-Si) which can be used in various forms including mono-crystalline (mono-Si) and poly-crystalline silicon (poly-Si). Crystalline-type modules are the most conventional, most efficient and most commercially predominant PV technologies available at present (National Institute of Building Sciences, 2015). From the prevalent 'solar grade silicon', the bulk materials are separated using the crystallinity process to obtain crystals by the resulting yields of the atomic arrangement to form the crystal structure. A single crystalline material typically has larger crystal sizes arranged in a more regular and orderly manner of atoms in the layers of crystal framework than the materials that composed of numerous smaller crystals. As such, PV cells made from mono-crystalline silicon are highly efficient, due to the ability to yield the highest light-to-electricity conversion efficiency from the almost perfect crystal structure in the material properties comparing to other types of solar cells.

Poly-crystalline silicon which consists of small crystals is less expensive to produce than mono-crystalline material. The material is becoming increasingly popular in the use of PV cells although they are less efficient. As the silicon purification and the crystalline wafers forming processes used in obtaining highly pure, near-perfect single crystalline material are very energy intensive and hence

high cost of production. A variation type of poly-crystalline silicon known as the ribbon silicon can be produced by pulling a thin sheet of silicon melt to result in a poly-crystalline structure. This type of cell is becoming another alternative technology where material quality and efficiency can be as high as the crystalline-based PV cells for a lower production cost (Watts, 2009).

2.2.2.2 Second Generation Cells - Thin Film

Second generation solar cells known as thin-film technologies are made from non-crystalline materials such as amorphous silicon (a-Si), or non-silicon materials including cadmium telluride (CdTe) and copper indium gallium diselenide (CIS or CIGS). The technologies based on using lower amounts of active materials deposited as 'thin film' of semiconductor layers produced by innovative low-cost technique. As such, thin-film technologies generally have cost advantage from reducing material costs and expensive processes in obtaining crystalline products. However, the issue of low efficiency means more space of arrays is required to produce the same amount of electricity as a crystalline-type module (National Institute of Building Sciences, 2015). Given the flexibility of thin-film that can be applied directly onto various type of substrate such as glass, metal or flexible roof sheet, the technologies has been frequently used in building-integrated photovoltaic (BIPV) and other large-scale applications for a more cost-effective option. The focus of thin film developments on the use of alternative materials and construction processes are means of increasing cell efficiency and stability in energy conversion while reducing costs.

At present, amorphous silicon (a-Si) is the most developed thin-film technologies. The main advantage is the lower cost of production due the simplicity of material that can be deposited at very low temperature. However, amorphous silicon has much lower performance than first generation cells and suffers a drop in efficiency when exposed to sunlight. The effect can be reduced by stacking several thin film layers to reach higher efficiency however this practice leads to the expense of multiple layers and increased complexity. Of all thin-film technologies, cadmium telluride (CdTe) cells is the first solar panel that

can be manufactured at the lowest cost per watt and the ability in absorbing sunlight at ideal wavelength (NREL [National Renewable Energy Laboratory], 2011). However, its use poses concerns regarding the scarcity of Tellurium (Te) element as well as the toxicity of Cadmium. So far, copper indium gallium diselenide (CIGS-based) modules currently have the highest efficiency among all the commercial thin-film solar cells (NREL, 2011).

2.2.2.3 Third Generation Cells - Emerging Photovoltaics

Third generation cells, often known as emerging photovoltaics, encompassed multiple technologies in the use of a variety of alternative semiconductor materials. The common type of third generation cells include the combination of high efficiency crystalline products (first-generation) with a number of low-cost thin-film technologies (second-generation), in order to achieve the goal of producing low-cost, highly efficient solar cells. Primarily developments remain focused on reducing cost rather than improving efficiency and long life. As such, the technologies are still currently in the development phase and not yet commercially applied to the PV market.

Some of the promising technologies of third generation cells include tandem or multi-junction cells made of multiple layers of thin films with different material bandgaps to allow better light absorbance and improving energy conversion efficiency. The techniques are typically applied to amorphous silicon or high-efficiency material such as gallium arsenide (GaAs). Other related concepts include nanocrystal solar cells based on nanotechnology application to the layers of semiconductor materials for potential ability to capture full spectrum of light. Quantum dot solar cells also have a similar approach in using tiny crystals in absorbing materials to increase performance by harvesting multiple portions of solar spectrum through quantum mechanical effect. Another type is dye-sensitised solar cells (DSSC) which use the photosynthesis principles in converting any visible light into electricity. Other non-semiconductor technology such as organic solar cells which have low production cost and can be potentially cost-effective in the high volume PV production.

2.3 Factors Affecting the Operation and Efficiency of PV Electricity Generation System

The potential generation of solar electricity from photovoltaic (PV) depends on many factors. Although the incoming solar radiation is an essential component for PV production, only certain energies from sunlight reaching PV cells will work efficiently to create electricity (Renewable Energy World, 2015). This is due to several variables related to technological limitations, as well as other important parameters such as operating conditions that are necessary to take into account when determining the amount of output energy from a PV system.

2.3.1 Solar Radiation

The amount of solar radiation received on the surface is the most influencing factor for determining the electricity generation potential of a PV system. Solar radiation is the amount of sun energy reaching the earth's surface. PV system converts this sun energy directly into electricity.

The intensity of the solar radiation at a given location varies with geographical latitude, solar intensity throughout time of the day, temperature and seasonal effects, and atmospheric condition. At ground level, topographic variability including slopes and site elevations play an important role in influencing the amount of solar radiation reaching a surface. As the solar radiation available on the surface is highly variable, this variability affects the potential of a PV system in supplying solar electricity (Hofierka et al., 2014). In term of PV system design and installation, the orientation and angle, available sunshine hours, and system positioning under shading and aspect, are also very important factors to consider for assessing solar energy of the site (Armstrong & Ryan, 2009).

Solar radiation can be measured from the weather station around the world. In New Zealand, the incoming solar radiation data can be obtained from the National Institute of Water and Atmospheric Research (NIWA). The hourly

average measurements of incoming solar radiation are taken from the nearest weather stations throughout New Zealand. However, estimating the available solar energy by using the average value based on the solar radiation data from the nearest weather station is not always appropriate (Wood et al., 2013). This is because it can give an optimistic prediction without accounted for the local conditions and the performance capacity of the PV system. When the certain amount of sunlight strikes the surface of PV cells, much of the energy can either be reflected or absorbed by the semiconducting ability of the material that make up the cell (Renewable Energy World, 2015). Since only light of certain wavelengths is able to pass through the material, only some have enough energy to produce heat where much is lost before it could be converted into electricity (U.S. Department of Energy, 2013). In this case, it is necessary to account for these losses due to associated variables affecting efficiency at absorbing and converting sunlight of a PV system.

2.3.2 Module Orientation, Shading and Sun angle

In accounting for the site-specific factors in the design of a PV system, the efficiency of site orientation and solar incidence angle have great effects in term of positioning to make the most of the available local resource to obtain optimal performance. Considering New Zealand's geographical location in Southern Hemisphere means the sun passes from east to west through the north, i.e. rotating in the right-left motion through the northern sector of the sky. For this reason, the north facing surface (preferably in a range of 20 degree west to 30 degree east of true north) will be exposed to maximum solar insolation. This is considered to be the most suitable orientation for installing PV panels on the efficient roof space.

Shading losses by trees and surrounding obstacles can also limit the solar access of rooftop PV system. In winter, shadow casts from obstacles on the north side can be 2-3 times of the actual height (Armstrong & Ryan, 2009). The factor of overshadow cast by existing planting as well as neighbourhood elevating

structures must be taken into consideration to ensure the best positioning of the PV system.

Properly orienting, with an optimum inclination angle is also critical to PV energy yield. As the position of the sun in the sky is changing throughout the day, the optimum angle to capture maximum power is when the PV module surface are perpendicular to the sun rays. However, as the sun incidence angle increases, the amount of radiation reflected from the PV also increases which affect in solar radiation losses to reflection (Kalogirou, 2009). Since the optimal effects varies with the solar angle-of-incidence depending on the latitude and season, tilting the inclination angle of PV panel equal to the latitude of the location will typically provide the most year-round energy. Adjusting the arrays to steeper angle for ‘an extra 10 degree above latitude’ can optimize energy yield in winter when the sun is lower (Armstrong & Ryan, 2009, p.18). Flatter angle will favour the summer period because the sun is higher in the sky.

2.3.3 Effects of PV Technology Types

The performance of a solar cell is measured in terms of its efficiency at turning sunlight into electricity (Renewable Energy World, 2015). The conversion efficiency, which is defined as the percentage ratio of power generated to the solar incident on the PV panel, have different effects among active semiconductor materials, compositions and atomic structures in each PV technology type. The primary issue regarding the conversion efficiency in cell materials is the inability to respond to entire solar spectrum in certain wavelength. Therefore the unused energy contents are not converted into electricity but rather re-emitted and wasted as heat or light. Another major problem in some materials is the recombination of the electrical charge carriers including electrons and holes. They may be recombined before entering into the electrical circuit and contribute to the cell's current (U.S. Department of Energy, 2013). Factors such as natural and electrical resistance to electron flow, as well as reflective characteristic in certain materials causing light to be reflected away from the

cell's surface (such as untreated silicon) are also important parameters decreasing efficiencies in certain PV types (U.S. Department of Energy, 2013).

Due to the variations in PV technologies, the significant differences in the percentage ratio of rated module efficiency are apparent in each technology type. Depending on the manufacturing quality, there can also be the variations in specific energy yield between similar material products under different operating conditions. As such, the module rated efficiency is not necessary the best indicator of performance where other operating conditions of the entire system were also significant.

In order to obtain the more accurate prediction of the electricity production, many studies have developed theoretical approaches to determine the rate of module efficiency by integrating various factors affecting the performance of the PV system. While some studies are making assumptions in using average figures given by the manufacturer specification, other studies have taken a more serious measure by incorporating extensive computer simulation and complicated formula to determine the fraction of reverse current from different type of losses that can noticeably reduce the PV energy output (e.g. Kovach and Schmid, 1996's raytracing techniques by RADIANCE software). Up to the present, most of the studies have been interested in only specific factors affecting efficiency of PV panels and/or PV systems. There is not many studies that present all factors affecting efficiency and operation of the entire PV system in the literature (Meral & Dincer, 2011).

2.3.4 Effects of Ambient Temperature

There are various ambient conditions that affect the output of a PV system (Meral & Dincer, 2011). Among all major effects, ambient temperature is a parameter that has great influence and must be taken into account when analysing the output performance of the PV system. As determined by many studies, the efficiency of PV module decreased with increasing module temperature

(Yamaguchi et al., 2003; Ettah et al., 2009; Meral & Dincer, 2011). The relationship of the PV module efficiency and the PV module temperature is shown in Figure 2-7.

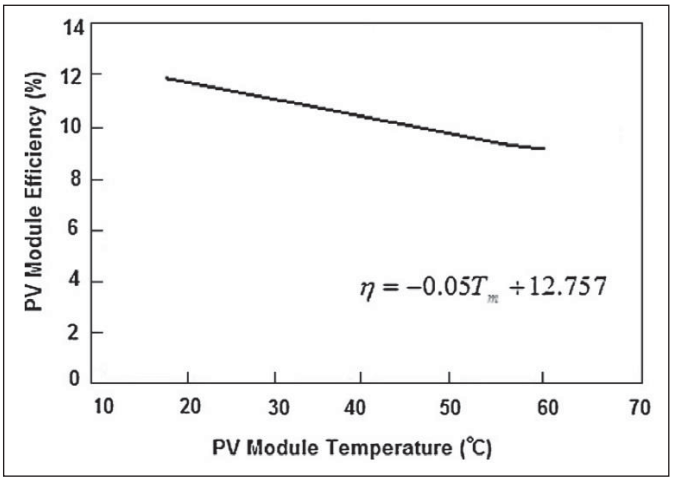

Figure 2-7: Relationship of PV module efficiency and PV module temperature (Source: Yamaguchi et al., 2003 in Meral & Dincer, 2011)

When operating solar cells at high temperatures, the cell efficiency reduces due to the effect of cell material properties that tend to lose voltage as temperature rises. As the PV module performance varies with actual location and prevailing environmental conditions to which they are subjected, different types of module tend to perform differently in certain weather conditions (Ettah et al., 2009). The effects are variable depending on the material type. Amorphous silicon modules have a lower temperature coefficient than crystalline products meaning they can be operated at higher temperature with less output degradation (Watt, 2009).

According to the study by Ettah et al. (2009), solar panel temperature increases more rapidly than the ambient temperature. This is the case where the solar radiation falls on the PV panel that is not converted to electricity but instead converted and absorbed as heat. The cell's heat absorbing characteristic of black material and glass cases also encourages temperature increase to the panel. Therefore it is important to match the cell material to the operation temperature

by either cooling and reducing heat stored inside the PV cells to improve efficiency and reducing the rate of thermal degradation of the module (U.S. Department of Energy, 2013; Meral & Dincer, 2011).

2.3.5 Effects of System Equipment

The related equipment including batteries, charge controllers, inverters, and peak power-trackers, all have influences in the behaviour of a PV system in the modification of efficiency and output energy. In case of batteries, the parameters related are the type, nominal capacity, maximum charge current as well as the ability to accept repeated deep charging and discharging without damage. According to the fact that PV cells have an optimum operating point (or maximum power point - MPP) where the values of the current and voltage result in a maximum power output (Kalogirou, 2009). However, this point varies with the radiation intensity and the cell temperature (Watt, 2009; Kalogirou, 2009). The efficiency is therefore depending on the charge controller in adjusting the varying battery voltage to the optimum operating level and preventing overcharging when temperature exceeds the set high voltage so the PV operates at its maximum power point (MPP).

The fundamental purpose of an inverter is to change DC produced from PV module to the useable AC electricity. As characterised by the energy conversion efficiency, the main function is to keep a constant voltage on the AC side and convert the input energy into the output energy with maximum efficiency (Kalogirou, 2009). In the case of a grid-connected PV system, the less efficient inverter may not have enough power to drive the PV generated power into the main AC supply effectively for energy to smoothly flow outward (Meral & Dincer, 2011). The use of maximum power point tracking (MPPT) technique is a method to monitor the output voltage and allow the converter circuit to extract the maximum power available from a cell. Only inverters that operate at maximum efficiency throughout MPP range will achieve the highest possible energy yield (Watt, 2009).

2.4 Economics and Applications of Grid-Connected PV System

The most common type of solar PV use in the urban environment is grid-connected system that is tied to the utility grid with no batteries to store extra electricity (National Institute of Building Sciences, 2015). In this type of application, the grid acts as a storage facility receiving excess electricity at times when PV producing surplus, and supplying electricity when PV cannot meet the household demand (EECA, 2001). Grid connection gives the advantage in the ability to sell surplus energy and reduce storage losses involved. The system usually connects to the local electricity network through an inverter with metering installation to measure the import/export quantities transferred. Depending on the interconnection agreements and applicable metering rules of the distribution company, it is necessary for the consumers to understand this transaction structure in order to benefit from effective utilization of energy generated and compete with the retail price of electricity (Coughlin & Kandt, 2011; EECA, 2001).

The capital costs by the PV modules and associated balance of the system (BOS) are the main considerations. The corresponding price drops from massive-scale production has made PV become more cost-effective when calculating the system cost per 'Watt peak' (Wp) basis. Together with the pressure to price reduction throughout the construction chain, the upfront cost of PV has fallen to the rate approaching grid parity in which the levelized cost of PV generated electricity (LCOE) is comparable with the grid electricity prices in many locations (Branker et al., 2011). In New Zealand, research by Miller et al. (2015) have found that PV is now an attractive investment for some types of household with higher day-time load where they can offset more of their higher retail electricity price. If the cost of PV continues to fall (as shown in Figure 2-8), and the electricity prices increase substantially, the region with high solar radiation will be suitable for large-scale PV investment (Miller et al., 2015).

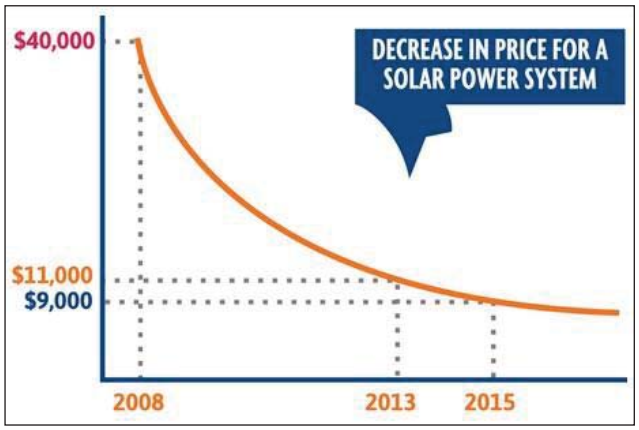

Figure 2-8: The price of a standard 3kW solar power system in New Zealand (Source: My Solar Quotes Limited, 2015)

Assessing economic viability of a grid-connected system is complex due to many associate factors which include the technical performance and the presence of regulatory measures that set the economic incentives for the PV system. The growing body of literatures have combined several modelling approaches to address the economic viability of grid-connected PV systems from the consequences of different scenarios. While some studies focused on the impact of retail electricity structures by the varying time of use (e.g. Darghouth et al., 2013; Ong et al., 2010; Mills et al., 2008 and Borenstein, 2007, in Jagemann et al., 2013). Other studies extended the approach by applying the household optimisation model to analyse the profitability of investments, using the range of associated costs to predict when the system life cycle production costs reach grid parity (e.g. Ayompe et al., 2010). Ren et al. (2009, in Jagemann et al., 2013) determined the cost-optimal capacity of grid-connected application by minimising the annual electricity costs. Castillo-Cagigal et al. (2011 in Jagemann et al., 2013) evaluated the function of battery storage system and focused on the active demand-side management in order to maximise the in-house consumption of self-produced PV electricity.

From many perspectives, it was found that the cost-effectiveness of grid-connected application relies heavily on the size of PV system installed to achieve meaningful savings (Coughlin & Kandt, 2011). Jagemann et al. (2013) analysed the effects of optimizing the size of PV and found the higher economic

consequence in reducing the electricity costs by consuming self-produced instead of earning from grid supplied electricity. Murray (2005) also emphasizes that good system sizing and appropriate load to resource matching are crucial for lifecycle economics of the renewable energy system. This is particularly important under the current New Zealand market condition where the invariably buy-back rates are significantly less than the retail prices as well as the net metering that allows excess energy to be credited are not offered. Consequently, balancing power generation with power consumption does not result in the balance of revenue and expense hence over-producing can lead to underutilization of excess power (Wood et al., 2013; Murray, 2005). One of the key challenges noted for the system design to become economical is one that is sized to provide all the electricity demand and generate no more than it directly consumed.

In the absence of feed-in tariffs, net metering and other regulated pricing principles of electricity buyback arrangements to ensure grid-connected benefits in selling excess electricity (independent of government subsidies), shifting the pattern of demand to maximize self-consumption is an economic alternative to operate PV generated electricity in the more efficient manner than feeding the surplus energy into the grid (e.g. Wood et al., 2013). In order to do this, it is important that the operational issues related to the nature of daytime energy usage pattern and domestic loads must be well understood to properly select and size a PV system to match the user needs and increase accuracy of energy demand predictions (Wood et al., 2013; Coughlin & Kandt, 2011; InGrid, 2014). The increasing share of self-consumption will reduce the reliance on the market financial structure and increase savings from the offset electricity costs (EPIA, 2013). Adding to the uncertainty derived from the intermittent nature of solar energy due to the variability of insolation that cause conflicts to the network from the rapid changes of output voltage (Baker et al., 2013). Grid energy storage is often proposed as a solution to smooth out intermittent generation by controlling the voltage levels to remain within grid operating conditions and shifting peak energy to focus on the efficiency from the demand side (Baker et al., 2013).

Given the complexity and conflicts of grid-connected renewable generation systems, the energy policy formation and execution needs to be underpinned by reliable energy resource data and robust numerical modelling in order to understand the behaviour of the physical systems (Bruckner et al., 2005; Gomez-Munoz & Porta-Gandara, 2002 in Murray 2005). Chaurey et al. (2004 in Murray, 2005) also indicates that the lack of information on the techno-economic performance is a problem in grid-based system design which in turn becomes a major obstacle to the acceptance of renewable energy through energy policy. While the economics of PV technology is continuingly advancing as the ongoing amount of research and development heavily focuses on improving the efficiency and affordability of PV systems. However, all aspects of technical, financial, regulatory and institutional play important roles in deciding the viability of distributed generations (Chaurey et al., 2004). It is assumed that continuing and additional market support mechanisms will lead to a dynamic expansion of worldwide installed capacity that allow grid-connected energy system to achieve the distributed electricity at or below grid prices (grid parity) (Ayompe et al., 2010). The predictability in economic, social, environmental, and technological dimensions for the system design is a key mechanism that will drive public contribution to gradually transform the policy dependent market into the one driven by consumers seeking greater long-term certainty in their PV investments (Bruckner et al., 2005; Watt, 2009).

2.5 Urban-Scale Solar Mapping Projects in New Zealand

Several international studies have attempted to predict the solar energy potential on rooftops of a city or a large-scale region, i.e. Spain (Izquierdo et al., 2008; Ordonez et al., 2010), Ontario/Canada (Wiginton et al., 2010), Valparaiso/Chile (Araya-Munoz et al., 2014), Hawaii/United States (Carl, 2014). Some authors have applied the roof area and population relationship to quantify total roof area for PV deployment i.e. Germany (Lehmann & Peter, 2003 in Wiginton et al., 2010), India (Kumar, 2004; Pillai & Banerjee, 2007 in Wiginton et al., 2010), Brazil (Ghizi, 2006 in Wiginton et al., 2010), Spain (Izquierdo et al., 2008), Ontario/Canada (Wiginton et al., 2010). Ordonez et al. (2010) utilized the

statistical construction data and the digital urban maps to obtain the mean roof surface area for each building type in Andalusia region of Spain. Carl (2014) applied the geographic information systems (GIS) and Light Detection and Ranging (LiDAR) data to obtain useful roof surface area for estimating PV potential in the town of Kailua Kona in Hawaii.

There are only a few projects carried out in New Zealand, each with rather limited information available. These projects have a similar purpose in using solar mapping to assist energy policy formulations in the region. However, they differ in context and scale of analysis, which are varied depending on the research goals and purposes of the analysis. Due to the limitations of the resource concerning roof data and other site-specific information, different approaches and techniques have been utilised. The review of these projects informs the solar mapping direction and the opportunities to develop and expand upon these aspects of PV analysis in New Zealand.

2.5.1 Auckland Solar Mapping Projects

A study by Ghosh and Vale (2006) of the potential solar energy, focused on the local-scale residential neighbourhood relating to urban planning strategy for comparing different type of urban neighbourhood arrangements. This study's aim was to make the recommendations on roof forms and configurations that signify higher collection rates of solar energy available on rooftops. The study determined spatial distribution of residential roof extensively in order to estimate and compare corresponding energy by the ratio of utilization from the total available roof areas. A calculation model was developed using GIS-based methods for solar energy planning. The total roof areas were determined diagrammatically and calculated using a geometric method that considered the roof orientation within 45 degree north for solar efficient roof area. Detailed categories of different building roof area were presented to provide for the basis of appropriate roof designs that can maximise PV generation.

The solar potential of Auckland study by Hugh Byrd (2013) took a different approach from Ghosh and Vale (2006). Within the similar case study site of Auckland, Byrd (2013) investigated the maximum solar potential available from installing PV systems on buildings throughout the city. The purpose was to evaluate the contribution of the energy produced from PV in supplying the electricity load of a city. From the investigation among building types and urban forms, the research showed that the low density suburban housing with large roof area are capable of producing surplus electricity when compared to the energy demands given from HEEP studies for household energy consumption. It was found that the surplus energy was sufficient for charging electric vehicles in Auckland. The study also challenged the conventional thinking that suburbia is energy inefficient. The results of the research also reversed the argument for a compact city based on transport energy use, with the conclusion that a dispersed city is more efficient for energy production when designed accordingly.

The calculation techniques adopted in this study were based on a detailed cross-section of Auckland housing where the samples are taken as representative of the city throughout different densities of main buildings types. The data analysis was undertaken on the basis of selected meshblocks. The annual average solar radiation was calculated using solar simulation of Ecotect software to compare solar energy generation potential in different suburbs and land use.

2.5.2 Solar PV Potential for Each Region in New Zealand

The estimation of solar potential in New Zealand by Eltayeb (2013) has adopted the approach by David Mackay's study on *Sustainable Energy-Without the Hot Air* by applying Mackay's idea to New Zealand, in comparison to United Kingdom. Eltayeb (2013) has followed the approach by making rough estimates of the amount of energy from solar thermal, solar photovoltaic and solar farming in kWh/day/person for every region in New Zealand. By using Mackay's formula which incorporated the distribution of population density per m^2 and the average solar radiation of the region to calculate PV potential per day per person, the solar radiation maps produced by NIWA were utilized to obtain the average solar

radiation values in MJ/ m²/day for each region in New Zealand. The study concluded with the recommendations that solar thermal is a better option for New Zealand in term of energy production and cost.

2.6 Modelling Solar Radiation

This section of literature review discusses the key concepts and addressing methods for modelling solar radiation. It also describes the research phases for measuring and mapping building rooftop area for calculating PV potential of a city.

2.6.1 Solar Radiation Components

Solar radiation or insolation is an important parameter concerning the available power from the sun energy received on the earth surface. Defined as the site's 'solar quality' (EECA, 2001), solar radiation can be represented in the number of different ways upon the relation between global, direct and diffuse irradiance. On a horizontal surface, global irradiance (also referred to as Global Horizontal Irradiance [GHI] or solar intensity) is a measure of the total energy from the sun per unit area in watts per square meters (W/ m²) received by a surface horizontal to the ground with the components of direct irradiance and diffuses irradiance (NREL, 2011). The direct irradiance (or Direct Normal Irradiance [DNI]) is the straight line radiation received by a surface perpendicular (normal) from the direct path of the sun at its position in the sky (NREL, 2011). The diffuse irradiance (or Diffuse Horizontal Irradiance [DHI]) represents the energy received on the surface after being scattered by the atmospheric molecules and particles (NREL, 2011). On the tilted plane, there is a reflected irradiance exists (often referred to as albedo) from the reflection of the ground and surrounding features, displaying as the third component which makes up a small proportion of the total global irradiance. It is usually insignificant compared to direct and diffuse, for all practical purposes global radiation is said to be the sum of direct and diffuse radiation only (NREL, 2011).

Understanding the amount of total energy received on a given site is of particular interest in the field of solar energy utilization. The quantity present by each type of radiation can indicate the potential of solar energy output from various solar systems and technologies. On a practical level, direct irradiance is the largest component of the total global irradiance (Fu & Rich, 1999). This can be intercepted by the highly concentrating solar collectors with two-axis tracking system following the direct beam from the position of the sun (EECA, 2001). Other solar conversion systems, such as the flat plate collectors, are more related to the global irradiance. At such the insolation figures are one of the most important considerations when designing the solar energy systems to be installed for the specific location.

2.6.1.1 Factors Affecting Solar Radiation

At the global scale, latitude of the geographical location is the main factor concerning the amount of solar radiation received on a surface. Due to the earth's geometric rotation and revolution around the sun (Fu & Rich, 1999), the latitudinal gradients of the specific location effect the distribution of solar insolation in a number of ways. In general, solar intensity increases with the location of closer proximity to the equator (Eltayeb, 2013). Another factor is the solar intensity as functions throughout time of the day. Given that the maximum value occurs at midday when sunrays are perpendicular to the surface, and lower figures of solar intensity during sunrise and sunset when sunrays are almost parallel (Eltayeb, 2013). New Zealand's geographical location in Southern Hemisphere (latitude between 34.00° - 48.30°, longitude between 165.80° - 179.40°) means the sun passes from east to west through the north, i.e. rotating in the right-left motion through the northern sector of the sky. For this reason, the north facing surface will receive maximum solar insolation. The seasonal effects result in the earth's orbital variation and the sun angles at different times of the year, associated with the geographical difference in the extent of atmospheric attenuation such as cloud cover and water content, also influence the amount of solar radiation reaching the surface.

In the local context, topography is the major factor contributing to the distribution of insolation (Fu & Rich, 1999). The shadow casts by the topographic variability, elevation, slope and orientation of the surface can create strong local gradients of insolation, which in turn determines the spatial dynamics of the location (Fu & Rich, 1999). Furthermore, topography changes the proportion of direct and diffuse radiation (Ruiz-Arias, 2009). In the urban scale where the building geometry consists of differently oriented and inclined surfaces, the shadow pattern generated around the complex morphology of the urban setting becomes a very important factor added to the complexity of solar energy estimation when compared to a flat, non-shaded surface (Jonsson et al., 2012).

2.6.2 Solar Radiation Modelling: Existing Approaches

The insolation value of a location is an important consideration for various energy applications. Unfortunately, accurate maps or measurements of solar radiation on inclined surfaces are very scarce and rarely available due to the requirement of dense collection from station network (Jonsson et al., 2012 and Fu & Rich, 1999). At present, the available solar radiation data are the ground measurements or satellite information monitoring from locations throughout the world e.g. from space-based observations of solar irradiance (started in 1978 which associated with weather stations) or meteorological geostationary satellite. However, in most cases, the solar radiation data estimated from satellite image provides less accurate values compared with ground measurements due to the cloud effects of the sky conditions (Tovar-Pescador et al., 2006). Other solar radiation data sources include the climate prediction models or forecast models produced from national meteorological service by data assimilation from a modern analysis system. This type of dataset was typically used for the metrological and climatological studies (Jonsson et al., 2012).

The most common form of solar radiation data is often referred to the global irradiance. The estimation of each solar component can be obtained by using the theoretical relationship to divide the solar radiation of a location into the separate fraction of direct, diffuse and reflected irradiance (Jonsson et al., 2012). However,

this data processing technique based on a simple calculation of solar radiation components is more relevant in the larger scale of analysis as it only provides reasonable estimates in the homogeneous terrain. Often it is not accurately applicable in the complex environments that subject to strong topographic effects or urban geometric variations where the increase of diffuse radiation component can decrease the accuracy of the estimate values drastically.

The realistic evaluation of a site-specific solar capacity by considering all sources of influencing factors is fundamental for system design and installations. Among several factors, shadow casting effect is a major factor limiting the solar access of buildings (Levinson et al., 2009). Recent analyses on solar PV potential have been using techniques to incorporate shading losses and identify the sun-casting effects on the surface (e.g. Kassner et al., 2008; Karteris et al., 2013). Examples such as Redweik et al. (2013) conducted a solar radiation model using a shadow algorithm to calculate shadow maps of direct and diffuse solar radiation on each point of the surface. Nguyen & Pearce (2012) also developed a new shading algorithm using LiDAR data to incorporate both terrain and near surface shadowing effects. Levinson et al. (2009) characterized rooftop shading using the LiDAR data of surface height to geometrically calculate the fraction of annual insolation losses to shading by trees and building obstacles.

A number of theoretical approaches and empirical irradiation models have been developed to predict the incoming solar radiation in complex environments. These primarily differed in the way they deal with the complex issue of the diffuse component of radiation and its distribution through different choices of sky model (Perez et al., 1987). For decades, conventional methods have treated the diffuse radiation as being isotropic (the sky is assumed to be uniform and the radiation is derived equally from all directions). Some cases have ignored the reflected radiation from surrounding topographic features due to the assumption of its minor contribution to the total irradiance (Fu & Rich, 1999). The uniform sky model provides an unrealistic depiction of the sky. Other developed models have attempted to address the distribution of diffuse and reflected radiation in a

more rigorous way through anisotropic sky conditions (accounted for sky variables such as cloud cover and position of the sun) (e.g. Oke, 1987; Arnfield, 1982; Aida 1982; Evan 1980, Perez et al., 1987 in Robinson, 2006). With this focus, choices of overcast sky model, clear sky model, or all-weather model have been developed to provide a more realistic sky representation for daylighting analysis on different site conditions. Among different sky models, the anisotropic method originating from Perez et al. (1993)'s all-weather model have been found to give the most accurate performance when applied to various locations (Jensen, 1994 in Robinson & Stone, 2004; Jonsson et al., 2012).

2.6.3 Tools for Spatial Solar Radiation Modelling in Urban Environment

Solar radiation modelling in urban environment is a complex process which needs to incorporate multifactor and variables in the integration between the urban form and solar energy inputs (Amado & Poggi, 2014). Particularly, the strong presence of urban geometry around the complex urban structures constitutes various sky obstructions, and consequently affects the urban microclimate through the radiation exchange pattern of the surface. The common parameters that are significant to the radiation geometry of the urban climate are the canyon geometry - the ratio of the mean height and widths of the buildings (H/W ratio), and the sky view factor (SVF) - the ratio of the radiation received by a planar surface and that of the entire hemispheric radiating environment (Lindberg, 2007). In this sense, SVF is a measure of the clearness of the sky in relation to the radiation path to a surface in term of the degree of obstacles i.e. buildings (Svensson, 2004). A number of studies have shown that the canyon geometry and the SVF are the main causes of 'urban heat islands' (UHI), affecting the net radiation and the temperature pattern due to the thermal properties in built-up areas and the counter radiation from obstructions (Svensson, 2004). Therefore they are considered to be important parameters in numerous models for analysing solar radiation in urban geometry (e.g. Oke, 1987; Arnfield, 1982; Aida 1982; Evan 1980, Perez et al., 1987, Ratti & Richens, 1999 in Robinson, 2006).

There are two types of models used for predicting solar radiation on the surface: point-specific models and area-based models (Fu & Rich, 1999). Point-specific models 'calculate irradiation at a point' (Mardaljevic & Rylatt, 2003, p.28), based upon the surface geometry, and the sun position from a specific point. This type of model incorporated the local topographic effect by empirical relation, visual estimation, or by using the hemispherical type of photographic image (fish-eye photographs) (Fu & Rich, 1999; Tovar-Pescador et al., 2006)). However, the method for deriving the SVF value is not straightforward and is limited to the data availability in the area of high building density and geometry (Lindberg, 2007). Point-specific model can produce a highly accurate result for a point of location but does not provide for the calculation over the entire area in the large scope of analysis (Fu & Rich, 1999 and Mardaljevic & Rylatt, 2003).

In contrast, area-based models can compute insolation for every location over the entire geographical area (Tovar- Pescador et al., 2006). This method calculates the surface orientation and shadow effects using the topographic information from a digital elevation model (DEM) integrated within a GIS (Dubayah & Rich, 1995, 1996; Rich et al., 1995 in Fu & Rich, 1999). The use of DEM provides a new technique for obtaining the SVF and other topographic influences on the spatial distribution of solar radiation in the area of complex topography (Tovar- Pescador et al., 2006).

2.6.3.1 Modelling Based on the DEM and GIS

In the last decades, a new technique for estimating solar radiation in the complex topography has been enhanced through the use of terrain elevation data and topographic surface information of DEM. DEM is commonly constructed using remote sensing techniques such as photogrammetry, LiDAR; or through field mapping and direct land surveying data. The application of DEM is mainly integrated within a GIS to determine terrain attributes such as slope, aspect and elevation, for the amount of solar radiation, at every point of DEM (Ruiz-Arias et al., 2009). Using the sun position in relation to the specific point, the analysis can take into account the measure of sky obstruction to determine the composition of

direct and diffuse radiation from the total global irradiance values (Tovar-Pescador et al., 2006).

The accuracy of solar radiation modelling in the urban environment depends on how appropriate the geometrical data is represented (Jonsson, 2012), i.e. the resolution of DEM (Dubayah & Rich, 1995; Rich et al., 1995 in Tovar-Pescador et al., 2006). While the application of vector data such as Computer Aided Design (CAD drawings) is more common for representing building geometries in higher accuracy and precision. In comparison, a raster DEM has advantages over the vector-based spatial information from the increased spatial extensions which enable the larger areas of the city to be examined at a much lower computational cost (Lindberg, 2007). The recent development of high-resolution raster data originating from LiDAR has been proven to give accurate details of spatial information suitable for solar irradiance calculation in raster environment (Jonsson, 2012). Unfortunately, this technology still has a comparatively high cost and requires extensive processing procedures to be developed in many areas (Araya et al., 2014).

With the topographic information from DEM, GIS application gives the capabilities for integrating, overlaying, and displaying the analysis of geographical referenced data. Particularly it allows the spatial-temporal relationships between different parameters of solar irradiance variations to be examined and visualized in one system. Currently, a number of GIS-based software packages offer several different methodologies in their approaches of solar modelling used to achieve these functions. Examples such as ArcGIS adopting SolarFlux model (Dubayah & Rich, 1995; Hetrick et al., 1993 in Tovar-Pescador et al., 2006) and Solar Analyst (Fu & Rich, 1999 in Tovar-Pescador et al., 2006). IDRISI uses Solei model (Miklanek & Meszaros, 1993), GRASS GIS developed r.sun model (Suri & Hofierka, 2004), and later developed SRAD model (Wilson & Gallant, 2000) also designed to run inside ArcGIS platform (Ruiz-Arias, 2009). Despite the flexibilities within these tools, each modelling

software package has different strengths and limitations and produces variations in results due to the parameters used in the chosen solar radiation model.

In New Zealand, the SolarView calculator developed by NIWA estimates the available solar energy that can be collected by solar panel at a particular location. The programme combines an image of the local landscape with irradiance data from the nearest weather station, and determines the cumulative solar energy received along the sun path during each day in kWh/m² (NIWA, 2014). However, SolarView indicates the amount of solar energy hitting the solar device, not the amount of output power of the PV array.

2.6.3.2 3D Solar Evaluation - Computer-Based Daylighting Simulations

GIS-based software relies on the high-resolution DEM to provide for accurate inputs of geographical data in order to perform accurate solar radiation evaluation. However in many cases, the available DEM only described height information of topographic terrain without any surface elements such as plant canopies and building structures. Ground features need to be manually reconstructed into DEM through vector-to-raster data conversion. This process can be challenging and could introduce errors to the data used (Rich et al., 1995 in Fu & Rich, 1999; Jonsson, 2012).

On the other hand, vectorised data representation of building geometries is more common within the building energy sector for urban planning and architectural applications, due to the ability to accurately describe objects in three dimensions (Jonsson, 2012). A number of digital simulation tools have been developed for architectural design purposes which are suitable for solar analysis and energy evaluation. Computer-based daylighting simulation software such as Ecotect, AG132, 3ds Max-Design have been widely used for creating accurate simulations through the range of building energy analysis functionalities. These software functions calculate the daylighting effects on building performance based on the relationship between sky conditions and building orientations. The

solar analysis capabilities integrate with these tools can visualise building obstructions on the sky vault (i.e. SVF), and simulate solar access from building envelopes (Souza & Rodridues, n.d.; Kensek & Suk, 2011). The solar evaluation tools that adequately support the early design phase are particularly useful in supporting important decisions for future developments. With these tools, the evaluation can be made in both existing buildings as well as 'planned buildings' from conceptual design. This ability distinguishes the daylighting simulation software from GIS-based tools which only deal with the existing objects present on the surface.

Among different software's daylighting analysis methods, 'the digital simulated representation of the sky is one of the most important factors in daylighting calculations' (Kensek & Suk, 2011, p.3). The choice of sky selection is critical for accurate analysis due to the implications of different sky conditions. The most widely utilized sky models (mathematically developed models of virtual skies by CIE) such as CIE clear sky (less than 30% cloud), CIE overcast sky (completely cloudy 100%), are typically based in the software for daylighting simulations. The choice of which to use depends on the site's condition of the buildings.

Given the advances in numerical modelling arising from increased computational power, several dynamic simulation programs are now capable to integrate increasingly sophisticate sky models which are sensitive to the influence of sky obstructions in reducing incoming solar radiation and contributing to diffuse irradiance (Robinson & Stone, 2004). While the widely used software such as Ecotect uses the CIE overcast sky model as a default, it does not support other sky options. In comparison, AGI32 software offers 15 sky conditions available to choose from, including both clear sky and overcast sky options. 3ds Max adopted the most advanced daylighting field including both CIE sky as well as empirical solar radiation model such as that of Perez all weather sky model (Perez et.al, 1993) in the analysis (Kensek & Suk, 2011).

2.7 Calculating Rooftop Area

This study seeks to identify the areas of available rooftop surface in the city of Invercargill, New Zealand, in an effort to determine the solar harvesting potential for PV electricity generation. In order to do this, it is important to determine total rooftop area that may be utilized from the existing buildings.

The ability to determine the amount of available rooftop areas suitable for solar system installations on a large scale can be a difficult task (Arnette, 2013). To produce this analysis, it is necessary to obtain available roof surface area to be used as an input data. Ideally for advanced solar analysis by computer-simulations, the existence of digital 3D model of individual buildings containing every shadow casting objects in the built environment would be desirable. Several studies have developed methods for extracting roof surface outlines. To date, the common methodologies have been utilizing the LiDAR data to generate the 3D digital elevation model (DEM) of the site (e.g. Kassner et al., 2008; Kanters et al., 2013; Redweik et al., 2013). This approach has proven to be very accurate, not only in defining rooftop areas, but also in accounting for geographical aspects and vegetation useful for rooftop shading analysis (Levinson et al., 2009). Nevertheless, this technique requires detailed processes of advanced 3D modelling integrating with high computational power and technical knowledge of filtering and segmenting LiDAR data, to derive the building outlines and roof shape reconstruction.

Among several efforts made on large-scale solar potential analysis, other methodologies develop the 3D model of buildings through the use of stereo aerial imagery (e.g. CH2MHill Solar Automated Feature Extraction, 2008 in Levinson et al., 2009; Araya-Munoz et al., 2014). SUN-AREA (2012) has also fully utilized GIS-based analysis on high-resolution LiDAR by means of aerial survey, and becoming the largest solar cadastre project so far for covering more than 650,000 rooftops (SUN-AREA, 2012).

Unfortunately, the geometrical data from LiDAR or other appropriate digital image data for 3D modelling simply do not exist in many locations. Since there is no immediate statistical information available, a methodology for determining available rooftop area need to be developed for the appropriate scale of analysis (Izquierdo et al., 2008). In this respect, the difficulties remain on the size and scope of the study area. Several efforts have been made to develop a method to extract the available roof area for a location, but often the same technique is not directly applicable to different scale of the study site (Wiginton et al., 2010; Izquierdo et al., 2008). Some techniques focused on a single building and immediate surroundings of a small neighbourhood to classify land use designation in urban planning projects (e.g. Gadsden et al., 2003; Ghosh & Vale, 2006 in Wiginton et al., 2010), but it is not feasible to apply the similar approaches into a regional-scale solar farming for the renewable energy planning purpose (e.g. Arnette, 2013).

Despite the lack of technically-advanced data resources from local limitations, it is still possible to determine the available areas of rooftop in the local-scale residential developments. Araya-Munoz et al. (2014) used the topographic groundwork data obtained in the study to produce spatial-geometry database of the buildings. Ordonez et al. (2010) developed a methodology based on building characterization by utilizing the available governmental database for statistical construction data to determine the gross roof surface area for each building type. Several more simplistic approaches examine a small-scale representative sample of building typologies to extrapolate the results to the whole region level (Karteris et al., 2013). Furthermore, several studies have identified the relationship between population density and roof area in different locations around the world (e.g. Lehmann & Peter, 2003; Kumar, 2004; Ghisi, 2006; Pillai & Banerjee, 2007 in Wiginton et al., 2010). Izquierdo et al. (2008) developed a new methodology using the relationships between accessible data such as land uses, population and building densities based on stratified sample of representative building typologies in Spain. This method was found to be highly accurate and also applicable in the larger scale.

Another method found to be efficient, comprehensive and accurate was proposed by Wiginton et al. (2010). Built on the concept of population-roof area relationship from accessible census data, the study demonstrates techniques to merge the capability of GIS and image recognition to quantify the available roof areas for PV potential in the large-scale province of Ontario, Canada (Wiginton et al., 2010). The methodology developed consists of a five-step procedure, starting by dividing the region into smaller geographic units of census subdivisions. These units were sampled to determine the relationship between population- roof areas from population density distribution, an approximation value of roof area per capita was then plotted against the total number of population to give an estimation of the gross roof area for the whole region.

2.8 Calculating PV Potential from Rooftop

Understanding the available solar radiation and having obtained roof surface areas of the site are essential components to determine the suitable areas for solar energy applications. Since the performance effectiveness of the solar energy technology at the neighbourhood and household levels can vary widely depending on a range of site-specific factors. Knowledge of site-specific access to local resources is critical for ensuring the best possible benefit from the technology can be obtained. From this perspective, not all sites are suitable for every solar energy options (Armstrong & Ryan, 2009).

2.8.1 Solar Efficient Roof Area

Several considerations must be taken into account in order to compute the suitable areas for solar energy systems accurately. Major factors such as building orientation, inclination angle, shading, insolation pattern, as well as other competing uses are all important parameters influencing the fraction of available roof area accordingly. Moreover, the technical capability of roof to install a solar system is also considered to be another key limitation. According to Ghosh & Vale (2006), 42% of the solar efficient roof areas would be lost due to inappropriate roof design referring to the area of roof which cannot accommodate

the size of solar panels adequately assuming 4m² per household. Kanter et al. (2014) also consider the minimum surface of the solar system (m²) as an important parameter used to analyse the efficiency of roof surface. Particularly the insufficient space can be seen in the hip or valley segments of the roof as well as other spaces used to accommodate other architectural elements of the buildings such as dormers, sheds and chimneys.

In order to assist with the variable components associated in this matter, many research initiatives have come up with the numerical model for obtaining reduction factors that can be used for calculating suitable fractions of roof area. In each case, the reduction factor coefficient value, derived from taking into account the limiting factors in various combinations, is used to multiply with the total roof areas to obtain the fractions available for PV deployments (Wiginton et al., 2010). As such, enormous efforts have been placed to analyse extensive sets of factors in order to derive useful indicators of reduction potential values.

However, it can be seen that different researchers placed different emphasis on the criteria used in the process. Depending on locations and scope of analysis, Izquierdo et al. (2008) formulated the shadow coefficient and the facility coefficient with the output being focus on shading and other competing uses of roof space. Similarly, Pillai and Banerjee (2007) estimate 30% total roof areas to be solar efficient. While Ghosh and Vale (2006) determine the coefficient value of solar efficient fractions to be the percentage of building orientation within 45 degrees of true north in New Zealand. Wiginton et al. (2010)'s five-step method have taken a conservative approach in utilizing the combination of coefficient values formulated from different literatures for roof area reduction process of the analysis.

The fractional coefficients can represent appropriate approximations of roof reduction percentage especially the ones which considered all sources of influence on the fraction of available roof area (Wiginton et al., 2010). However,

the use of a constant value for roof reduction across the rooftops can be inaccurate in many cases as it only gives an overview of potential roof area (Izquierdo et al., 2008). A separate simulation using computer-based simulation tools can give more accurate reduction factors to obtain roof area available for PV. As discussed in the earlier section, computer-based simulation software such as Ecotect enables the building energy performance analysis by using the interrelation between building geometry and various combinations of influencing factors such as the site's geographic location, climatic condition, orientations and roof inclination angles. On this basis, the simulation tools assess the building performance by taking into account the solar radiation incidents and shadowing effects from surrounding environment in the urban landscape, and display the variations of expected incident solar radiation across the surface. The suitable fractions of roof area for PV application are indicated by the area showing higher solar access capacity.

2.8.2 Potential PV Energy from Roof Area

In order to estimate potential energy from the distribution of roof area, the computer-based simulation method can calculate solar availability on roof surface in kWh/ m^2 of annual average solar radiation. However, the amount of PV energy output relies heavily on the conversion efficiency of each PV system. Additionally, it is necessary to account for losses throughout the system due to conduction, convection and radiation processing (Pollard & Amitrano, 2009).

The purpose of this study was to determine the solar PV potential from roof area, it was assumed that each PV system would be located on the most efficient location on the rooftops for maximum solar collection capacity. This study also assumed the appropriate installations of all individual system components and characteristics.

Based on the simulation tools typically used in several solar radiation prediction methodologies, such as PVWatts, PVGIS or Solar Analyst with GIS

integration, they are essentially focused on solar irradiation and not all of them are supporting PV potential calculations by accounted for the dynamic performances of PV systems. In many cases, several studies focused on estimating the potential energy output in terms of determining the energy balance from potential domestic energy distribution (supply) in comparison with the energy consumption of the household (demand). In order to do this, several techniques have been applied to formulate the methodology that takes into account the variability associated with PV potential. Wiginton et al. (2010) make the analysis on different type of PV panels based on pre-determined module efficiency values to calculate potential output from the annual average global solar radiation on a surface. Using the following equations:

$$E = I_{md} * 365 * e * A_{pv} \quad \text{..... Equation 1}$$

E is the total annual energy output. I_{md} is mean daily insolation calculated as annual average solar radiation in kWh/ m², e is module efficiency and A_{pv} is the available area of panels in m² (Wiginton et al., 2010).

From Equation 1, the extrapolated result across the region indicated that the significant contribution to the total per-capita's city grid demand can be obtained from the large-scale deployment of rooftop PV in Ontario (Wiginton et al., 2010).

In comparison, studies such as O'Brien et al. (n.d.), and Amago and Poggi (2014) took the sum of solar radiation incident on the surface (kWh/ m²) obtained from computer simulation tools (e.g. ESP-r software, O'Brien et al., n.d.; Ecotect software, Amago & Poggi, 2014), to estimate the energy production yield from a PV system by determining the performance ratio due to energy losses in the balance of system, collectors efficiency (%). The equation used by Amago & Poggi (2014) is shown as:

$$Y = Pr \times Me \times (Gr \times A) \quad \text{..... Equation 2}$$

Where Pr is Performance Ratio = 0.75 (O'Brien et al., n.d. used 0.7 for utilization factor), Me is nominal module efficiency (based on 1 kW/ m² global insolation, 13% is used by Amago & Poggi, 2014), Gr is the sum of annual solar radiation in kWh/ m² and A is the available roof area (Amago & Poggi, 2014).

There were significant differences between studies in the approaches to the choice of figures used for module efficiency, depending on the consideration in factors affecting the performance of solar energy system. While some researchers used assumptions (e.g. Byrd, 2013 using 12%; O'Brien et al., n.d. assumed 10% for solar collector and 35% for solar thermal), some studies took more serious approaches by using extensive computer simulation to determine the fraction of reverse current from different type of losses that could noticeably reduce the PV energy output (e.g. Kovach and Schmid, 1996's raytracing techniques by RADIANCE software). Jakubiec & Reinhart (2013) took more detailed approaches to module efficiency and derating factors by modelling the adverse effect from the urban ambient temperature and the incident irradiation on PV panel at each hourly time step. The study considered that the PV panel maximum power at its ideal conditions can be derated based on a temperature correction factor and thus used the predicted rooftop temperatures to calculate module efficiency. Huld et al. (2006, in Jakubiec & Reinhart, 2013) also predicted monthly average temperature profiles to use in calculating PV reductions.

The reviews of literatures and solar mapping applications covered the various approaches of solar radiation modelling and simulation tools to predict the amount of solar energy available for large-scale PV deployment. With currently limited resources to identify rooftop solar potential for a large-scale analysis in the chosen study area, the information informed the solar mapping direction and the opportunities to develop the methods for measuring and mapping building rooftop area suitable for the location and the scale of analysis. The methodology described in the following chapter seeks to incorporate the research goals and purposes in using solar modelling tools to quantify to total PV potential for residential rooftops in Invercargill.

CASE STUDY I - SOLAR HARVESTING POTENTIAL FROM ROOFS OF INVERCARGILL HOMES

CHAPTER 3: RESEARCH METHODS

This chapter presents the first case study of the research. This part of the work stream is to develop a site-specific PV analysis model for predicting solar harvesting potential of residential rooftops using Invercargill as a case study. The chapter provides the brief explanations of the study area characteristics and the overview of official data used for the conduction of the research. The methodology for determining the total rooftop area, building rooftop models as well as techniques used in analysing the city's solar energy potential are discussed here in detailed.

3.1 Description of Study Area - Invercargill City

3.1.1 Urban Context

Invercargill is New Zealand's southernmost city and the capital of Southland region. It is situated on the low lying flat land on the coastal edge of the Southland plains with the total land area of 491 km². The expansive landscape is enhanced by the vastness and the scale of pastoral surrounding which is subject to various seasonal climatic effects and frequent southerly storms. Due to the lack of topographical variations, the city grid layout occurs to enhance the planarity of the cityscape, which in turn serves to provide the city's linearity and clarity in its function. The formal north-south and east-west roads are clear dominant city structures providing the most significant means connecting the north and south sides of the city (Corson, 2010). This north-south reference to the urban layout also appears to contribute to the local identity of the residential neighbourhood character. The study area of Case Study 1 was selected from the existing buildings within the Invercargill City Residential Zone of Invercargill District Plan's Urban Boundary to assess rooftop solar radiation. Figure 3-1 displays the study area for Case Study 1.

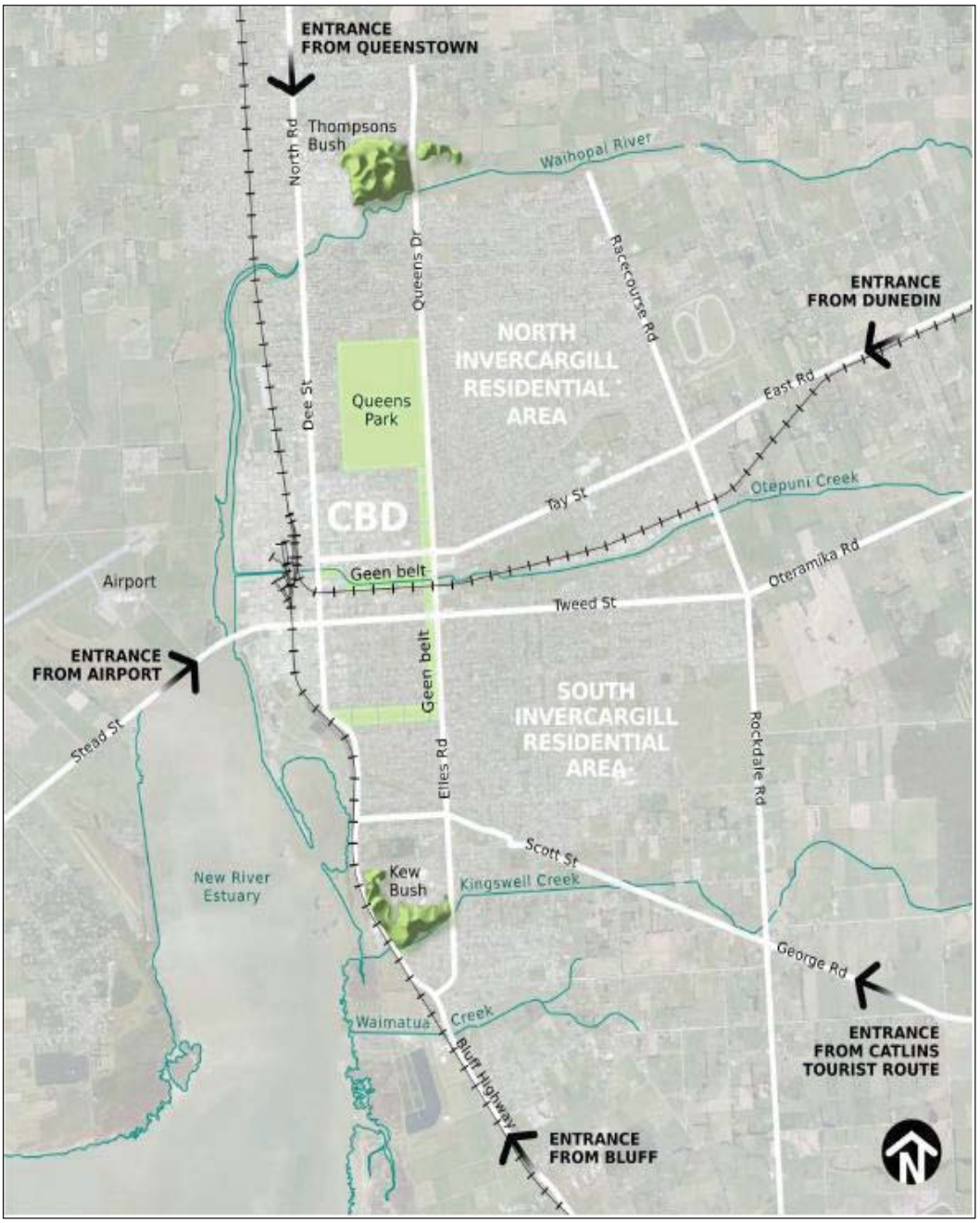

Figure 3-1: Study area - Invercargill City Residential Zone within the Invercargill District Plan's Urban Boundary (Source: Corson Consultancy, 2010, p.14)

3.1.2 Existing Building Stock

The residential areas are predominantly a mix of low-density, detached single-story typical New Zealand suburban housing. The building styles mainly ranges from pre-1950s, with the majority built around 1910 and prior to 1900s constructed primarily with timber framing. The aging housing stock reflects the inefficient housing quality and the issues around inadequate weather proofed and

deteriorated conditions. Figure 3-2 represents the typical housing styles in Invercargill.

Figure 3-2: Invercargill housing styles (Source: Corson Consultancy, 2010, p.20)

According to Statistics New Zealand (2013a) data, Invercargill City has the population of 51,696 people and a total of 22,560 dwellings, of which 21,216 are being occupied. Of these total dwellings, 89.4% are separate/detached houses,

10.3% are the two or more units joined together and 0.3% are the undefined temporary private dwellings including private caravans or holiday bach/crib. The city's built forms are oriented strongly to the spatial pattern of the road network rather than the sun hence limiting quality to gain maximum benefit from the solar penetration into the building's living environment. Wood and coal burners still remain the key source of heating contributing much to the city's air pollution built up, putting Invercargill's current air quality in breach of the Government's National Environmental Standards for Air Quality (NES) (Environment Southland, June 2014).

The poor quality of the current housing stock and high cost of heating in Invercargill are the relevant 'urban issues' addressed under the Regional Policy Statement concerning Section 5.10 Built Environment, as well as the Southland District Council District Plan Provisions in effects to Section 1.4 Urban Environment for "the need to provide opportunity for housing in the manner that maintain and enhances the quality of the environment" (Environment Southland, n.d., p.6). It is therefore the strategic vision for the city's Urban Renewal and Intensive Development within the scope of the New Zealand Urban Design Protocol and the Urban Design Strategy, for the opportunities to transform existing buildings into more functional energy-efficient housing supply by "renovate/redevelop and re-adapt them" to contribute to sustainable urban environment and modern lifestyles (Environment Southland, n.d., p.12).

3.1.3 Climate and Sunshine

Invercargill has a temperate oceanic climate with the mean daily temperature ranges from the lowest in July for 5.3°C to the highest in January for 14.2°C (Figure 3-3). The average high temperature ranges from 9.6°C to – 18.7°C but given the high latitude of the area of 46° 42', Invercargill summer could reach 25°C- 32°C for the extreme temperatures (NIWA, 2013).

Climate data for Invercargill (1981–2010)													[hide
Month	Jan	Feb	Mar	Apr	May	Jun	Jul	Aug	Sep	Oct	Nov	Dec	Year
Average high °C (°F)	18.7 (65.7)	18.6 (65.5)	17.1 (62.8)	14.9 (58.8)	12.3 (54.1)	10.0 (50)	9.5 (49.1)	11.1 (52)	13.1 (55.6)	14.4 (57.9)	15.8 (60.4)	17.5 (63.5)	14.4 (57.9)
Daily mean °C (°F)	14.2 (57.6)	13.9 (57)	12.5 (54.5)	10.4 (50.7)	8.0 (46.4)	5.9 (42.6)	5.3 (41.5)	6.6 (43.9)	8.5 (47.3)	9.9 (49.8)	11.4 (52.5)	13.0 (55.4)	10.0 (50)
Average low °C (°F)	9.6 (49.3)	9.3 (48.7)	7.9 (46.2)	5.8 (42.4)	3.8 (38.8)	1.9 (35.4)	1.0 (33.8)	2.2 (36)	4.0 (39.2)	5.4 (41.7)	7.0 (44.6)	8.6 (47.5)	5.5 (41.9)
Precipitation mm (inches)	115.0 (4.528)	87.1 (3.429)	97.4 (3.835)	95.9 (3.776)	114.4 (4.504)	104.0 (4.094)	85.2 (3.354)	75.6 (2.976)	84.2 (3.315)	95.0 (3.74)	90.4 (3.559)	105.0 (4.134)	1,149.3 (45.248)
Avg. precipitation days (≥ 1.0 mm)	13.0	10.3	12.3	12.3	15.3	15.6	14.2	12.8	13.1	13.8	13.3	14.3	160.4
% humidity	80.6	83.3	84.2	85.3	87.0	87.7	88.1	85.8	81.3	80.0	78.2	78.6	83.3
Mean monthly sunshine hours	185.9	167.2	142.6	117.2	87.5	78.7	97.9	123.0	139.8	173.0	181.3	188.2	1,882.2

Figure 3-3: Climate data for Invercargill (1981-2010) (source: NIWA, 2013)

New Zealand has more clear sky days and relatively higher sunshine hours than some oversea countries with higher rates of solar energy use. While the daily solar energy value in most New Zealand sites are similar to Australia and slightly higher than Europe (EECA, 2001), Invercargill has the lowest daily average among New Zealand cities due to its southernmost position (EECA, 2001). Solar record by NIWA (2013) (Figure 3-3) showed that Invercargill has only 1,682 sunshine hours per year comparing to New Zealand highest sites of Blenheim and Nelson with 2,475 and 2,472 sunshine hours per year respectively (Figure 3-4). However, due to its latitude, Invercargill has longer daylight hours during summer and much shorter daylight hours in winter.

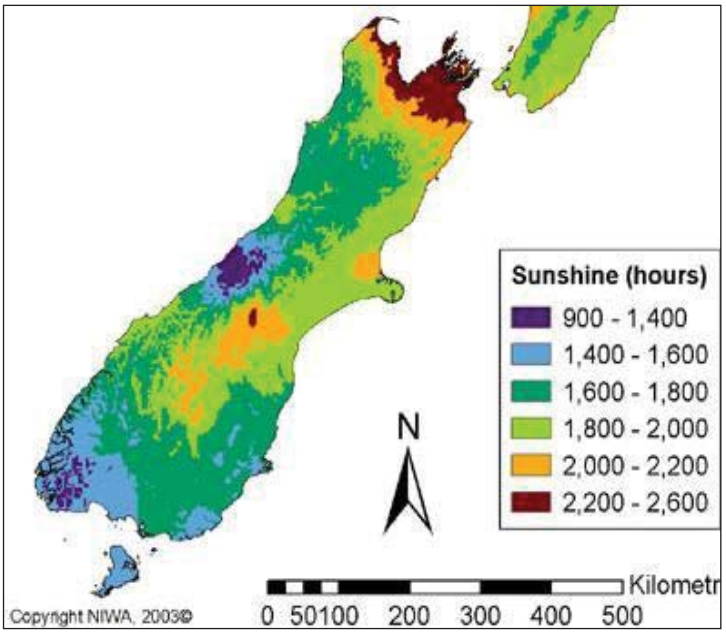

Figure 3-4: New Zealand mean annual sunshine hours by locations (source: NIWA, 2013)

The New Zealand solar energy resource was measured by NIWA at over 90 NIWA's atmospheric research station, using a number of instrumental techniques to measure global irradiance by the rate of energy flow per unit area on a horizontal surface. The estimation of available solar energy around New Zealand sites were recorded in the solar radiation map of NIWA climate database as shown in Figure 3-5.

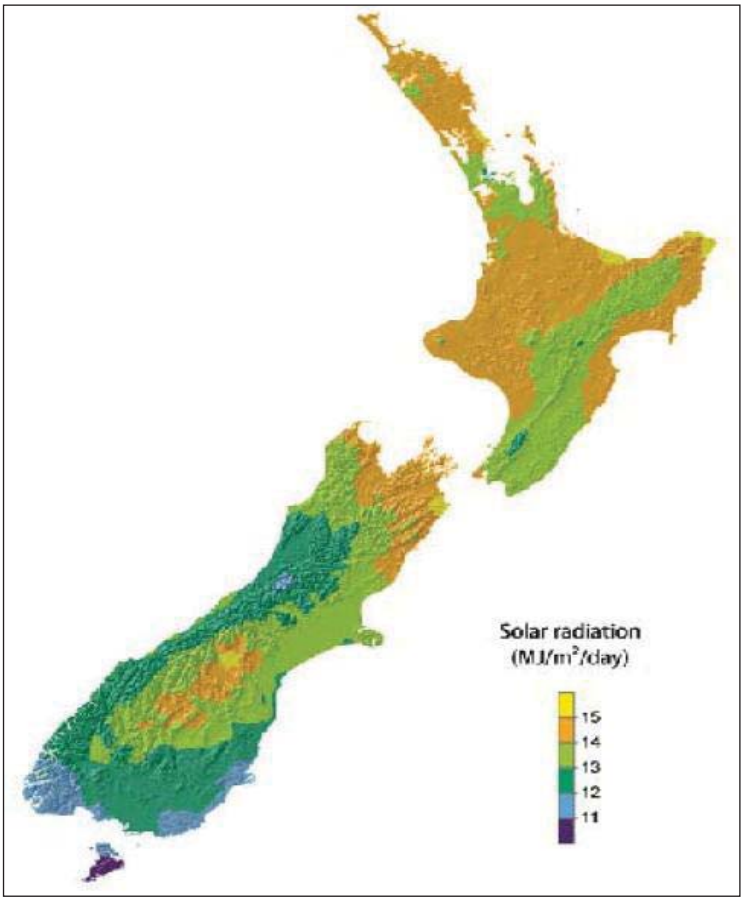

Figure 3-5: Solar radiation in New Zealand (source: NIWA, 2005)

The data from this solar radiation map supported the overview of solar radiation energy pattern in New Zealand. For Invercargill, the map showed the average incoming solar radiation ranges around 12-13 MJ/m²/day or 3.47kWh/m²/day (1 kWh = 3.6 MJ). Prior studies by EECA (2001) (Figure 3-6) indicated that the monthly average of daily global irradiance were similar in most locations for New Zealand and Australia, based on the maximum value of 30MJ/m²/day in summer and 12 MJ/m²/day in winter. Invercargill has the average

daily value of 15% lower than other major New Zealand sites due to the pattern of cloudiness and the effect of latitude influencing the pattern of measured irradiance (NIWA, 2005). The higher proportion of clear-sky days around Nelson and Blenheim explains the effects of the higher incoming solar irradiance in these areas, while Central Otago and Southland has lower percentage of clear skies due to complex thickness of cloud type over. However, the solar record for Invercargill of 4651.9 MJ/m²/year or 1292.2 kWh/m²/year still presents a comparably good prospect of potential capacity for several solar energy applications (EECA, 2001).

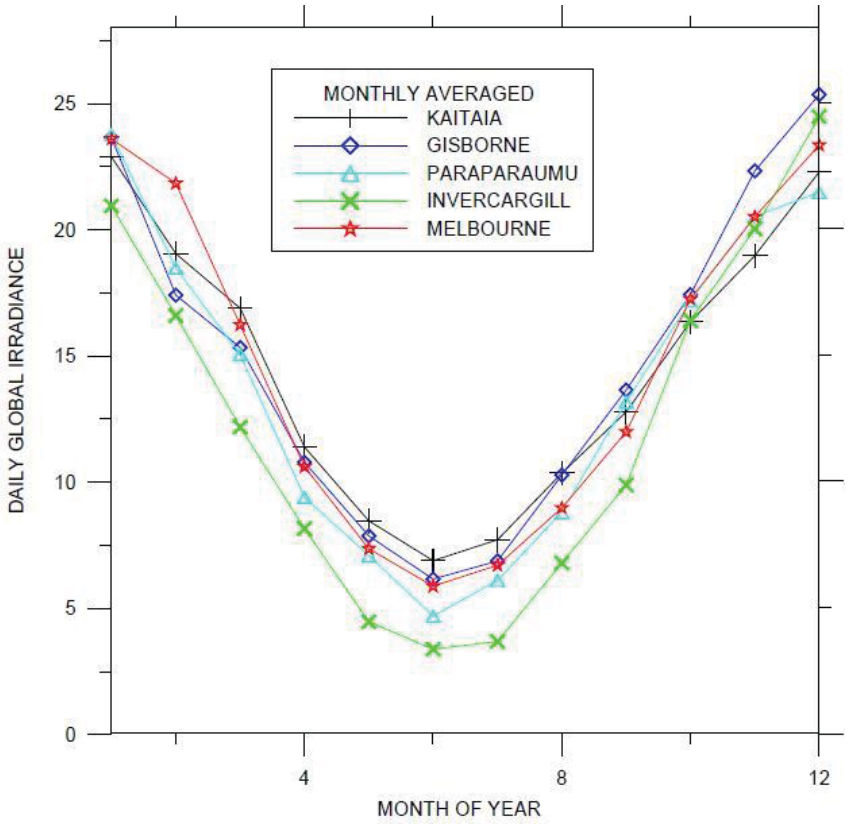

Figure 3-6: Monthly averaged daily global irradiance comparing Invercargill to other locations in New Zealand and Australia (source: EECA, 2001, p. 14)

3.2 Research Design

The main objective of this research strand is to develop a model that can be used to calculate the solar harvesting potential from solar efficient rooftop area of residential buildings throughout a city. Invercargill City was selected as a case study due to its potential characteristics of a well-established community and a sufficient housing stock that could be utilized for achieving energy sustainability from solar energy options. The geographical location in a vast flat plain with minimal topographic variations gives the city a practical advantage for the study of solar energy potential.

A number of research tasks were outlined to calculate rooftop PV potential for the study area. The focus was on an estimation of available roof areas that are solar efficient and suitable for installing PV systems. In order to do this, it was first necessary to identify a set of sample buildings for which to digitize rooftops. These selected rooftops were then digitized using the information from aerial map for roof pattern and building outlines, and housing typologies analysis for building height and roof pitch. Solar simulation function in Ecotect software was utilized to identify the solar efficient roof area and annual average solar radiation. The variables obtained from the distribution of roof area were used for statistical analysis to calculate total roof area per person and solar efficient roof area per person. The equation built in this study by combining two existing equations was used to calculate solar PV potential per person. Finally, the result per person was applied to the entire study area by the number of population.

The development of this study's research design was applied into a model – Rooftop PVGen Model, based on this study's developed workflow to combine the process of computer-simulation, PV modelling and mapping incoming solar radiation data. Figure 3-7 displays the flowchart of Rooftops PVGen Model which outlines the research design for Case Study 1. The following step-by-step methodology developed for Rooftop PVGen Model was also discussed in details.

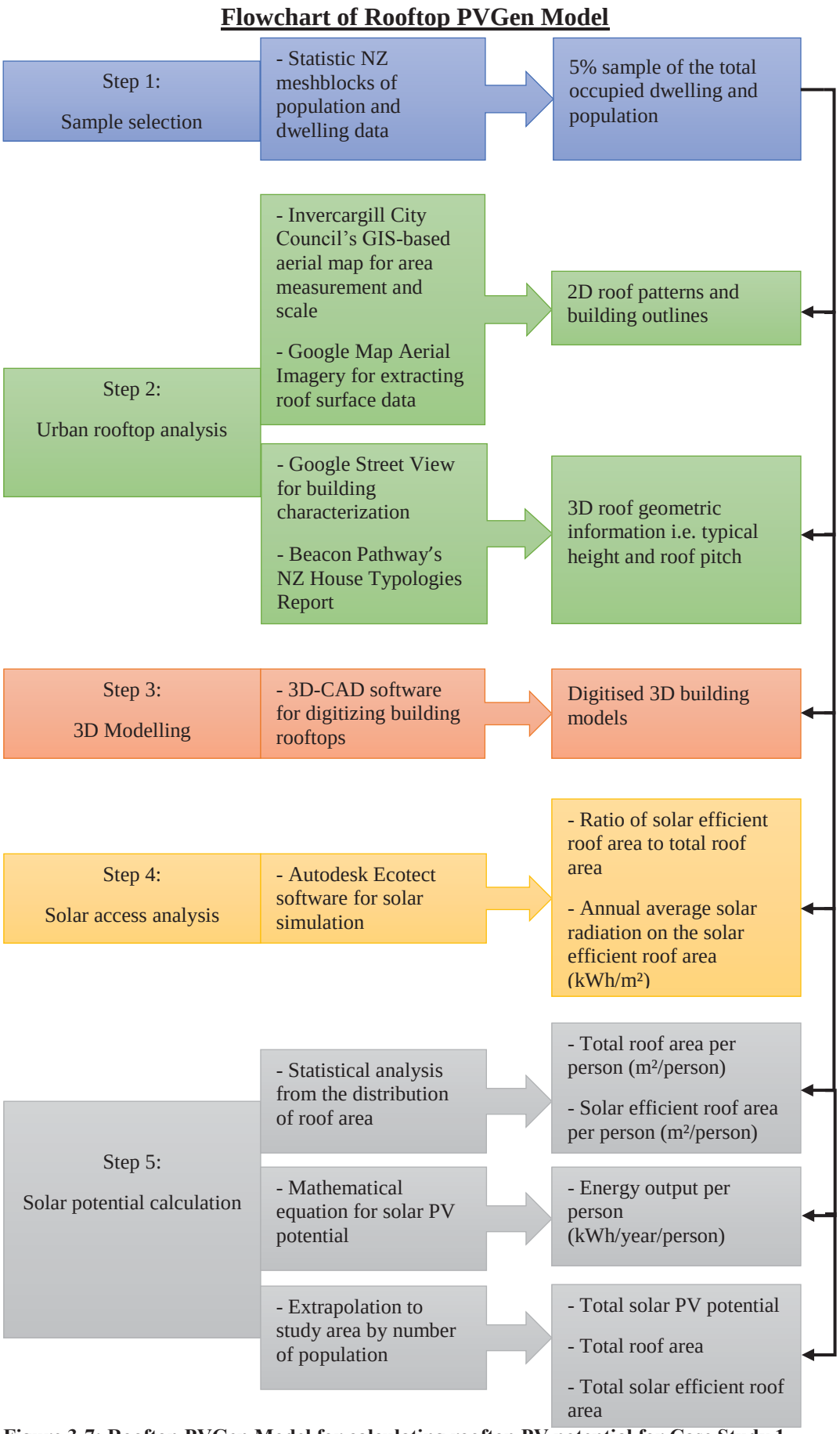

Figure 3-7: Rooftop PVGen Model for calculating rooftop PV potential for Case Study 1

Step by Step Details of Tasks Outlined in Rooftop PV Gen Model

Step 1 - Sample selection

- **Statistic New Zealand meshblocks – census map of population and dwelling data**: This is the smallest unit of census subdivisions. The typical residential building samples of the city were selected to represent the common building typologies in the urban context. The 5% sample size of the representative area was selected from the number of dwellings and the population counts in the meshblocks of the Statistic New Zealand census data. The ratio of resident population and buildings (number of people in occupied dwellings/unit area) was obtained from each geographical area unit in the Invercargill City census map. Figure 3-8a and Figure 3-8b display the geographical area units and meshblocks for the study area.

- **Sample size:** The size of 5% sample was selected to create an appropriate sample size for this study. It was determined that of all 17,706 occupied dwellings, a 5% sample size (or 885 buildings) would be feasible to digitize within this study's timeframe. Each representative meshblock was selected based on the number of occupied dwellings to match the number of required 5% sample size calculated for each area unit. In some area units with less occupied dwellings in each meshblock, two meshblocks were selected to make up the exact number of the required occupied dwellings.

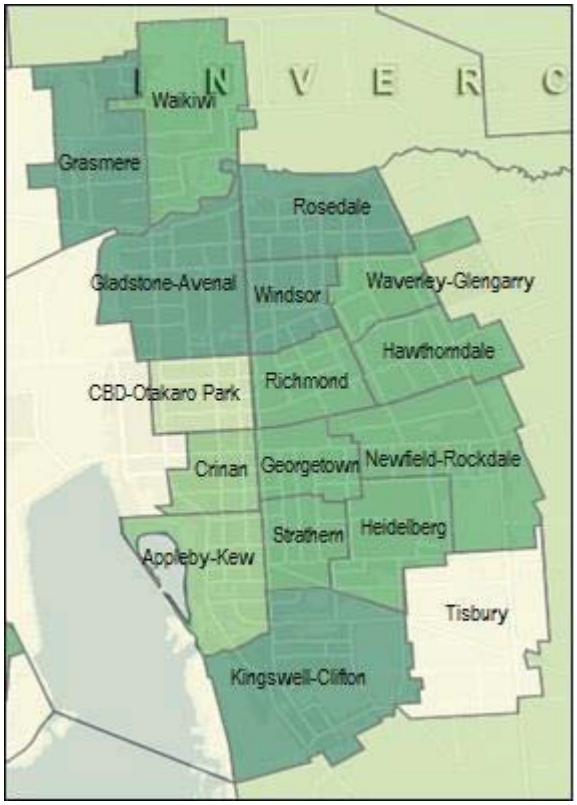

Figure 3-8a: Invercargill City suburbs and boundary as defined in the geographical area unit of Statistic New Zealand census data (Source: Statistic New Zealand, 2013)

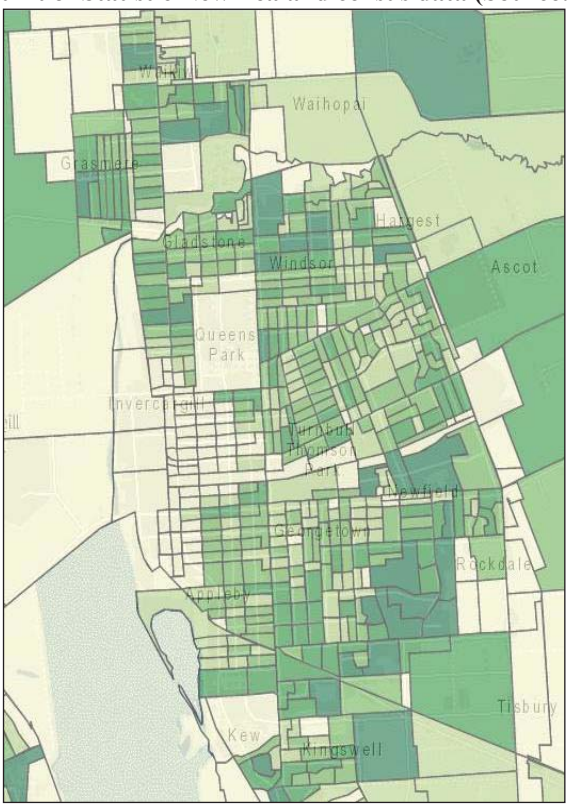

Figure 3-8b: Invercargill City meshblocks in the geographical area unit representing the Statistic New Zealand census data of population and dwelling counts (Source: Statistic New Zealand, 2013)

Step 2 – Urban rooftop analysis

- **Invercargill City Council's GIS-based aerial map**: Based on the layers of Invercargill properties boundaries. The GIS-based aerial map has operational map layers showing the cadastral-based data concerning property boundaries designated with residential lot sizes and street legends (Figure 3-9). This GIS function provides for the gross land area in relation to the meshblock size to obtain the correct measurement to scale.

- **Google Map Aerial Imagery for extracting roof surface data**: It is important to note that there was no building footprint or rooftop data available in any accessible database for the study area. The Google Map aerial imagery was used as the reference of roof patterns and building outlines. Although Invercargill City Council's GIS based aerial map has better image resolution but Google Map provides three-dimensional display of street view and buildings. The aerial images from the representative sample set were exported and scaled with CAD software i.e. AutoCAD. The 2D outlines of roof pattern were drawn diagrammatically upon the roof surface area of each residential building.

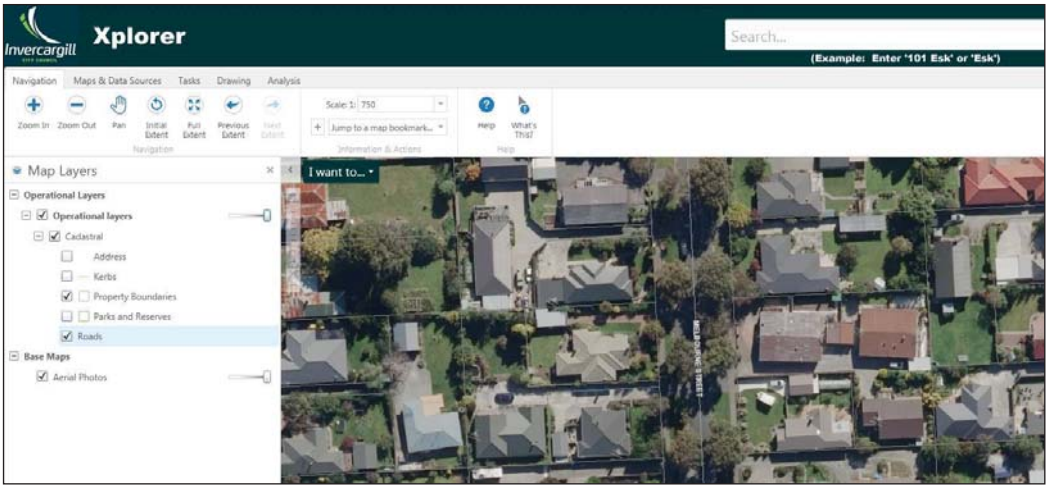

Figure 3-9: Example of available Invercargill City Council's aerial map with GIS-based data layers (Source: Invercargill City Council, 2014)

- **Google Street View for building characterization**: To gain three-dimensional (3D) roof information, the geometric characteristics of building height, roof design and configurations as well as slope segments were determined by the assessment of building types. Based on their prevalence of component

characteristics shown in 3D visual images from Google Street View, each building was characterized according to description of era and construction types of New Zealand house typologies reported by Beacon Pathway (Ryan et al, 2008). Building geometric information of each representative house type was obtained to use for digitising rooftop model.

Step 3 – 3D Modelling

- **3D-CAD software for digitizing building rooftops**: The 3D building models located in each selected meshblock were created using the geometric information for each building typology and the visual information obtained from Google Map aerial imagery. Among the factors taken into account for digitizing were orientation, roof structural form and degree of roof inclination angle, typical building height as well as floor plan size where applicable. This is to identify the 3D form of roof area to use for solar access analysis.

Step 4 - Solar access analysis

- **Ecotect software for solar simulation to determine solar efficient roof area**: The digitized 3D models were imported and displayed in the Ecotect software's simulation environment. The study employed the function of the solar simulation tool to perform the assessment of solar radiation incident on roof surface area over a year. The modelled geometric information including roof surface dimensions, orientation towards north, and roof inclination angles in relation to the horizontal planes enabled the solar access analysis to display the distribution and availability of solar radiation on roof surface. The suitability rankings in term of solar harvesting potential were categorized by the level of solar efficiency indicated on each roof.

Step 5 – Solar Potential Calculation

Distribution of roof surface area

- **Total roof surface area**: total roof area and the number of resident population in the sample meshblocks were identified to calculate the total roof surface area per capita (roof area in m^2/person) for each sample set. The relationship between roof area and the number of population was used for extrapolation to estimate total roof surface area for the entire study area.
- **Solar efficient roof area and annual average solar radiation**: the amount of solar efficient roof area (m^2) and annual average solar radiation kWh/m^2/year were obtained from solar access analysis method. The ratio of the solar efficient roof area in relation to the total roof surface area was calculated for each sample set.

Solar PV potential from solar efficient roof area

- **Solar potential calculation using proposed mathematical equation**: From the ratio of solar efficient roof area and the annual average solar radiation obtained from the solar access analysis method, these variables were used for the calculation of solar PV potential by the mathematical equation adopted in this study. By taking into account the ratio of solar efficient areas and the total roof area per capita (roof area in m^2/person), the potential energy output (kWh/year/person) from solar efficient roof area were estimated for each geographical area unit's sample set.

Extrapolation to study area

- **Total solar PV potential of residential rooftops in Invercargill**: The energy output per person in each sample set was extrapolated by multiplying them to the number of population in the entire geographical area unit and the whole study area.

- **Total roof surface area and total solar efficient roof area in Invercargill**: Multiplying the total roof area per-capita and the solar efficient roof area per-capita to the number of population in each geographical area unit for the sum of total roof surface area and total solar efficient roof area of Invercargill City.

3.2.1 Extracting Roof Surface Area

Digital data was not available for Invercargill as there was no existing building footprint or roof print information available from any accessible database. The building roof outlines had to be manually traced from aerial photographs for extracting each surface area and the structural elements for 3D modelling. The process of hand digitizing every rooftop in the study area would be a time-consuming task and it was not a feasible method for a large-scale analysis. Due to time constraints, the methodology proposed was made to employ a statistical analysis by using a sample set of rooftops to extrapolate out to the total set of buildings to characterize the city.

3.2.1.1 Representative Sample Selection

A total of 885 representative samples of residential buildings were selected from the established meshblocks. Each meshblock dataset is a polygon shapefile containing the count of occupied dwellings and the number of people inhabited within each block area. A number of meshblocks are grouped into the larger geographical area units defined by suburban boundaries of the city. The inner city typically comprises of non-residential areas including commercial buildings, hotels, light industrial, and large retail clustered within the CBD. The residential accommodations, agricultural lands, parks and open spaces locate around the periphery of the city. These meshblocks usually contain smaller number of occupied dwellings (between 0-15 dwellings) together with the number of unoccupied dwellings within the area.

The study area was sorted according to the area units within the urban boundary of Invercargill District Plan’s Residential Zone. The non-residential

units were filtered out to identify the number of residential lots to be considered for the analysis. In order to find the appropriate sample meshblock size, a 5% sample size was calculated for each area unit to find a number of sample buildings to digitize. Table 3-1 displays the counts of occupied dwellings with the resulting numbers for the 5% sample size in each area.

Table 3-1: Sample design for digitization

		Occupied Dwellings		Number of People		
Number	**Area unit**	**Census Data**	**Calculated 5% Sample Size**	**Whole area unit census population counts**	**Population counts in chosen meshblocks**	**Selected Meshblock ID**
1	Grasmere	1353	68	3357	168	3101500, 3102500
2	Waikiwi	942	47	2490	144	3103500
3	Gladstone-Avenal	1524	76	3657	180	3118700, 3118800
4	Rosedale	1533	77	3828	198	3121000, 312000
5	Windsor	1479	74	3051	144	3125500, 3125600
6	Waverley-Glengarry	969	48	2289	120	3131400, 3131500
7	CBD-Otakaro Park	315	16	693	30	3106600
8	Richmond	1230	62	2787	138	3137400, 3128300
9	Hawthorndale	909	45	2244	111	3134200
10	Crinan	798	40	1752	96	3111600, 3109900
11	Georgetown	951	48	2289	102	3142800, 3144100
12	Newfield-Rockdale	1188	59	2907	135	3140300, 3142200
13	Appleby-Kew	795	40	1914	75	3113700
14	Strathern	1029	51	2409	120	3149000, 3149400
15	Heidelberg	1194	60	3216	156	3147400
16	Kingswell-Clifton	1395	70	3381	189	3153403, 3152301
17	Tisbury	102	5	288	21	3154000
	Total	**17706**	**885**	**42552**	**2127**	
	%	**(885/17706)x100% = 5%**		**(2127/42552)x100% = 5%**		

In each area unit, a meshblock that contained the matching number of occupied dwellings with the determined sample size was chosen. Buildings in these meshblock were used to digitize as the representative samples. In some area, two

meshblocks in a suburban unit were required to make up the exact number of the determined 5% sample size. These meshblocks contained the residential house types and ranged from different population densities near the city centre to the outer suburbs. The resident population data in these selected meshblocks are also shown in Table 3-1.

3.2.1.2 Building Characterization - Representative Building Typology

This study targeted to analyse the buildings with a residential function as classified in the residential zone within the urban boundary of Invercargill City. In order to provide for the indication of the housing characters that dominates Invercargill housing stock, the residential buildings are assigned into broad categories relating to the prevalence and incidence of building component characteristics. The most common type is the separate/detached house group which accounts for 89.4% of the total dwellings (Statistics New Zealand, 2013). The variability in these houses' physical characteristics are indicative of different eras of construction types that reflects the changes in parameters of building height, roof system and typical house sizes in each building typology. This analysis is carried out to determine the information of "typical" building and roof structures to ensure the digitized building models of sample building types are the representative of the housing stock in the study area. Table 3-2 summarizes the main characters of different New Zealand house typologies to provide for key information for analysing each representative house type.

Table 3-2: New Zealand house typologies summary (source: Ryan et al, 2008)

Building Typologies	Main Characteristics							Location
	Era/ Age	General Description	House Form	Roof System		Stud Height (m)	Typical Plan Size (m^2)	
				Roof Type	Pitched (Degree)			
Early Housing	Pre-1890	Timber frame/Pre industrial standard	Single square verandas	Gable/ Metal	30-45	2.4-3.0	80	Early settlement area
Villa	1880-1920	High pitch/Large cavity roof	Simple square	Gable/ Iron	30	3.0-3.6		Wealthy new area, villa suburbs
Bungalow	1920-1930/ 1940	Simple plan/English cottage style	L or T shaped porches	Gable/ Hipped over porches	24-27	2.8		Margin of villa suburb
Art Deco	1925-1935	Stucco featuring flat roof	Curved	Mono-pitched/ Flat	<15	2.8	<110	Small fraction scattered around
State House	1930-1970	Wooden cladding/Brick/Mass housing	Simple square	Hipped	30	2.7	<100 about 87	Edge of cities in groupings
Multi-Unit Housing	1960s	Sausage flats/ Limited construction details	Rectangular	Skillion	<20	2.4		Older inner city suburbs
70s House	1970-1978	Pre-insulation/Variation in styles	Simple rectangular	Plain gable/ Skillion	<20	2.4		Large developer subdivision
80s House	1978-1989	Beazley Box/Large suburban house	Rectangular L shape	Plain gable/ Iron	<20	2.4		Developer subdivision
Early 90s	1990-1996	Pre-revamped Building Code	Rectangular variable	Low pitched	<20	2.4		Clustered in new suburb
Last Decade	1996-2007	Post-insulation upgrade	Variable	Truss/ Mono-pitched/ Flat	<20	2.4		New housing development

3.2.1.3 3D Modelling – Digitizing Rooftops

The aerial imagery obtained from Invercargill City Council's GIS-based aerial map is utilized as base map containing designated property boundaries. The maps are exported and scaled in AutoCAD software application. The initial data of roof patterns and building layouts are extracted from these images to provide for the size of roof surface to use for the construction of the building rooftop model.

The buildings in the selected meshblocks were digitized using the initial roof pattern data as shown in Figure 3-10. These outlined AutoCAD layer of roof

patterns were used to construct realistic three-dimensional model of buildings, where the geometric dimensions were created from the key characteristic information summarized in each building typology (Table 3-2) together with the visual information obtained for Google Street View. The models of the main building types in each selected meshblock were reassembled to display a representative cross-section of each suburban area of Invercargill City (an example shown in Figure 3-11).

Figure 3-10: Example of digitized roof patterns on the sample set of buildings (Source: Invercargill City Council, 2014)

Figure 3-11: Example of 3D building model of the representative samples in an area unit. Base map sourced from Google Map's aerial image. Each colour of the model indicates different types of housing typology within the selected meshblock.

3.2.2 Solar Access Analysis

The study used the computer-based analysis as a tool to assist in the assessment of incoming solar radiation that can be received on the external surfaces of each roof segment area of the buildings. Autodesk Ecotect analysis software was chosen as the appropriate solar simulation tool for its capability to analyse the variation of solar incidence across the surface, providing a display of the distribution and availability of incoming solar radiation over the entire city block.

The software function of solar access analysis refers to the availability of incident solar radiation which is calculated on the points and surfaces of the input model. Solar radiation calculations use hourly recorded direct and diffuse radiation data from the Invercargill weather file loaded into the system. The latitude and longitude of the site and the selected weather file are the main input parameters for the software to generate the calculations on the correct zone of the site's global position. The remaining conditions required are the associated geometric building information as presented in the structural properties of surface dimensions, orientation towards north, and roof inclination angles in relation to the horizontal planes. The total incident calculations from these input parameters of the digitized buildings taking into account the overshadowing and shading effects from its surrounding parameters, enable the solar access analysis function to reveal parts of the roof that are solar efficient suitable to place solar PV panels for maximum solar collection across the applied surface areas.

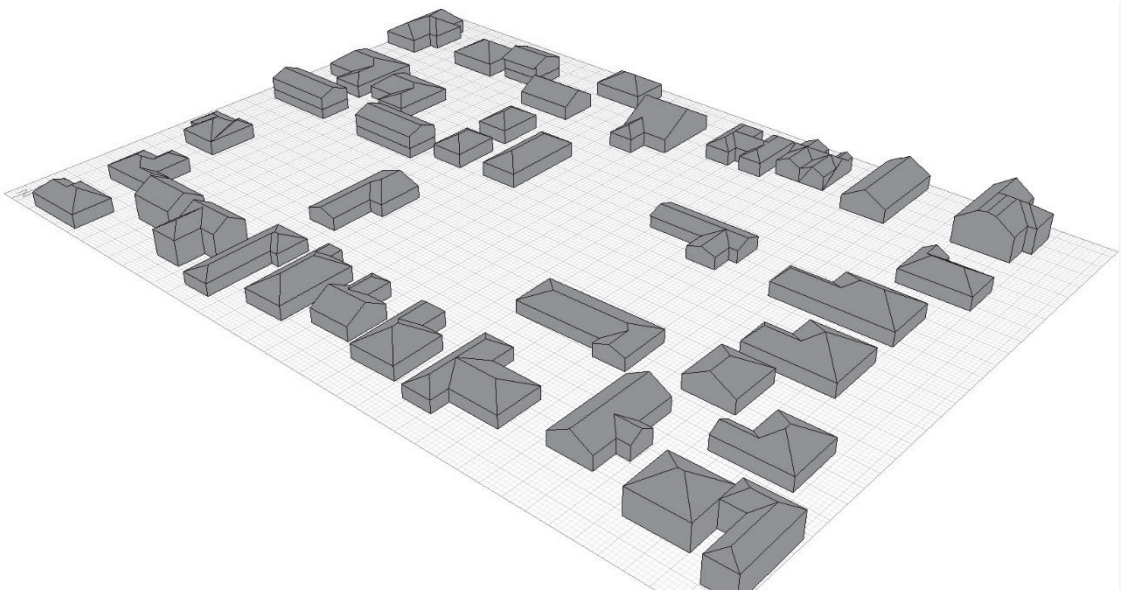

Figure 3-12: Imported model of sample buildings displayed in Ecotect environment

As discussed in the literature review section, Ecotect analysis offers limited choices of only two different sky conditions for daylighting simulations, CIE overcast or uniform sky models. Based on Invercargill's site conditions which have high levels of cloud cover obscuring the sky, the overcast sky model is appropriate representation to select for this assessment. Ecotect uses a geometric version of the split flux method which incorporated the relationship between sky components with the external and internal reflected components for calculating daylight factor (Reinhart, 2012). The measure of sky illuminance where the relative angle of particular sky patch makes with the surface angle, ultimately determines the proportion ratio of daylight level exposed on the point of surface.

Ecotect calculates overshadowing impact from surrounded adjacent buildings by using the shading masks generated from the inter-zonal adjacency on the sun-path diagram of the specified global position to reveal the surfaces under shadow over the selected time period. The projected shading area represents the ratio of shade measured by the analysed number of rays that hit other objects in the model compared to the total number of rays in the section. When the overshadowing accuracy function is set to the highest level, more rays would be generated to achieve the highest shadow precision. The degree of azimuth and altitude relates

to the number of sky subdivisions where the sky dome is divided up over the entire surface. The smaller the subdivisions means increasing sky segments, which ultimately refines the shading mask and increases accuracy upon the calculations. However, the higher precision adjustment of input parameters would increase the processing time of the simulation. For this study, the default values were utilized in a number of settings for the practical purpose of maintaining reasonable processing time.

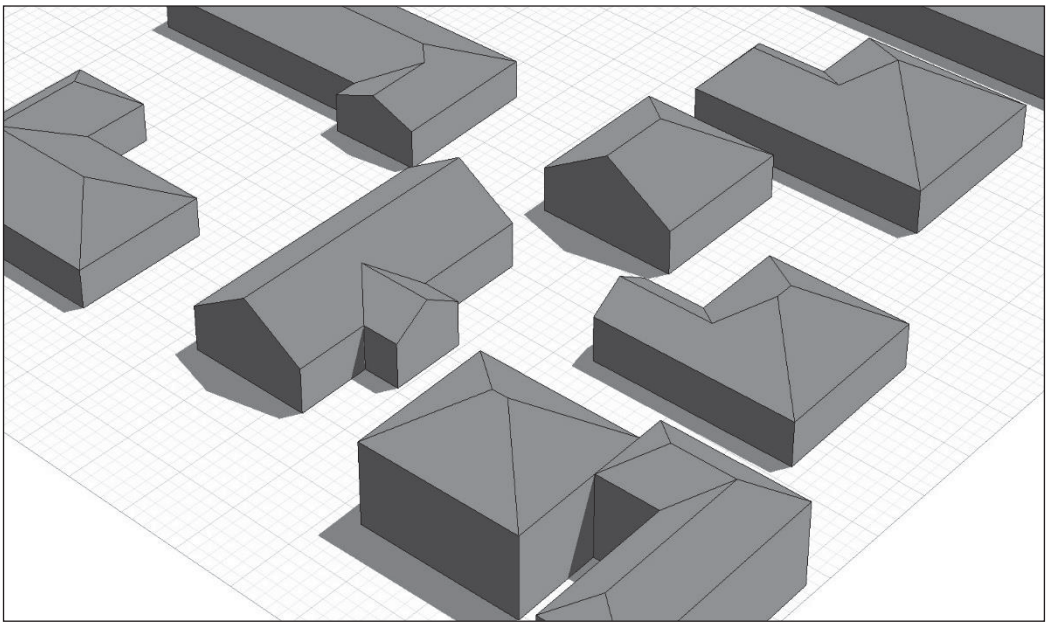

Figure 3-13: Example of overshadowing on the surfaces (shading effects from the surrounding structures)

Ecotect shading simulation displays the numerical summary of solar exposure with the breakdown proportion of each solar radiation component. Some area may include the effects of ground reflected radiation which would be particularly significant for the highly detailed ground surface terrain geometry. Where Ecotect assumes the reflectivity values of 0.2 for the ground surface calculations, the geometric overshadowing, reflective effects and available radiation calculated each day separately within one month can take 30 times longer simulation times. Since the terrain parameter in this study was assumed to be minimal due to the flatness of Invercargill City within Southland plain, the option of ground reflection was left as a default value.

From the imported model, Ecotect identified each surface plane as one object according to the default resolution obtained from the digitized model object attribute. For the analysis purpose to determine the most accurate result, these surface planes were set to be divided into smaller grids of rectangular tiles. Based on the standard size solar panel of 800x1600mm or about 3.7 m², as such, the size of surface subdivisions was appointed by the resolution of 2mx2m setting according to the size of rectilinear PV array. Figure 3-14a and Figure 3-14b show examples of simulation results where the surface subdivisions were applied onto the building models.

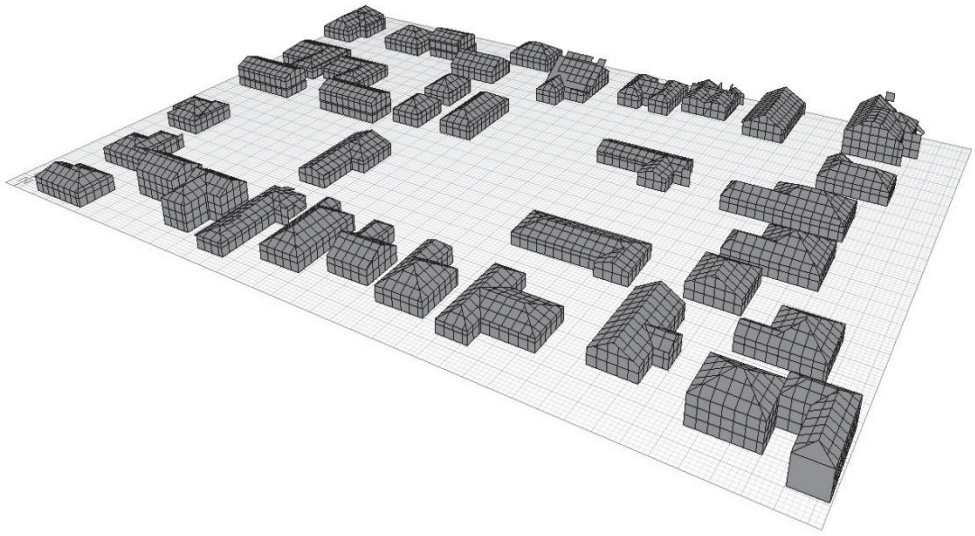

Figure 3-14a: Example of 2mx2m surface subdivisions applied to the building models before solar simulation

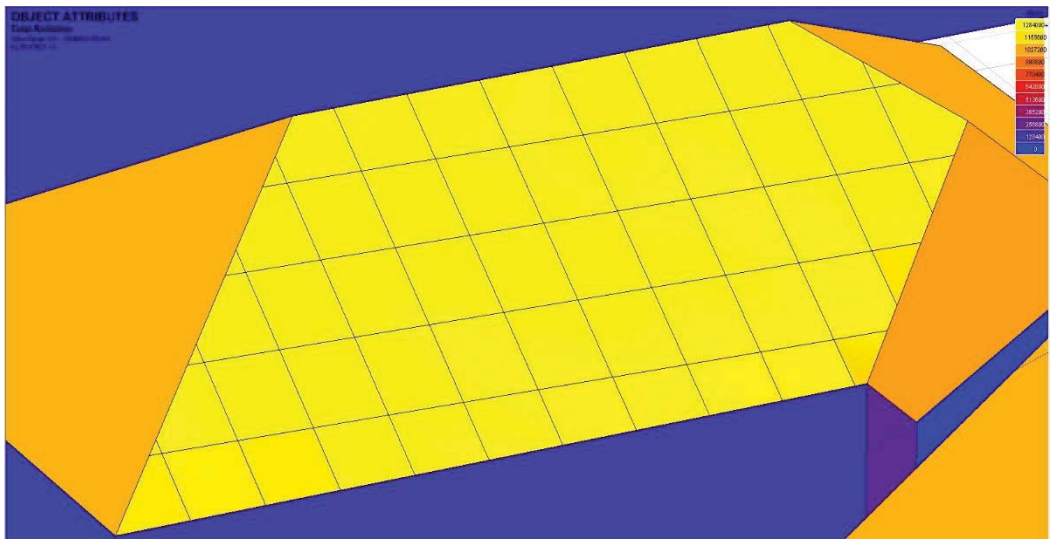

Figure 3-14b: Result of solar simulation on the 2mx2m surface subdivisions on rooftop

Computer processing time increased greatly with higher resolution due to surfaces being subdivided. The processing time for 10 hours was increased for solar simulation of each building model. Higher processing capacity tools would be required in order to achieve such level of resolution. The initial trial result showed only a slight variation between each tile where the amount of insolation obtained within the highest range values was the same as before applying the surface subdivisions. As such, the decision was made to run the analysis using the default value in this parameter for practical purposes of maintaining computational processing time. Table 3-3 summarises the input parameters for Ecotect solar access analysis settings in this study.

Table 3-3: Summary of input parameters for Invercargill solar analysis settings in Ecotect

Input	Description	Value
Terrain	Ground surface elevation geometry	Default horizontal flat surface of analysis plane
Building geometry	Import digitized buildings model from 3D-CAD	Automatic input parameters as digitized
Orientation	Aspect of building surfaces in relative site context direction toward the sun.	Automatic input parameters as digitized model locations
Latitude Longitude	Global position of Invercargill	46° 42'
Weather data	Invercargill climatic data downloaded in Ecotect	As recorded
Calculation period	Time period selected for calculating solar radiation	all year
Sky type	Choices of sky model representing the sky conditions used to calculate the distribution of incoming diffuse radiation to the surface.	Overcast sky
Surface subdivisions	Resolution size of each surface plane to be analyzed e.g. size of tiles across the surfaces.	Default
Azimuth Divisions	Size of sky segments subdivisions of sky dome to be calculated for each zenith angle. The lower degree (minimum value 2°) increases the accuracy given a more refined shading mask.	5°
Altitude Divisions	Sizes of sky segments subdivisions of sky dome. Each altitude band has certain number of azimuth segments.	5°
Overshadowing Accuracy	Adjustment for the calculation of overshadowing masks level of precision, the higher settings the more rays are generated.	High
Diffuse proportion	The solar exposure component with the choice of ground reflection or direct light only which ignoring all diffuse and reflected radiation.	Ground Reflection – default value
Calculated data	The option of how the analysis values will be totaled up from the choice of cumulative, average daily or peak values.	Cumulative values

Figure 3-15a and Figure 3-15b display the examples of incoming solar radiation analysed over the selected one-year period. The variations of the amount of solar radiation reaching the surface are visualized by colour gradients. The highest range of value above 1,148,000 Wh/m² outputs displayed in yellow indicates parts of the roof that were receiving maximum range of annual solar insolation across the entire surface.

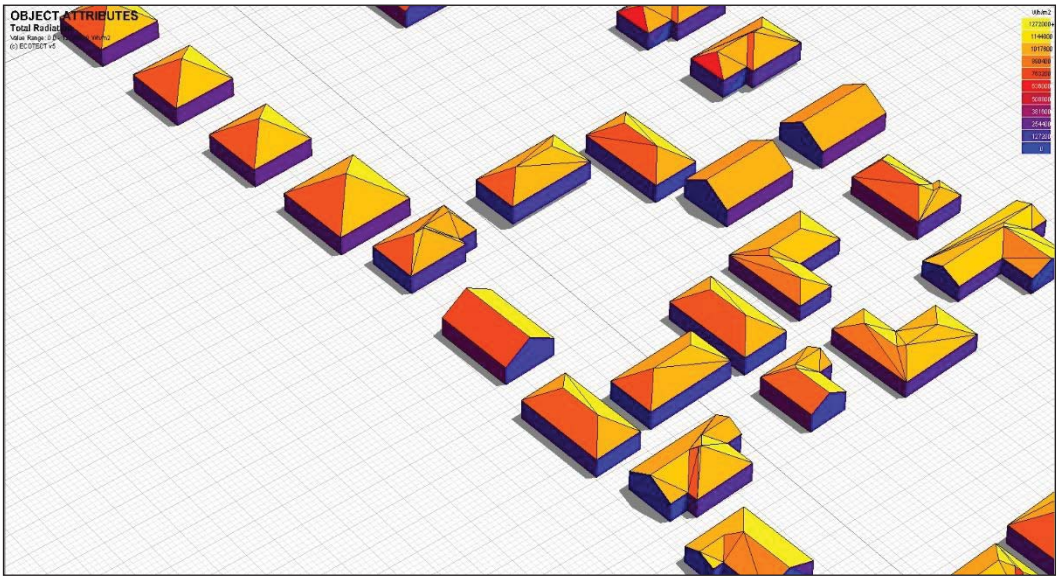

Figure 3-15a: Display of incoming solar radiation on roof surfaces

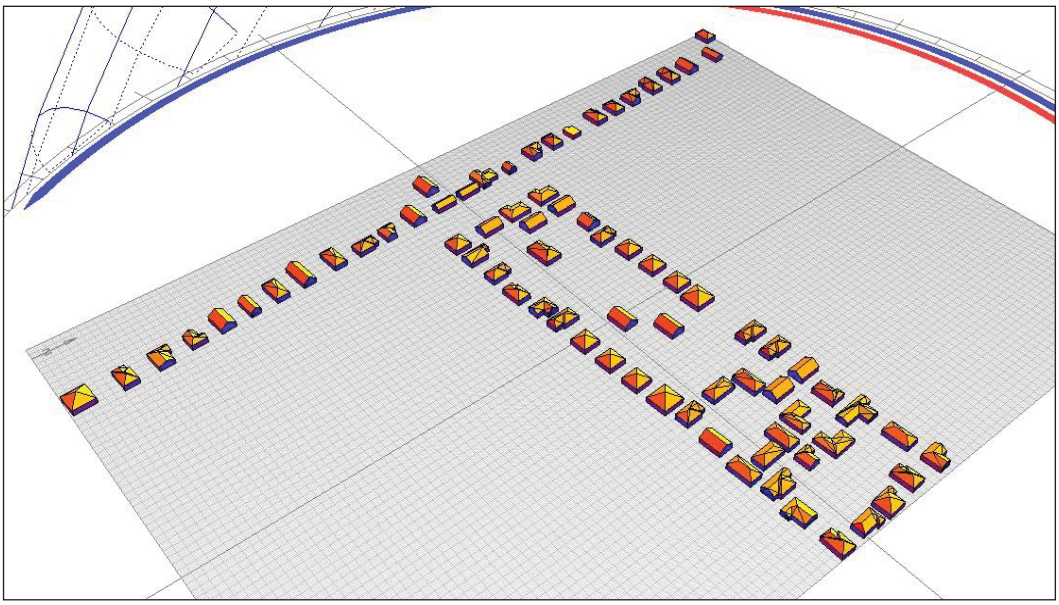

Figure 3-15b: Display of incoming solar radiation across the entire surfaces of the sample city blocks

3.2.3 Determining Solar Efficient Roof Area

Once the sample building models were analysed for solar radiation through the simulation process in Ecotect, the solar efficient area were identified by the area of highest range of solar radiation. The simulations were repeated for each separated suburb model. The findings were later compiled to obtain the result for calculating the total solar efficient roof area in order to find the ratio of solar efficient roof area in relation to the total roof surface area in each suburb.

In order to extract the amount of highest potential roof area from the variation of each graphical output, the numerical summary table containing the text field of value for all visible objects in the model was utilized (Figure 3-16). The solar simulation output also showed that the highest solar radiation area appeared on the northern parts of the roof. Based on the factor of building orientation, other roof aspects received relatively less amount of solar radiation reaching the surface. It was also shown that building walls received less amount of solar radiation comparing to roof surfaces. Ecotect simulations analysed every surface of each building. The data was manually cleansed to remove all wall surfaces and roof surfaces that were inefficient for solar generation i.e. south facing roofs. The modified data was selected from the highest value range. Figure 3-15 outlines the numeric surface area data and total radiation for every individual object in the model accordingly.

Report: Object Attributes - All							
Description: Lists attributes of objects in model.							
Model:	Grasmere						
Object Attributes							
Object ID	**Object Type**	**Orient. (°)**	**Tilt (°)**	**Area (m2)**	**Total Radiation Wh/m2**	**Direct Radiation Wh/m2**	**Diffuse Radiation Wh/m2**
0	Wall	176.61	0	3.2	92073.086	2281.772	89791.312
1	Wall	86.61	0	4.8	207193.297	94953.68	112239.617
2	Wall	176.61	0	14.4	80570.398	2002.96	78567.438
3	Wall	-93.39	0	12	221749.922	92674.711	129075.211
4	Wall	-3.39	0	17.6	425538.344	257180.578	168357.766
5	Wall	86.61	0	7.2	128814.312	44635.426	84178.883
6	Floor	176.61	-90	4.5	112239.617	0	112239.617
7	Ceiling	86.61	90	4.5	1161058	594249.312	566808.75
8	Ceiling	-3.39	63	8.488	1269217.875	741188.438	528029.438
9	Ceiling	-3.39	63	16.975	1239304.625	728110.438	511194.219
10	Ceiling	-93.39	63	0.281	1031014.625	508601.812	522412.812
11	Ceiling	-93.39	63	20.202	994416.188	488836.781	505579.406
12	Ceiling	-93.39	63	8.873	994241.375	488661.969	505579.406
13	Ceiling	-93.39	63	0.912	1044614.875	516584.344	528030.5
14	Ceiling	-93.39	63	3.858	992093.188	486513.906	505579.281
15	Wall	176.61	0	9.075	111305.555	4678.111	106627.445

Figure 3-16: Microsoft Excel numerical list of individual object area and total radiation received on each surface (roof areas are shown as ceiling in the object type list due to the software default setting)

In this case, roof surfaces with highest total radiation values in the range between 1,144,800 Wh/ m² to the maximum (approximately 1,263,000 + depending on the maximum value of each suburb model) were isolated from the list by data processing techniques in Microsoft Excel to quantify the net efficient solar potential roof area available for PV installation. The total amount of solar radiation received on these surfaces was also retrieved from this data to find the average value which was needed as a variable input for solar potential calculation.

Table 3-4: Summary of output data obtained from Ecotect simulation by each suburb samples

From each suburb sample set	**Unit**
Total solar radiation available from this block's sample buildings	Wh/m²/year
Annual average solar radiation of solar efficient roof surfaces	Wh/ m²/year
Net areas of solar efficient roof surfaces	m²
Gross rooftop surface areas of buildings	m²

3.2.4 Existing Methods for Calculating PV Potential

The amount of solar radiation received on the surface is the most important factor signifying potential energy from the rooftop. However, other variables that affect the energy outputs are the performance capacity and module efficiency of the PV systems. The study conducted by Amado and Poggi (2014) adopted mathematical equations that included these factors in PV potential calculation. This study adopted the combination of two equations present in the literature review for calculating solar PV potential to apply across the study area.

Equation 2 by Amado and Poggi (2014) was adopted to form a basis for PV output calculation in this study. The equation is consistent with the global formula in its principle technique for calculating annual solar energy output of a PV system. The comparison to show the similarity between Equation 2 (Amado & Poggi, 2014) to Equation 3 (Global PV formula - Photovoltaic-software, 2014) is presented as follows:

Y = Pr x Me x (Gr x A) ..... Equation 2

E = Pr x r x H x A ..... Equation 3

Y = PR x Me x Gr x A	Amado and Poggi (2014) Equation
E = Pr x r x H x A	Comparison to Global formula (Photovoltaic-software, 2014)
Y (E)	= Energy output (kWh).
PR	= Performance Ratio, coefficient for system losses (a default value).
Me (r)	= the yield of solar panel given by the ratio, electrical power of one solar panel divided by the area of one panel (a default value).
Gr (H)	= Global solar radiation (kWh/m²/year) (annual average or total sum of annual solar radiation depends on the analysis).
A	= Total solar panel area (m²).

Both equations calculate an energy output based on the variables of annual average solar radiation (kWh/ m²/year) (Gr in Equation 2; H in Equation 3), the Performance Ratio or the coefficient for system losses (a default value) (Pr in both equations), and solar panel yield (% module efficiency or the ratio of electrical power of one solar panel divided by the area of one panel) (Me in Equation 2; r in Equation 3). Both equations incorporate the distribution of total solar panel area (m²) (A in both equations) to obtain annual energy output (kWh) of a PV system.

According to these related approaches, the main contribution to the PV potential in buildings is the available roof area for PV installation (Izquierdo et al., 2008). MacKay (2009) has adopted the relevance of this factor by assuming a ratio of solar panel covering area of a city to the number of population per unit area (population density - m²/person), in order to evaluate energy potential per person from large-scale PV deployments.

MacKay (2009 in Eltayeb 2013) calculated the potential energy using the following equation.

Energy output/person = Module efficiency x Global solar radiation x (% of solar panel covering area x land area/person) ..... Equation 4

In comparison to the common approach of PV calculation shown in Equation 3 and Equation 4, MacKay's approach does not include the Performance Ratio which is a very important factor that account for all losses in the balance of system independently of the orientation or inclination factor of the panel. However, MacKay's approach in using the contribution of solar panel area and population relationship for large-scale PV potential evaluations was relevant to the purpose of this study. As such, a new equation was proposed by combining the relevant components of both existing Equation 2 and Equation 4. The ratio of solar covering area to total land area per person in Equation 4 was adapted to the ratio of solar efficient roof area to the total roof area per person, in order to obtain

the annual solar PV energy output by solar efficient roof area per capita from the calculation.

3.2.5 Proposed Method for This Case Study

The proposed equation by combining existing formulas is presented as follows:

Energy output/person = (PR x Me) x Annual average solar radiation x (% of solar efficient roof area x total roof area/person)

..... Equation 5

Where Pr is Performance Ratio, Me is nominal module efficiency as shown in Equation 2.

The Performance Ratio of 0.75 is chosen as a default value consistent with the standard commonly utilized by Amado & Poggi (2014) and industry professionals in New Zealand (Photovoltaic-software, 2014). The yield of a typical 1.28 m² solar panel is assumed to be 12% (Byrd, 2010) for the standard panel size of 800x1600mm.

Table 3-5: Summary of related variables for calculating solar PV potential by the proposed equation

From each suburb sample set	**Unit**	**Description**
Annual average solar radiation of solar efficient roof surfaces	kWh/m²/year	Amount of annual solar radiation of every solar efficient roof surfaces calculated by Ecotect analysis summed together and divided by the number to obtain the average.
Ratio of solar efficient roof area	%	Net areas of solar efficient roof surfaces divided by gross rooftop surface areas of buildings from each suburb sample size.
Total roof area per person	m²	Gross rooftop surface areas of buildings from each suburb sample set divided by total number of resident population counts in that sample meshblock.
Performance Ratio		Default value = 0.75
Solar panel yield/ module efficiency		Default value = 12% (=0.12)

The proposed Equation 5 provided the mean to calculate the solar PV potential energy output per year per person for each area unit's sample set. In order to extrapolate the result to the whole study area, each result obtained in kWh/year/person in the sample set was multiplied by the total number of resident population in the area unit (data recorded in Table 3-1), and summed to provide **the amount of total solar PV potential of residential rooftops in Invercargill**.

CHAPTER 4: RESULTS

The method described in Chapter 3 was applied to the housing stock of Invercargill. This chapter presents the results of the previous chapter for determining the solar efficient roof areas and analyse the solar energy potential of residential building rooftops for Invercargill City. The results reported are related to the analysis outcomes from the sample building models being assessed through multiple computer simulation efforts. Various statistical analyses and data processing methods have also been utilized in order to identify the relationships and patterns in the data that can be translated to the whole study area. The most relevant results are displayed and discussed here in detailed.

4.1 Distribution of Roof Surface Area

This study investigated solar energy potential using the three variables of:

- Total rooftop surface area,
- Net solar efficient roof area,
- Annual average amount of solar radiation reaching these solar efficient roof surfaces.

The Ecotect solar simulation methods allow these variables to be obtained from the modelling output reports of object attributes in each sample set. The following details outline the summary of these quantitative output data and solar analysis results for every suburban area unit in the study area.

4.1.1 Total Roof Surface Area

The gross rooftop surface areas were calculated from aerial photos to determine the relationship against the number of resident population in the sample set for the total roof surface area per capita (roof area in m^2/person) to use for extrapolation. Table 4-1 shows the summary of roof geometry and the calculation to indicate these relationships.

Table 4-1: Summary of results – Gross rooftop surface area for total roof area per person

Number	Area unit	Number of sample buildings	Gross rooftop surface area m^2	Average rooftop size (Gross rooftop area/Number of sample buildings) m^2	Population counts in selected sample	**Total roof area per person (Gross rooftop area/Population counts) m^2/person**
1	Grasmere	68	10331.60	151.94	168	**61.50**
2	Waikiwi	47	6575.69	139.91	144	**45.66**
3	Gladstone-Avenal	76	8256.86	108.64	180	**45.87**
4	Rosedale	77	11967.16	155.42	198	**60.44**
5	Windsor	74	10278.28	138.90	144	**71.38**
6	Waverley-Glengarry	48	7796.00	162.42	120	**64.97**
7	CBD-Otakaro Park	16	1375.77	85.99	30	**45.86**
8	Richmond	62	10273.73	165.71	138	**74.45**
9	Hawthorndale	45	7346.12	163.25	111	**66.18**
10	Crinan	40	4734.94	118.37	96	**49.32**
11	Georgetown	48	7220.04	150.42	102	**70.78**
12	Newfield-Rockdale	59	9177.61	155.55	135	**67.98**
13	Appleby-Kew	40	5749.25	143.73	75	**76.66**
14	Strathern	51	8483.04	166.33	120	**70.69**
15	Heidelberg	60	6808.84	113.48	156	**43.65**
16	Kingswell-Clifton	70	9535.56	136.22	189	**50.45**
17	Tisbury	5	869.15	173.83	21	**41.39**

From all residential buildings in each sample set, the values of the average rooftop size in Table 4-1 indicate the data range of residential low-density housing typical to suburban housing stock. This is based on New Zealand's average house size of 149m² (QV New Zealand, 2011). In comparison to these values which vary between suburbs, the smallest house size was found in the CBD. The CBD is typified by higher density housing such as multi-unit building type common in the city area. Larger houses tended to be located in the fringe

areas (Waverley-Glengarry, Richmond, Hawthorndale, Strathern), rural residential area (Tisbury), or in the areas with high proportion of larger modern homes built in new housing developments (Rosedale). Smaller average rooftop sizes (108m²-118m²) are more evident in the outer suburb of older settlement areas of Invercargill that are dominated by older housings. In this case, the findings of gross rooftop area results are consistent with the housing typologies confirming the positive correlation between house age and their size.

Table 4-1 shows the total roof area per person ranges from a minimum of around 41m²/person (Tisbury) to the maximum of 77m²/person (Appleby-Kew). This range was considered a reasonable estimate of roof area per person in New Zealand low density suburban context. The higher area per person was due to the lesser people per household. Despite the increasing average house size by new larger buildings, the average number of people per household is projected to fall from 2.6 to 2.4 people by the year 2006 - 2031(Statistic New Zealand, 2009a). Consistent with the national figure, the value within the urban boundary of Invercargill District Plan's Residential Zone are found to be currently sitting at the lower average of 2.4 people per household (according to 42,552 people per 17,706 dwellings of the study area) given the relatively small population size to the total number of dwellings in this city.

4.1.2 Solar Efficient Roof Area and Average Solar Radiation

North-facing Ecotect solar efficient roof was used to determine how much of gross roof area was solar efficient. Table 4-2 shows the solar modelling results of solar efficient roof surfaces as indicated by areas associated with highest range of total radiation values, along with the annual average solar radiation calculated by data processing of attribute values of these surfaces. The ratio of the net solar efficient roof areas to the gross rooftop were manually determined by visually analyse the Ecotect simulation results. This value was used to calculate the amount of solar PV potential.

Table 4-2: Summary of modelling results – Distribution of solar efficient roof area

Modelling results of each suburb's sample set obtained from solar access analysis - Ecotect Simulation Highest radiation range (min. to max. of the range) kWh/m²/year	Net efficient area m²	Ratio (Net efficient area /gross roof area)	Average radiation kWh/m²/year
Grasmere (1182.66 - 1271.15) 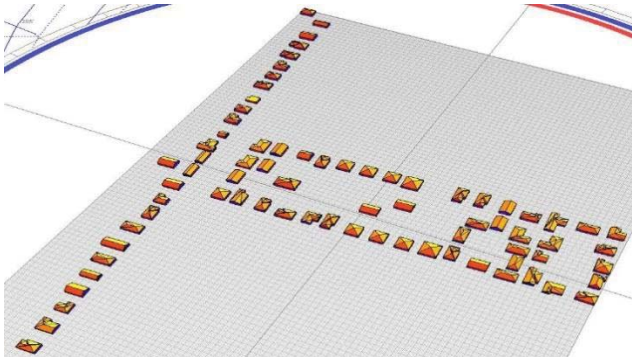	2744.94	**26.57%**	**1234.34**
Waikiwi (1158.44 – 1285.40) 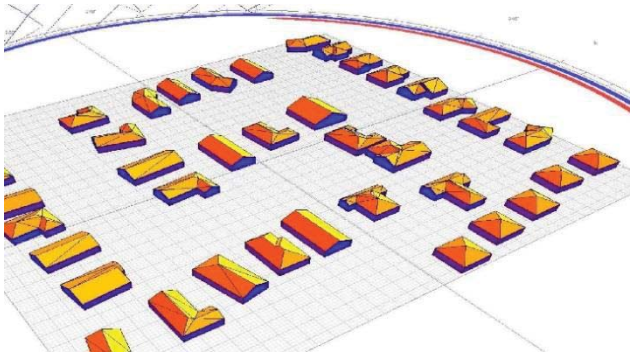	1649.70	**25.09%**	**1247.67**
Gladstone-Avenal (1164.21 - 1262.11) 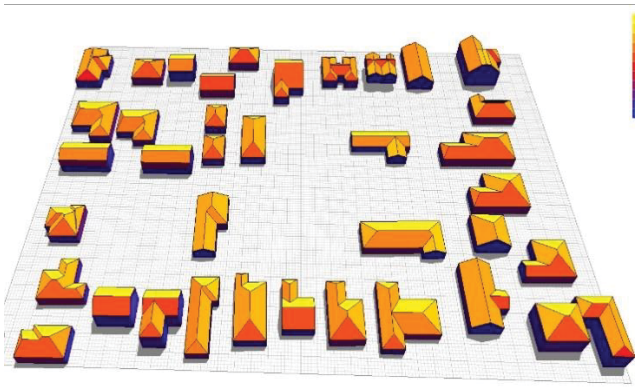	2159.95	**26.16%**	**1247.00**

Rosedale(1176.65 - 1289.65) 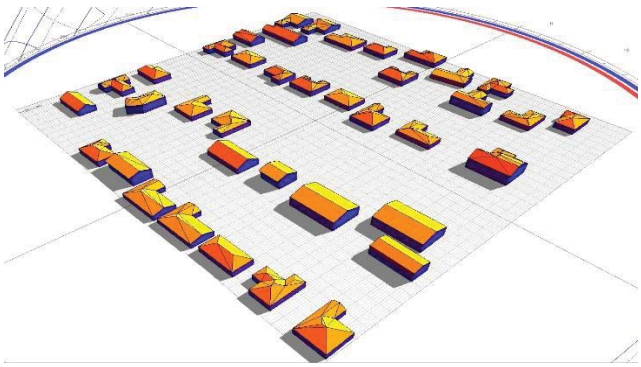	3677.28	**30.73%**	**1260.61**
Windsor (1194.67 - 1268.09) 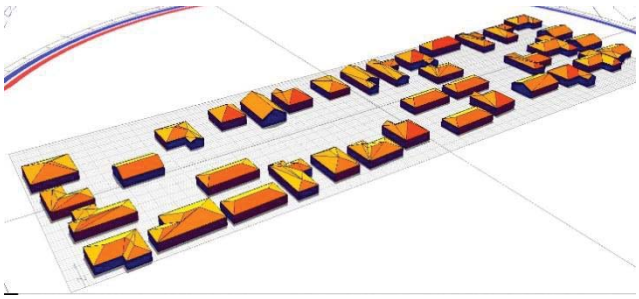	2287.70	**22.26%**	**1237.00**
Waverley-Glengarry (1167.58 - 1276.00) 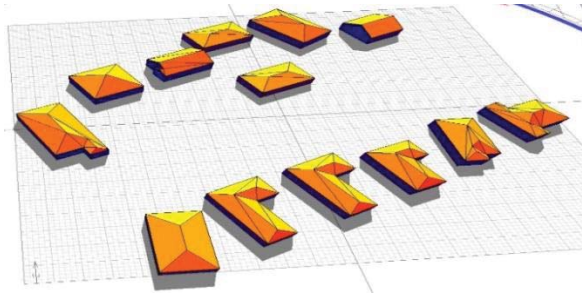	2528.79	**32.44%**	**1225.15**
CBD-Otakaro Park (1218.24 - 1271.12) 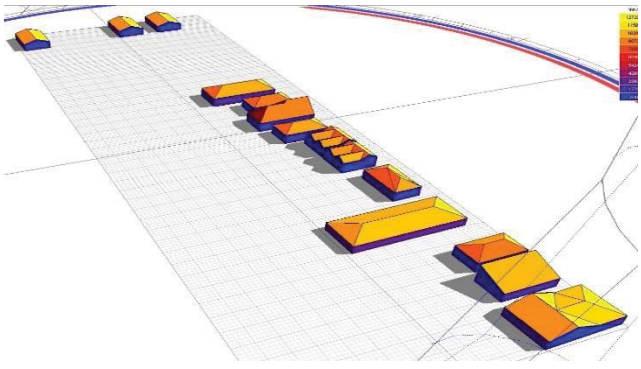	338.44	**24.60%**	**1259.53**

Richmond (1164.92 - 1265.93) 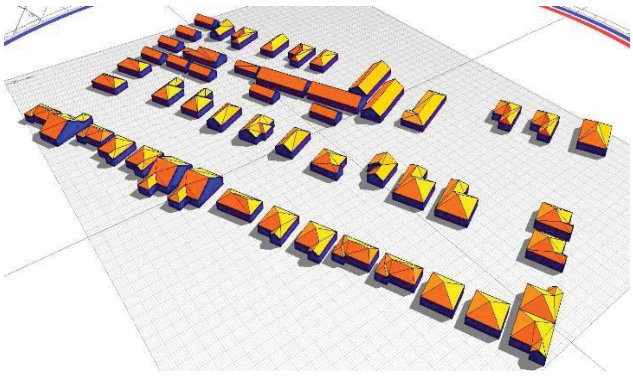	3811.77	**37.10%**	**1223.09**
Hawthorndale (1181.46 - 1269.14) 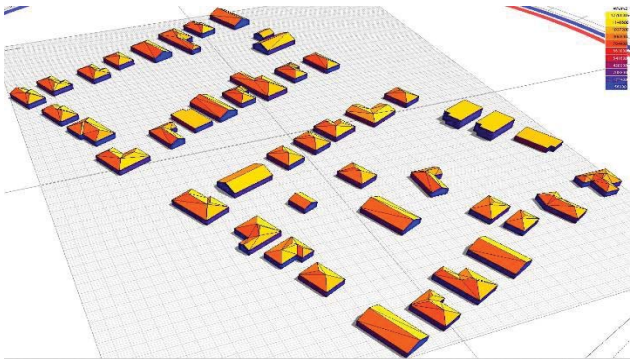	2431.47	**33.10%**	**1221.16**
Crinan (1239.56 - 1282.10) 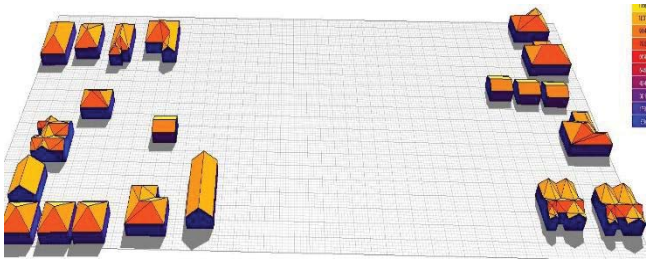	1138.94	**24.05%**	**1262.29**
Georgetown (1210.19 - 1289.49) 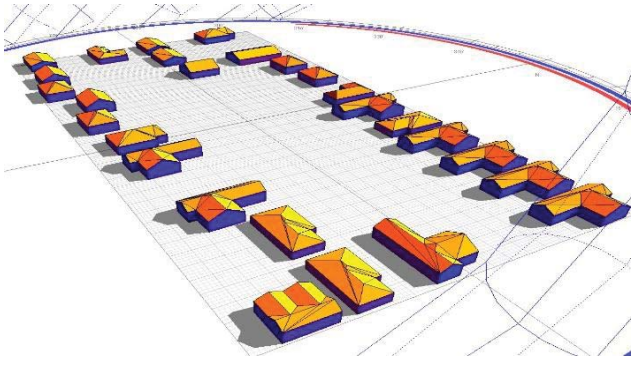	1732.34	**23.99%**	**1260.11**

Newfield-Rockdale (1198.41 - 1289.60) 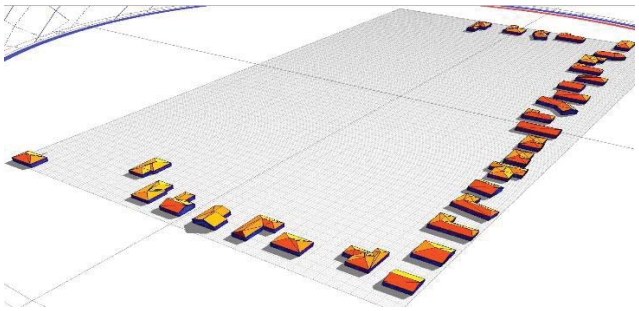	2775.27	**30.24%**	**1262.30**
Appleby-Kew (1219.94 - 1289.45) 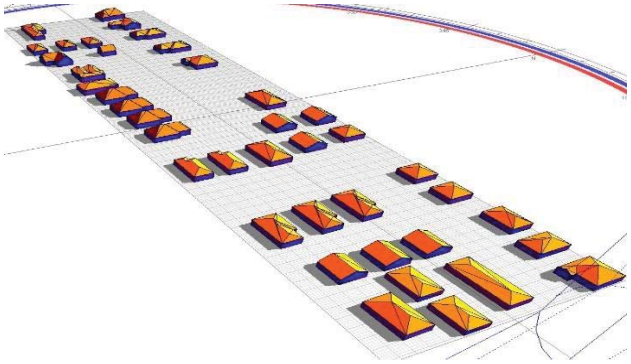	1789.75	**31.13%**	**1262.78**
Strathern (1206.27 - 1283.61) 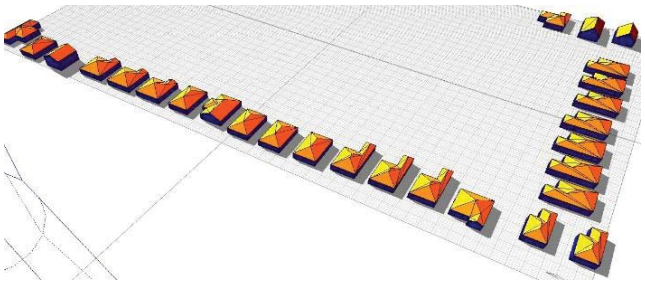	2464.02	**29.05%**	**1256.94**
Heidelberg (1173.38 - 1289.63) 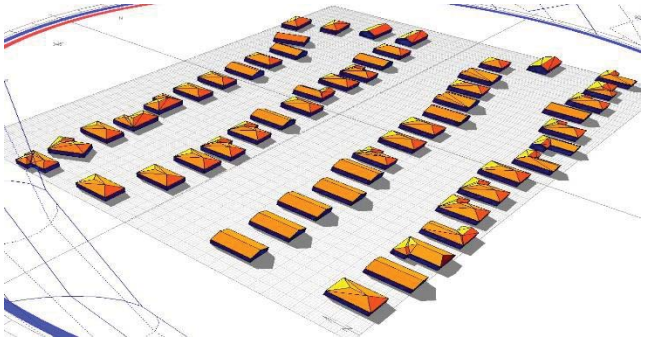	1272.67	**18.69%**	**1265.94**

Kingswell-Clifton (1194.45 - 1269.24) 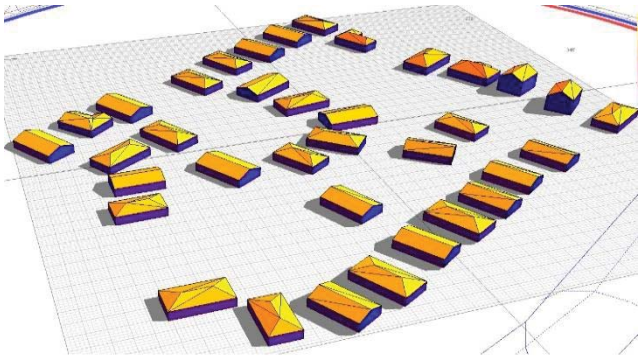	3786.42	**39.71%**	**1233.10**
Tisbury (1185.64 - 1283.07) 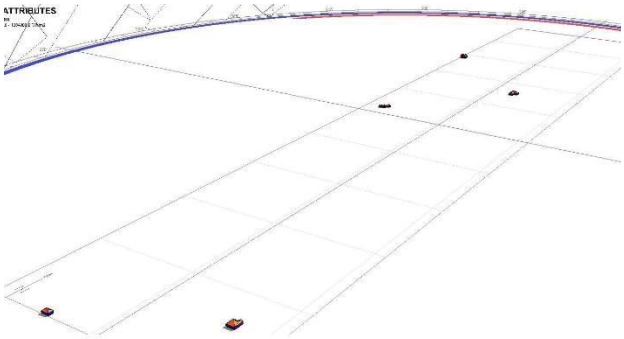	258.70	**24.80%**	**1239.39**

The results in Table 4-2 show that the annual average incoming solar radiations are relatively consistent across all suburbs. Each value lies within a close interval of expected range between 1221.16 – 1265.94 kWh/m²/year. This range agrees well with the solar radiation data report from NIWA (Figure 3-5 in previous chapter) showing Invercargill with daily average solar radiation of 3.33 – 3.61 kWh/m²/day which equals to annually 1216.67 – 1318.05 kWh/m²/year. Since the factors affecting total radiation value are corresponding with the prevalence of buildings in terms of positioning in shading and aspect, together with orientation and roof tilt angle. Nevertheless, the results of higher average solar radiation value in certain sites are mainly due to the higher proportion of solar appropriate roof space available in a favourable position and suitable roof angle for capturing higher amounts of direct sunlight.

In order to capture maximum capacity of solar radiation, the optimum inclination angle of the roof was calculated based on the site's latitude. For Invercargill's latitude of 46° 42', the best fixed tilt angle for gaining maximum insolation for the whole year basis would be 46 degree. The optimum efficiency of the inclination angle varies for different times of the year. Nevertheless, the solar access analysis have shown the north facing fraction of roof area within the inclined range close to the latitude to be most solar efficient. Roof tilt angles of the models that are outside these indicative figures have been identified as less optimum area for solar collection.

The suburbs Rosedale, Newfield-Rockdale and Appleby-Kew, all showed a high value in both radiation range as well as reasonable percentage of solar efficient area due to the majority of north facing aspect of buildings in these blocks. The suburbs Crinan, Georgetown, and Heidelberg, each also maintained an average value of over 1260 kWh/m²/year with the maximum value in their highest radiation range reaching above 1289 kWh/m²/year. It appears that these samples are north facing blocks containing certain parts of the roof that have access to maximum amount of sunlight despite their relatively low percentage of these solar efficient roof areas.

Considering the solar efficient roof areas are most significant for their contribution to the amount of PV potential due to the availability of roof area for the size of PV application. The ratio of the net solar efficient roof areas must be determined as the fractional coefficients to multiply the total roof area for the most appropriate estimates of solar efficient roof area available per person based on this data. From the solar simulation results, the figures obtained show that most suburbs obtained the solar efficient area in the close range between 22.26% - 30.73% of total roof area. This range is consistent with the estimated values of roof area reductions as reported in other literature such as Ghosh and Vale (2006) with 22%, 30% and 47% estimated from GIS software by five residential blocks in New Zealand.

The results also presented some relatively high values shown in Waverley-Glengarry, Richmond, and Hawthorndale with 32.44%, 33.10% and 37.10% respectively. This suggested that high solar efficient roof fractions consistently occurred in the north-west facing sample blocks. Kinswell-Clifton showed an exceptionally high value of 39.71% efficient areas due to the north-east facing aspect. The prevalence of these building aspect indicates that both north-east and north-west roof surfaces are able to gain access from the sun, despite the lower irradiation (around 1221.16 – 1233.10 kWh/m²/year) when comparing to the blocks containing large availability of roofs with true north facing orientation. Contrastingly, an interesting result occurs in Heidelberg which displayed the lowest fraction of 18.69%. This is due to the majority of buildings in this sample block are generally facing east, meaning they only possess small parts of the roof that are exposed to north.

4.2 Solar PV Potential from Solar Efficient Roof Area

4.2.1 Solar Potential Calculation by Proposed Equation

Finally, the calculation for the amount of solar PV potential from solar efficient residential rooftops in Invercargill was obtained. Using the data presented in Table 4-1 and Table 4-2 as the variables to apply for the solar PV potential equation described in the methodology. According Equation 5, first, the total roof area per person must be reduced to see the amount of solar efficient areas per person. The data were then used to calculate the potential PV outputs according to the annual average radiation by this distribution of roof area taking into account the performance ratio and the module efficiency of PV system. The results for each sample set are presented in Table 4-3.

4.2.2 Total Solar PV Potential of Residential Rooftops in Invercargill

Next, the energy output per person in each sample set is extrapolated by multiplying them to the population data available for the entire suburb and the

whole study area. Giving the capable value of maximum solar potential energy that can be made available throughout the residential urban area of the city.

Table 4-3: Calculation of solar PV energy potential by the proposed equation: Energy output/person = (PR x Me) x Annual average solar radiation x (% of solar efficient roof area x total roof area/person), PR = 0.75, Me = 0.12.

Number	Area unit	Solar efficient roof area per person (m^2) (% of solar efficient roof area x total roof area/person)	Energy output per person kWh/yr/person	Total solar PV potential kWh/year
1	Grasmere	**16.34**	**1815.10**	**6093295.33**
2	Waikiwi	**11.46**	**1286.43**	**3203200.12**
3	Gladstone-Avenal	**12.00**	**1346.73**	**4924987.31**
4	Rosedale	**18.57**	**2107.10**	**8065971.74**
5	Windsor	**15.89**	**1768.68**	**5396236.77**
6	Waverley-Glengarry	**21.07**	**2323.61**	**5318743.98**
7	CBD-Otakaro Park	**11.28**	**1278.83**	**886226.42**
8	Richmond	**27.62**	**3040.52**	**8473942.15**
9	Hawthorndale	**21.91**	**2407.47**	**5402364.33**
10	Crinan	**11.86**	**1347.82**	**2361377.20**
11	Georgetown	**16.98**	**1926.12**	**4408894.65**
12	Newfield-Rockdale	**20.56**	**2335.48**	**6789246.80**
13	Appleby-Kew	**23.86**	**2712.07**	**5190906.97**
14	Strathern	**20.53**	**2322.84**	**5595731.13**
15	Heidelberg	**8.16**	**929.49**	**2989254.42**
16	Kingswell-Clifton	**20.03**	**2223.35**	**7517145.55**
17	Tisbury	**10.27**	**1145.11**	**329791.06**
Total solar PV potential of residential rooftops in Invercargill urban area				**82,947,315**

The primary purpose of this study was to construct a solar simulation model using available data sources including factors that influence the approximate fraction of solar efficient roof areas. Nevertheless, these results can be considered a reasonable estimate within the range of other related research initiatives similar in the criteria used to account for shading, incoming solar radiation, building aspect and orientation in various combinations. As the basic approach has been taken to estimate the full solar PV potential that can be made available, assuming total distribution from the entire fraction of solar efficient area that all the residential rooftops in the samples could be delivered. Thus, the solar efficient roof areas per person ranging from 8.16 m^2 up to 27.62 m^2 represents a considerably high value in term of how an individual building may gain from utilizing all these areas with solar panels in an average 2.4 people per household in Invercargill.

Due to the low density housing, the energy harvesting from the large-scale PV deployment is potential large for the whole Invercargill urban area. This is estimated to be 82,947,315 kWh per year. The average energy output per person is in the range of 929.49 kWh to a substantial amount of 3040.52 kWh annually, assuming the PV module efficiency has a conservative value of 12%. If PV models had a higher actual efficiency then the yield would also increase.

The estimated result of potential energy output per person shows a promising aspect towards an achievable share of household energy consumption. The New Zealand energy demand reported on total average annual energy consumption (all industries) per capita for year 2013 is 9,497 kWh per person (MBIE, 2014b in Wikipedia, 2014a). When comparing the energy consumption on the household basis, the average annual household energy use identified by HEEP studies (NZ HEW, 2008) was 11,410 kWh per year, of which approximately 7,700 kWh accounted for electricity consumption. Based on an average 2.4 people per household in Invercargill, the estimated potential energy indicated the considerable contribution from residential rooftops PV system towards Invercargill suburbia energy requirements.

This research on investigating the solar PV potential in buildings from the available roof area found results similar to Izquierdo et al. (2008) and Byrd (2010). This provides further evidence to confirm the potential for solar harvesting in low density suburbs due to large roof per person house size. In this study, relatively large amount of available solar efficient area indicates the significant influence that large-scale PV deployment may contribute towards distributed energy generation of the household level. As such, in order to understand the potential implications of the available rooftop areas to benefit the whole city, it is necessary to compare the estimated solar harvesting amount in relation to the total roof surface and household energy demands in Invercargill study area.

4.3 Extrapolation to Study Area

So far, the study results related to the analysis outcomes derived from the methodological model based on the 5% sample size of total occupied dwellings in the targeted study area i.e. Residential Zone within the Invercargill District Plan's Urban Boundary. The findings from the 5% of house sampled are assumed to represent the relationships and trends significant to the whole study area. Since the developed model has been established on the statistical data for the relationship between the number of occupied dwellings and the number of resident population in each sample set, the average value per-capita obtained in the variables are important indicators that allow the data to be compared with related works.

4.3.1 Total Roof Surface Area and Solar Efficient Roof area in Invercargill

In order to meet the objective of the research to estimate the solar harvesting potential from the available rooftop areas in Invercargill, it is necessary to extrapolate from the sample set results to the total population for the outcome that can be applied to the entire city's potential. Table 4-4 shows the extrapolation, by

multiplying the value per-capita to the number of population in the area unit, for the sum of total roof surface area and total solar efficient roof area.

Table 4-4: Extrapolation of roof surface data to total residential occupied dwellings in the study area

		Census data		Calculated extrapolation data	
Number	Area unit	Number of occupied dwellings	Number of people	Total roof surface area (m^2)	Total solar efficient roof area (m^2)
1	Grasmere	1353	3357	**206447.51**	**54849.78**
2	Waikiwi	942	2490	**113704.64**	**28526.06**
3	Gladstone-Avenal	1524	3657	**167751.87**	**43882.98**
4	Rosedale	1533	3828	**231365.09**	**71094.08**
5	Windsor	1479	3051	**217771.06**	**48470.64**
6	Waverley-Glengarry	969	2289	**148708.70**	**48236.67**
7	CBD-Otakaro Park	315	693	**31780.29**	**7817.96**
8	Richmond	1230	2787	**207484.68**	**76981.18**
9	Hawthorndale	909	2244	**148510.75**	**49155.12**
10	Crinan	798	1752	**86412.66**	**20785.66**
11	Georgetown	951	2289	**162026.19**	**38875.75**
12	Newfield-Rockdale	1188	2907	**197624.54**	**59760.81**
13	Appleby-Kew	795	1914	**146720.86**	**45674.42**
14	Strathern	1029	2409	**170297.03**	**49465.20**
15	Heidelberg	1194	3216	**140366.86**	**26236.58**
16	Kingswell-Clifton	1395	3381	**170580.57**	**67734.85**
17	Tisbury	102	288	**11919.77**	**2956.57**
Whole study area		**17706**	**42552**	**2559473**	**740504**

Table 4-5: Summary of obtained data as indicators for potential implications on the whole context

Indicators	Calculation	Data
Overall average rooftop size	(2559473.06/17706)	**144.5 m²**
Ratio of solar efficient area	(740504/2559473)x100%	**28.93%**
Efficient roof area per building	144.55 x 28.93%	**41.82 m²**
Number of solar panels the efficient area could hold (based on standard module size of 800x1600mm = 1.28m²)	41.82/1.28	**32 panels per rooftop**
Typical annual electricity consumption per household	(NZ HEW, 2008)	**7,700 kWh**
Total electricity consumption in overall residential occupied dwellings	7,700 kWh x 17706	**136,336,200 kWh**
Proportion of potential solar energy distribution to the total electricity demand	(82,947,315/136,336,200)x100%	**60.84%**

According to the total census data, Invercargill has a population of 42,552 people living in 17,706 dwellings. The total roof surface area of all residential buildings in the Residential Zone within the Invercargill District Plan's Urban Boundary was found to be 2,559,473 m². Of all this total area, the solar efficient rooftop surface with appropriate solar harvesting potential for PV deployment was 740,504 m² which equals to 28.9 % of the total. Considering the energy potential could be generated from this total amount of solar efficient area was estimated at 82,947,315 kWh per year based on the solar panel yield of 12% efficiency. This would satisfy approximately 60.8% of the residential electricity used in Invercargill's urban area, based on the 7,700 kWh typical annual electricity consumption per household, assuming all solar energy is usable and not wasted during periods when energy harvesting exceeds demand e.g. during midday and midsummer.

However, this calculation assumes that all electricity generated from PV systems can be used to offset the household electricity needs. In reality this offset

may not be as valid as it is likely to be generated as non-peak times when sunshine is higher rather than in the evening peak time electricity usage. Unless the energy generated can be stored in the grid or with the battery usage, the actual practical offset value would be less than 60.8%.

Based on the extrapolated total roof surface area, overall average rooftop size obtained for the 17,706 buildings of the study area was approximately 144.5 m², which was a very close value based on the New Zealand's average house size of 149m² (QV New Zealand, 2011). The effective roof area of 28.9% which equals to 41.8 m², allowing the installation of about 32 standard size solar panels per rooftop. The result represents an immense opportunity to harvest sustainable energy from Invercargill's residential rooftops.

4.4 Model Findings and Discussion

This section discusses the results as well as the overall outcomes in relation to the research objectives of **Case Study 1 – Solar harvesting potential from roofs of Invercargill homes.** It also provides the review for the reliability of data by the methodology used in obtaining the results and the analysis of the data sources. The section also outlines the recommendations for areas of improvements, implications and potential for future analysis using the developed model to assess solar harvesting potential on rooftops in other locations.

4.4.1 Review of the Methodology and Findings

The aim of this research was to determine the solar harvesting potential from the available rooftop area and locations that are suitable for solar PV deployment of existing residential buildings in Invercargill, Southland region, New Zealand. From this purpose, the work strand of Case study 1 provided a solution to overcome the limitations of resource concerning the roof data and other associated building parameters for evaluating solar potential from residential rooftops in Invercargill City.

The Rooftop PVGen model has been developed to suit the implementation in this context. The work highlighted the process of obtaining large-scale rooftop data by using the digital aerial map and building characterisation method to gain the three-dimensional roof structural information for digitizing rooftop models. The work utilised New Zealand statistical census map of population and dwelling data to measure the solar efficient roof area from a 5% representative sample of buildings for the analysis. The solar PV potential was calculated using Equation 5 proposed in this study by combining the principle components of existing formulas to investigate the contribution to the solar PV potential in buildings using roof area and population relationship as the key indicator for extrapolation to study area. The study compared the technical potential of rooftop PV energy with the total energy consumption in the residential sector.

Based on the findings presented in this study, the total amount of solar PV potential of 82,947,315 kWh per year was estimated from the total solar efficient roof area of 740,504 m². This equates to approximately 60.8% of the residential electricity used in Invercargill's urban area, based on the 7,700 kWh typical annual electricity consumptions per household. These findings derived from the estimated 2,559,473 m² total roof surface area of all residential buildings in the Residential Zone within the Invercargill District Plan's Urban Boundary which comprised of 17,706 occupied dwellings in the census data.

For the study, solar PV potential was calculated from the distribution of total amount of solar efficient roof area. The research purpose was to investigate the maximum potential energy, based on the assumption that the entire solar efficient roof area could be used for PV installations. However, in reality the entire rooftop is not available for PV installation due to many limiting factors such as chimney, vent, and skylight to receive other roof uses, as well as complex roof design that could limit the capability for system layout. Nevertheless, the estimated ratio of 28.9% solar efficient roof area from the total roof area (approximately 41 m² from 144 m² roof surface) is still considered a reasonable estimate as it is consistent with the estimated values of roof area reductions. This is similar to the efficient

value reported in other literature such as Ghosh and Vale (2006) with 22%, 30% and 47% estimated for five residential blocks in New Zealand. By focusing on the idea of a city to maximize the use of available resources, this presents an important clue to gain an understanding about the pattern of rooftop energy production by the magnitude of average house size of the city as a whole, rather than as an individual function of a rooftop distribution potential.

The outcome from the calculation of PV potential has illustrated a reasonable representative value assuming full potential from large-scale PV production of all the residential buildings in the study area. The method for measuring this potential from solar efficient rooftop area, based on the census data of population and dwellings relationship, was found to give an appropriate analysis. However, the accuracy of outputs from solar simulation and PV modelling relies heavily on the quality of data sources. Additionally, with a number of simplifications that were necessary for the feasibility of the research design, the uncertainties of the outcome could be introduced at each step of the analysis. These are described in the next section.

4.4.2 Reliability of the Outcome, Model Limitation and Potential Uncertainties

The research outcome of solar PV potential and roof surface data were estimated based on the methodology developed for the practicality of the research design to overcome resource limitations and the lack of available data. In this case, it is necessary to be aware with the model limitations and potential uncertainties inherent in the process of findings at each step of the analysis, which are discussed in details.

Step 1: Sample selection

- Statistical inaccuracy of the sample size and selections. The analysis was carried out based on the coarse data from selected sample set to obtain the

averages from a representative value of total population. The 5% sample size may not provide accurate representation of the whole study area.

- The sample buildings in the selected meshblocks only represented building characters in the certain locations of the suburban development. These buildings may not contain appropriate variations of rooftop area and house size in the suburb.

Step 2: Urban rooftop analysis

- Simplified roof pattern and building outlines.
- Potential errors from manual extraction of roof surface data. This has a direct consequence on the amount of total roof surface area and the solar efficient roof area.
- Assumptions on the degree of roof angles and building parameters based on the representative building typologies.

Step 3: 3D Modelling

- 3D building models built on simplified building geometries and roof configurations from the assumptions of urban rooftop analysis process.

Step 4: Solar access analysis

- Inaccurate digital representation of the urban environments.
- The study assumed minimal shading effects based on restricted variations of the site's topography. The solar simulation was performed on the flat horizontal plane of the software environment.
- The analysis did not account for roof area losses to shading from trees and neighbourhood obstacles, due to the lack of elevated elements information in the surrounding area. It was not possible to manually digitise these features under this research timeframe. The absence of shading effects and shadow cast from existing trees and other miscellaneous features has direct implications on the amount of solar access of rooftop PV system.
- The analysis did not account for the roof area losses for other competing uses and inappropriate slope segments to accommodate PV installations.
- Simplified settings for solar access analysis and simulation.

Step 5: Solar potential calculation

- Simplifications of the overall system design and associated factors in the proposed equation for the practicability of the analysis.
- Calculation of PV potential based on the distribution of the entire solar efficient roof area.

Due to these procedures being taken manually, a 5% sample of the city was measured. This data was plot against the number of population of the whole study area. As the sample size has direct implications on the accuracy of the results, greater modelling efforts using a larger sample size could contribute to improve the accuracy and the reliability of the outcome. Due to the constraint in obtaining more samples from this scope of analysis, the availability of roof data have the strongest implications in the methodology for predicting solar PV potential from roof area.

A higher-precision digitizing procedure could also improve the modelling outcomes. With an appropriate way to identify the input parameters, this can make possible for the computational simulation to obtain the best solution that influences the quality of the output. The elevated elements such as trees and other obstacles should also be included in the analysis to account for shading effects. The related approaches for solar potential calculation should take into account the reduction factors for roof area available for PV installation. Since not all of roof area could be used for standardised rectangular PV panel, the area around the edges and the slope segments that could not accommodate the size of the panel should be reduced. Beyond other standard errors from the analysis itself, great precautions have been taken at each step to minimize the errors as much as possible for the reliability of the study outcome.

4.4.3 Implications for Future Analysis

The results from the research outcomes showed that large roof areas in suburban flat terrain locations can generate significant electricity to meet the

residential demand. This has direct implications on urban energy planning practices in relation to the significant potential from low density residential suburban area. The developed model represents a decision-support tool to implement effective energy system, in order to promote the city's transition towards sustainable energy from renewable distributed generation at a local level in New Zealand.

Rooftop PVGen model can be customized for different settings. Future research may apply the model with different input data from various topographical situations or use other building typologies in other cities. In local scale, the topography is the most important factor in determining the distribution of solar radiation at the surface, the current proposition has been understood that the shading effects in Invercargill are very restricted to the south-facing areas given its planarity with no topographical variations. The majority of single-story, low density residential developments theoretically have minimum issue on shadows casting from adjacent buildings and other ground reflected obstacles. This can provide the basis for model testing in other geographical locations with the significance of shading that may arise from the topographical variations in different context of solar applications. A further improvement of the model could include an algorithm to convert total north facing roof area to roof area that suits standard rectangular PV panels.

The second strand involved the validation of Rooftop PVGen Model proposed in the first strand of the research, to test the reliability of the developed method for predicting the PV outputs. The methodology presented in Rooftop PVGen Model was applied to calculate the rooftop PV potential and estimate the performance of existing photovoltaic installations. The aim was to conduct the performance prediction for comparing the modelled estimate energy output with the actual generation data from the PV systems that are installed in New Zealand schools under the Schoolgen programme. The energy generation of each Schoolgen system was evaluated and compared to assess the system parameters and operating conditions that affect PV performance.

CASE STUDY 2 – MODEL VALIDATION USING EXISTING DATA FROM PV GENERATION ON SELECTED NEW ZEALAND SCHOOLS

CHAPTER 5: MODEL VALIDATION

This chapter presents the second case study of the research. Schoolgen programme provides real data of electricity generation produced from the PV systems of Schoolgen schools. This data source enabled the validation of the model for the opportunity to compare the predictions from model developed in the first strand to the amount of PV energy under actual state of operations. This chapter discusses the methods and the use of Schoolgen data for model validation phase of the research.

5.1 Description of the Case Study

5.1.1 About Schoolgen Programme

Schoolgen is a sustainability programme developed by Genesis Energy to bring solar PV generation to schools across New Zealand (Schoolgen and NZ Power Company Genesis Energy, 2006-2015). As one of the largest electricity generator and energy retailer, Genesis Energy adopts a holistic approach in expanding the organisation's commitment toward sustainability by incorporating social, economic and environmental aspects to promote renewable generations. Under the key objective to raise the community's awareness with the concept of solar energy solutions, the Schoolgen programme funds the installation of solar generation systems and provide educational resources to selected schools around New Zealand. The programme was launched in 2006. Schoolgen was initially supported by the Ministry for the Environment's Sustainable Management Fund until 2010 when Genesis become the only sole sponsor. A new partnership with the Wellington City Council through Smart Energy Capital in 2013 has continued

to co-fund the progress and expand the uptake of PV installations to more schools in Wellington region.

Figure 5-1: Schoolgen launched (Source: Schoolgen and NZ Power Company Genesis Energy, 2006-2015)

By the end of 2014, Schoolgen had provided 71 schools with either a 2 or 4 kW of solar PV system. The total capacity of more than 100 kW Schoolgen installations makes it so far the largest distributed solar power station in New Zealand (Schoolgen and NZ Power Company Genesis Energy, 2006-2015). With the PV systems installed, schools can generate a portion of their required electricity, which contributes to direct savings in utility costs by offsetting the imported amount from the grid. The PV generated patterns are recorded and displayed with the real-time generation data in the Schoolgen online database to provide for the educational learning/teaching resources available for students and public access to explore the role of solar for renewable energy.

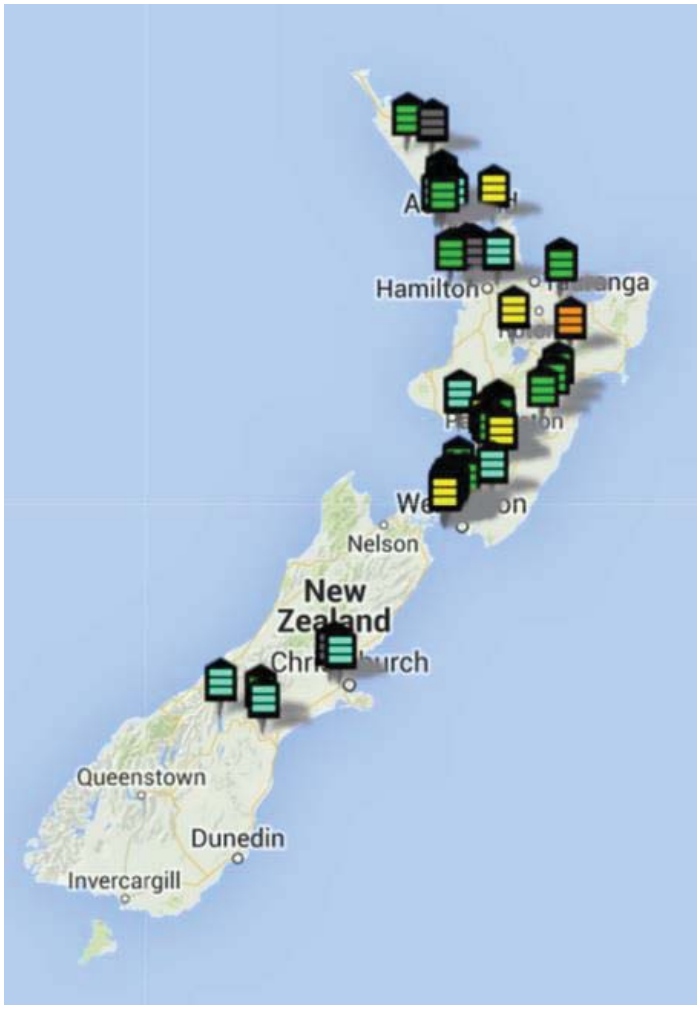

Figure 5-2: Locations of Schoolgen schools across New Zealand (Source: Schoolgen and NZ Power Company Genesis Energy, 2006-2015)

5.1.2 Description of Schoolgen PV Systems

The PV system installed at a Schoolgen school consists of solar PV panels connected in one or two strings and typically functioned to generate electricity (Schoolgen and NZ Power Company Genesis Energy, 2006-2015). They are not the solar thermal collectors which can be used to heat water. The system has an inverter connected to convert the energy produced to direct current (DC power), which is produced by the PV system at about 400 volts into the alternating current (AC power) at 230 volts for use in the school (Schoolgen and NZ Power Company Genesis Energy, 2006-2015). The AC side of the inverter is connected and synchronised with the local distribution board to ensure the producing voltage can smoothly flow outward from the PV panels. The energy produced by the panels is then introduced to the school distribution network to be locally used

within the school prior to and in conjunction with other imported energy from the grid (Schoolgen and NZ Power Company Genesis Energy, 2006-2015).

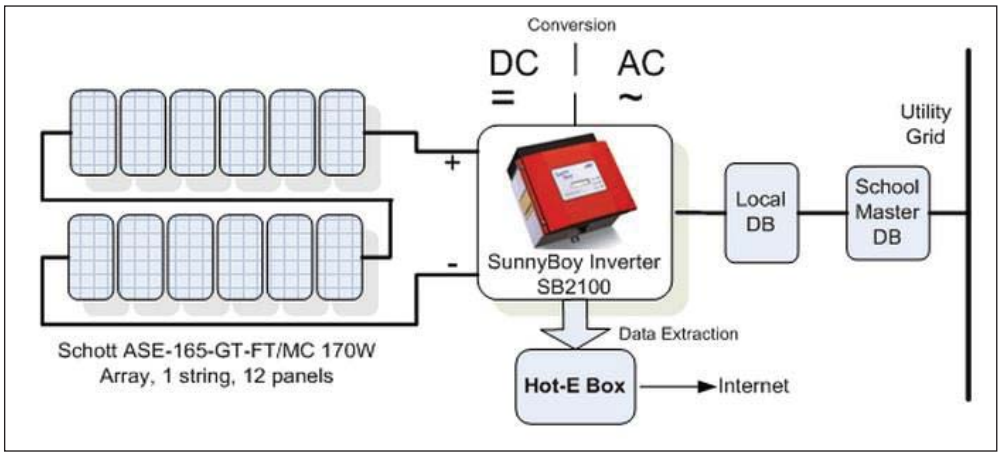

Figure 5-3: Typical circuit diagram of the PV system installed at a Schoolgen school (Source: Schoolgen and NZ Power Company Genesis Energy, 2006-2015)

A typical Schoolgen PV system is installed as grid-connected type. As such the inverter is equipped with the isolating transformer device to detect system islanding which can impose danger to utility workers if the solar distributed generation continues to feed power into the main system even though the power from the utility grid is not present. In the case when the PV system generates surplus electricity to export to the grid, the inverter also monitors grid voltage, waveform and frequency to ensure the generated power is delivered at the exact same grid voltage (230 volts) and frequency (50 times per second). Any imported energy from the grid can simply combine with the conditioned AC power to meet the domestic load demand. However, since the base capacity of PV system installed in Schoolgen schools can only generate a maximum possible output of either 2 or 4 kW at a given point of time, this amount produced by the peak sunlight during school hours is assumed to be fully utilised by the school consumption with no surplus electricity. During weekends and school holidays, the energy generated will also be most likely consumed by the school's base demand such as refrigerators, hot water cylinders and computer servers. Therefore Schoolgen schools do not have an import/export meter installed to

monitor the amount of energy transfer to the utility grid (Schoolgen and NZ Power Company Genesis Energy, 2006-2015).

The PV modules installed in the majority of Schoolgen schools are the poly-crystalline silicon which is the thin slice wafers of the silicon material. Another type of PV technology used in a few of South Island locations are the thin-film silicon called “micromorph” which is specifically designed to be more efficient than a traditional thin-film material. This micromorph is a type of tandem cell made of two thin-film layers of microcrystalline and amorphous silicon combined to capture a broader part of the solar spectrum and allow better light absorbance from different material bandgaps. However, the efficiency of thin-film per square meter is lower than the crystalline silicon type due to a much thinner layer of reduced material so more roof area is required to produce the same amount of power with these thin-film modules. The intended purpose of micromorph installation is for trial the performance of this technology in term of its efficiency, reliability and cost-effectiveness in comparison to the conventional crystalline type (Schoolgen and NZ Power Company Genesis Energy, 2006-2015).

5.1.3 Electricity Generation Data

The amounts of energy produced by the PV panels at all of the Schoolgen schools are recorded by the data extraction device called the Hot-E box. This Hot-E box is designed to capture the electricity generation data from the inverter and send this data to the school LAN (local area network) where the statistic pattern collected in the Microsoft Excel spreadsheet is converted into weekly, monthly, and yearly energy generation graphs before being uploaded to the Schoolgen website. The programme database keeps the massive records of PV generation data of all Schoolgen schools every 30 minutes since the panels were first installed. This data of each school can be accessed and downloaded directly from the Schoolgen website where the amount of electricity generation in a specified time period can be displayed in conjunction to the amount of solar radiation available on the site of PV installation. The solar radiation data is obtained from

the nearest NIWA weather station reported in the units of Mega-Joules per square meter (MJ/m2) (1 kWh = 3.6 MJ).

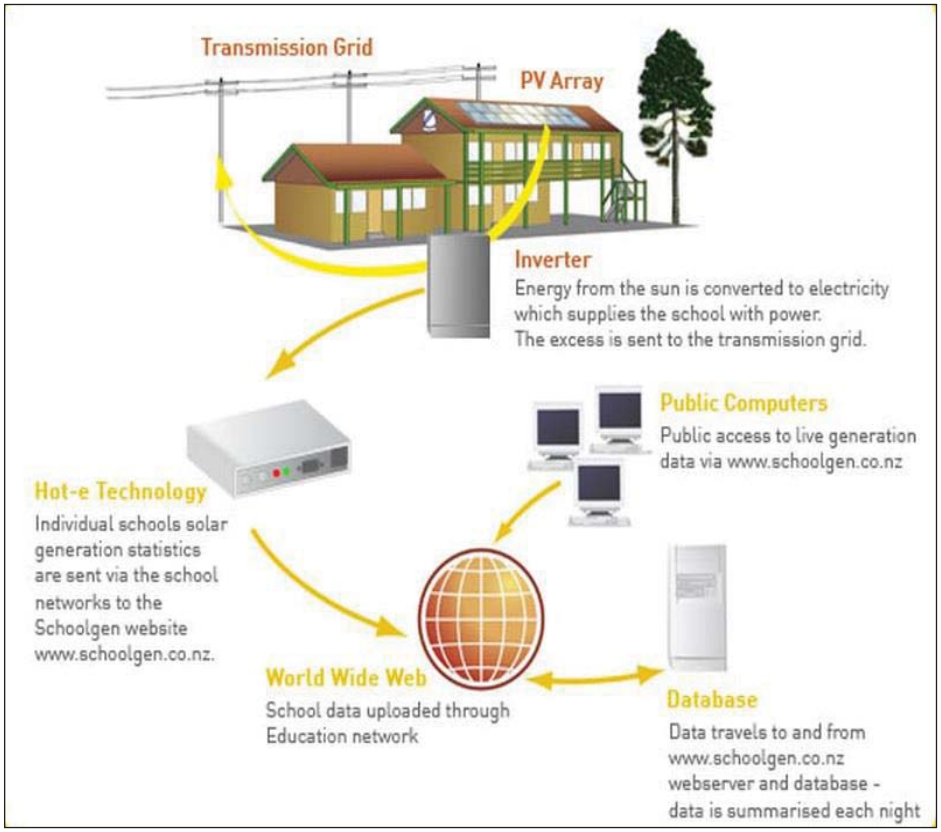

Figure 5-4: Diagram of how the PV generation data were collected from all the Schoolgen schools (Source: Schoolgen and NZ Power Company Genesis Energy, 2006-2015)

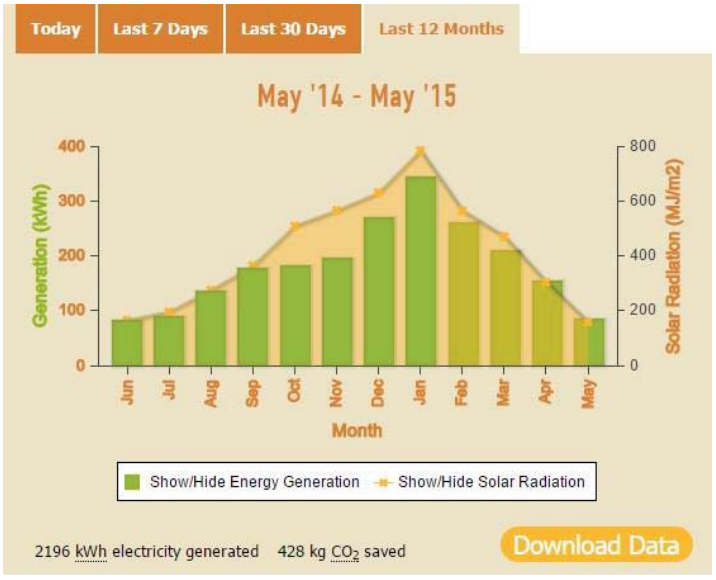

Figure 5-5: Example of PV generation data of a Schoolgen school in a defined time period (Source: Schoolgen and NZ Power Company Genesis Energy, 2006-2015)

Apart from the displayed amount of electricity generation, the comprehensive programme also reports the avoided amount of carbon dioxide (CO2) emissions by the use of PV generated electricity. Schoolgen calculates the carbon emissions by multiplying the PV generated amount obtained in kilowatt-hours (kWh) with the official New Zealand emissions factor of 0.195 kilograms of CO2 per kWh (Schoolgen and NZ Power Company Genesis Energy, 2006-2015). This is an average value of CO2 emission factor sourced from the Energy Greenhouse Gas Emissions 1990-2007 publication which provides CO2, CH4, and N2O emissions that occur from a range of combustion fuels used by New Zealand energy sector recorded in the New Zealand Energy data file (MfE [Ministry for the Environment], 2013). However, the CO2 emission factor provided is an indicative figure on the basis of direct fuel combustion. It is important to note that this is not the full cycle emission factor and does not incorporate emissions associated with the extraction, production and transportation of the fuel (MfE, 2013).

The specific details of how PV systems were set up in Schoolgen schools are contained in each school profile record. The system details explain the exact geographical information of the installed panels with its direction and tilt angle in relation to the pitch of the roof. The number of panels as well as individual size and module capacity are also displayed to show the difference between system types. This variability in size, orientation, inclination, and climatic parameter by each school’s location are the key factors that affect the electricity output from the PV installation of different Schoolgen schools.

Latitude:	-40.05499
Longitude:	175.774115
Location:	4 Henderson St, Kimbolton
Type of school:	Primary
Date of PV installation:	4/11/2009
Type of panels:	Schott ASE-165-GT-FT/MCI 170W
Size of individual panels:	1620mm x 810mm x 50mm
Number of panels:	12
Output capacity of a single panel:	170W
Output capacity of a PV system:	2.050 Kw(P)
Inverter size:	1700 watts
Location of panels:	Main classroom block roof
Direction of the roof:	North facing
Pitch of the roof:	15 degrees
Pitch of the panels:	Flat to roof
Nearest weather station:	Palmerston North Ews

Figure 5-6: Example of a Schoolgen school's PV system details (Source: Schoolgen and NZ Power Company Genesis Energy, 2006-2015)

5.2 Model Validation Methods

This strand of the study utilised the data from Schoolgen database for model validation. As Schoolgen programme contains the most comprehensive list of real-time generation data of PV production on the active site available for public access. The actual Schoolgen PV generation data was compared to the estimated PV potential calculated in the model developed in the first strand of this research.

In this strand of the research, the applicable methods of Rooftop PVGen model were applied to calculate the potential generation of Schoolgen PV systems. The comparison of the modelled output potential against the actual PV generation recorded by the Schoolgen data was the principle research strategy for this part of study to evaluate the capabilities of the analysis tools, as well as the opportunity to analyse the system efficiency and performance capacity of PV in the actual state of operation. The scope of this study was conducted in the framework of quantitative-base project and relied on the available data from official collection and the case study's website and databases. Following the step-

by-step procedure of Rooftop PVGen model, the methodology utilised for this research phase is summarised as follows:

Step 1 - Schoolgen selection

- **List of Schoolgen schools**: All Schoolgen schools' system details were obtained and sorted by location from the most northern area to the furthest south of school locations. Only 2 kW and 4 kW installed capacity of Schoolgen PV system were selected for the analysis. The schools with expanded capacity, and the schools where the recent installations did not cover full year database, were not included in the analysis.

Step 2 – Building rooftop analysis

- **Google Map Aerial Imagery for extracting roof surface data of school buildings:** From the geographical information indicated in the school's PV system details, the location of the school was searched through google map where the aerial imagery was displayed to use as a reference for digitising the spatial distribution of roof patterns and building outlines. The aerial image were exported and scaled with 2DCAD. Each PV panels were drawn over the school's building rooftop.
- **Google Street View for 3D roof information:** The geometric characteristics of building height, roof design and configurations as well as slope segments were determined.

Step 3 – 3D Modelling

- **3D-CAD software for digitizing building rooftops:** 3D building models and PV panel models on the rooftops were digitised from the visual information obtained from the aerial image and google street view. Most of the system parameters required for digitising are listed in the school's PV system details including the pitch of the roof, degree of PV mounted angle, orientation, numbers of the panels and the individual size. The assumptions on school's typical building height were also made where applicable.

Step 4 - Solar access analysis

- **Ecotect software for solar simulation to determine solar radiation incident on PV panel area**: Ecotect solar simulation and analysis tools were used to to perform the assessment of incoming solar radiation that can be received on the Schoolgen PV panels. Each digitised school building with roof-mounted PV panels was exported to the Ecotect environment to determine the amount of solar radiation available by the size of panel area.

Step 5 – Solar Potential Calculation

- **Solar potential calculation using PV mathematical equation**: The amount of solar PV potential energy was calculated using the amount of available solar radiation received on the panels obtained from Ecotect simulation to apply in the mathematical equation adopted in this study. By taken into account the annual average amount of solar radiation (kWh/m²/year), the total area of installed PV panel (m²), the performance ratio and module efficiency (%) of the PV system, this will give the result of PV energy output based on the incoming solar radiation exposed on the PV panel surface.

Step 1-5 of Rooftop PVGen model was utilised for the calculation to obtain the amount of PV potential generation from each Schoolgen PV system. The next step was designed for the methods of model validation in order to meet the purpose of this research strand.

Data analysis

- **Comparison of the model findings with actual PV generation:** The result of PV energy output modelled for each Schoolgen sample was compared to the Schoolgen PV generation data monitored from the actual state of operation. This allowed the assessment of the modelled findings and the actual production. Discrepancy between the two set of figures will determine the validity of the simulation tools and PV analysis principles developed in the Rooftop PVGen model.

- **Capacity factor:** The generation output and performance capacity of Schoolgen PV systems is analysed by the value of capacity factor as an indication for comparing the performance variability between Schoolgen schools. This is the ratio of the actual generation output obtained in one-year period divided by the maximum rated capacity of the system.

Flowchart of Rooftop PVGen Model for Schoolgen application

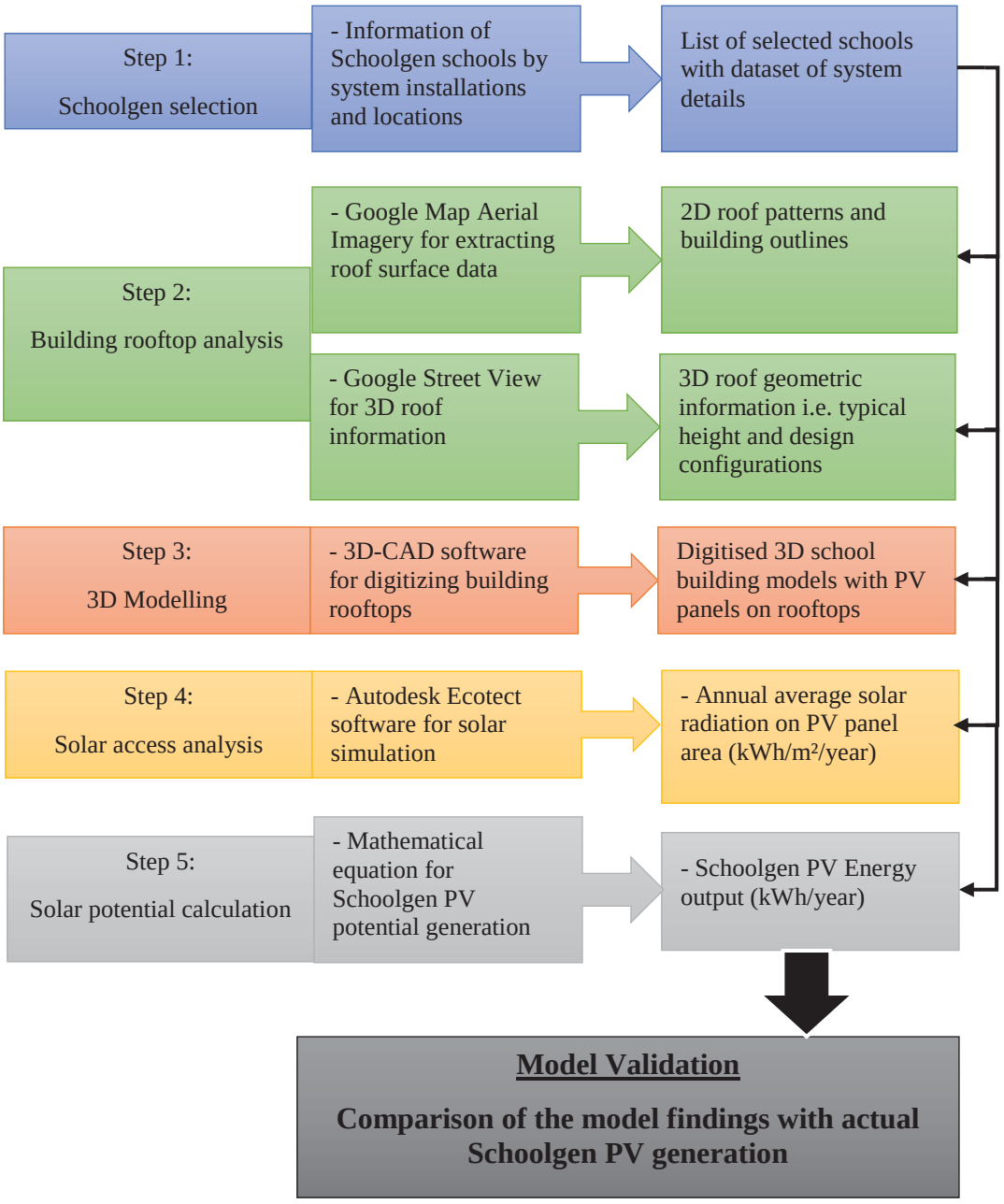

Figure 5-7: Rooftop PVGen Model for calculating rooftop PV potential for Case Study 2

5.2.1 Schoolgen Selection and System Installation Data

Information of Schoolgen schools can be accessed directly from the Schoolgen programme website. The analysis covered the energy generation data on an annual basis, in order to take into account of all seasonal variations that affect the energy availability from PV production. However, the systems that were newly installed did not cover a full year performance dataset. Only PV systems installed for more than one year which is the total of 66 Schoolgen were included in the analysis. The information obtained at this initial stage were related to the school geographical location, roof direction, and the number and size of the individual panel for digitising school buildings with specific dimension of roof-mounted panels. The total area of panels (m^2) across the building rooftop was calculated from the given information on the individual panel size by the total number of panels in the system details. From the comprehensive set of data, Table 5-1a and Table 5-1b were sorted by locations to provide a summary of technical information on how each PV system was installed at selected Schoolgen schools.

Table 5-1a: List of Schoolgen schools for digitization (2kW capacity installations)

	School	Location	Direction of the roof Degree	Roof Pitch Panel Pitch Degree º	Panel length m	Panel width m	Individual panel area m2	Number of Panels	Total area of installed panels m2	Panel type	Output capacity of single panel W	Total installed capacity
1	Mangakahia Area School	Mangakahia	N	15	1.64	0.99	1.6236	8	12.9888	CSUN250-60P	250	2000
2	Wangarei Heads Primary School	Whangarei	NE	20	1.64	0.99	1.6236	8	12.9888	CSUN250-60P	250	2000
3	Westlake Girls High School	North Shore	16º East of N	12	1.62	0.81	1.3122	12	15.7464	Schott ASE-165-GT-FT/MCI 170W	170	2040
4	Northcote Collge	North Shore	5º West of N	12	1.6	0.85	1.36	12	16.32	Sharp NT-R5E3E polycrystalline	175	2100
5	Greenhithe Primary School	North Shore	N	27	1.6	0.85	1.36	12	16.32	Sharp NT-R5E3E polycrystalline	175	2100
6	Glendowie College	Orakei	25º West of N	45	1.62	0.81	1.3122	12	15.7464	Schott ASE-165-GT-FT/MC 170W	170	2040
7	Pakuranga College	Horwick	15º West of N	15	1.6	0.85	1.36	12	16.32	Sharp NT-R5E3E polycrystalline	175	2100
8	Henderson Valley Primary School	Waitakere	N	15	1.62	0.81	1.3122	12	15.7464	Schott ASE-165-GT-FT/MC 170W	170	2040
9	Tirimoana Primary School	Waitakere	5º East of N	15	1.6	0.85	1.36	12	16.32	Sharp NT-R5E3E polycrystalline	175	2100
10	Silverdale Primary School	Albany	N	15;27	1.6	0.85	1.36	12	16.32	Sharp NT-R5E3E polycrystalline	175	2100
11	Hamilton Girls High School	Hamilton	N	15	1.62	0.81	1.3122	12	15.7464	Schott ASE-165-GT-FT/MCI170W	170	2040
12	Maeroa Intermediate School	Hamilton City	N	15	1.62	0.81	1.3122	12	15.7464	Schott ASE-165-Gt-FT/MCI170W	170	2040
13	Fairfield College	Hamilton	N	40	1.62	0.81	1.3122	12	15.7464	Schott ASE-165-GT-FT/MCI170W	170	2040
14	Forest Lake Primary School	Hamilton	N	20	1.62	0.81	1.3122	12	15.7464	Schott ASE-165-GT-FT/MCI170W	170	2040
15	Matamata Primary School	Hamilton	N	15	1.62	0.81	1.3122	12	15.7464	Schott ASE-165-GT-FT/MCI 170W	170	2040
16	St Pauls Collegiate	Hamilton	N	10	1.62	0.81	1.3122	12	15.7464	Schott ASE-165-GT-FT/MCI 170W	170	2040
17	St Peter Chanel Catholic School	Hamilton	N	20	1.62	0.81	1.3122	12	15.7464	Schott ASE-165-GT-FT/MCI 170W	170	2040
18	Vardon Primary School	Hamilton	N	15	1.62	0.81	1.3122	12	15.7464	Schott ASE-165-GT-FT/MCI 170W	170	2040
19	Te Kowhai School	Te Kowhai	N	15	1.62	0.81	1.3122	12	15.7464	Schott ASE-165-GT-FT/MCI 170W	170	2040
20	Mercury Bay Area School	Whitianga	N	20	1.62	0.81	1.3122	12	15.7464	Schott ASE-165-GT-FT/MCI 170W	170	2040
21	Raglan Area School	Raglan	N	15	1.62	0.81	1.3122	12	15.7464	Schott ASE-165-GT-FT/MCI 170W	170	2040
22	Taupo-nui-a-Tia College	Taupo	5º East of N	45	1.62	0.81	1.3122	12	15.7464	Schott ASE-165-GT-FT/MCI 170W	170	2040
23	James Street School	Whakatane	N	20	1.64	0.99	1.6236	8	12.9888	CSUN250-60P	250	2000
24	Whakatane Intermediate School	Whakatane	South	10;30	1.64	0.99	1.6236	8	12.9888	CSUN250-60P	250	2000
25	Te Kura O Waikaremoana School	Hawkes Bay	35º East of N	27	1.65	0.99	1.6335	8	13.068	Yingli YL250P-29b	250	2000
26	Napier Intermediate School	Napier	N	15	1.62	0.81	1.3122	12	15.7464	Schott ASE-165-GT-FT/MCI 170W	170	2040
27	Pukehou School	Hastings	N	10	1.62	0.81	1.3122	12	15.7464	Schott ASE-165-GT-FT/MCI 170W	170	2040
28	Hastings Intermediate School	Hastings	N	20	1.62	0.81	1.3122	12	15.7464	Schott ASE-165-GT-FT/MCI 170W	170	2040
29	St Johns Hill Primary School	Wanganui	N	12	1.62	0.81	1.3122	12	15.7464	Schott ASE-165-GT-FT/MCI 170W	170	2040
30	Wanganui Intermediate	Wanganui	N	15	1.62	0.81	1.3122	12	15.7464	Schott ASE-165-GT-FT/MCI 170W	170	2040
31	Awahou School	Manawatu	N	15	1.62	0.81	1.3122	12	15.7464	Schott ASE-165-GT-FT/MCI 170W	170	2040
32	Kimbolton School	Manawatu	N	15	1.62	0.81	1.3122	12	15.7464	Schott ASE-165-GT-FT/MCI 170W	170	2040
33	Mount Bigg School	Manawatu	N	12	1.62	0.81	1.3122	12	15.7464	Schott ASE-165-GT-FT/MCI 170W	170	2040
34	Aokautere School	Palmerston North	N	16	1.62	0.81	1.3122	12	15.7464	Schott ASE-165-GT-FT/MCI 170W	170	2040
35	Hokowhitu School	Palmerston North	N	15	1.62	0.81	1.3122	12	15.7464	Schott ASE-165-GT-FT/MCI 170W	170	2040
36	Newbury School	Palmerston North	N	12	1.62	0.81	1.3122	12	15.7464	Schott ASE-165-GT-FT/MCI 170W	170	2040
37	St Anthony's Primary	Pahiatua	N	15	1.62	0.81	1.3122	12	15.7464	Schott ASE-165-GT-FT/MCI 170W	170	2040
38	Paraparaumu Collge	Kapiti Coast	N	20	1.62	0.81	1.3122	12	15.7464	Schott ASE-165-GT-FT/MCI 170W	170	2040
39	Douglas Park School	Masterton	N	25	1.62	0.81	1.3122	12	15.7464	Schott ASE-165-GT-FT/MCI 170W	170	2040
40	Paremata School	Porirua	N	25	1.62	0.81	1.3122	12	15.7464	Schott ASE-165-GT-FT/MCI 170W	170	2040
41	Plateau Primary School	Upper Hutt	N	30	1.62	0.81	1.3122	12	15.7464	Schott ASE-165-GT-FT/MCI 170W	170	2040
42	Clifton Terrace Model School #1	Welllington City	20º East of N	15	1.62	0.81	1.3122	12	15.7464	Schott ASE-165-GT-FT/MCI 170W	170	2040
43	Wadestown School	Welllington City	N	30	1.62	0.81	1.3122	12	15.7464	Schott ASE-165-GT-FT/MCI 170W	170	2040
44	Eastern Hutt School	Lower Hutt	N	25	1.62	0.81	1.3122	12	15.7464	Schott ASE-165-GT-FT/MCI 170W	170	2040
45	Muritai School	Lower Hutt	N	15	1.62	0.81	1.3122	12	15.7464	Schott ASE-165-GT-FT/MCI 170W	170	2040
46	Raphael House	Lower Hutt	N	30	1.62	0.81	1.3122	12	15.7464	Schott ASE-165-GT-FT/MCI 170W	170	2040
47	Bank Avenue School	Christchurch	N	20	1.3	1.1	1.43	16	22.88	Auria M125000	125	2000
48	Middleton Grange School	Christchurch	10º West of N	20	1.3	1.1	1.43	16	22.88	Auria M125000	125	2000
49	Sumner Primary School	Christchurch	NE	20	1.3	1.1	1.43	16	22.88	Auria M125000	125	2000
50	Lake Tekapo School	Mackenzie	N	25	1.3	1.1	1.43	16	22.88	Auria M125000	125	2000

Table 5-1b: List of Schoolgen schools for digitization (4kW capacity installations)

	School	Location	Direction of the roof Degree	Roof Pitch Panel Pitch Degree	Panel length m	Panel width m	Individual panel area m2	Number of Panels	Total area of installed panels m2	Panel type	Output capacity of single panel W	Total installed capacity
51	Bayswater Primary School	North Shore	N	20	1.65	0.99	1.6335	16	26.136	Yingli YL250P-29b	250	4000
52	Stanley Primary Bay School	North Shore	22º East of N	35	1.65	0.99	1.6335	16	26.136	Yingli YL250P-29b	250	4000
53	Takapuna Normal Intermediate	North Shore	30º East of N	15	1.65	0.99	1.6335	16	26.136	Yingli YL250P-29b	250	4000
54	May Road Primary School	Auckland	17º East of N	15	1.65	0.99	1.6335	16	26.136	Yingli YL250P	250	4000
55	Amesbury School	Wellington City	44º West of N	10	1.65	0.99	1.6335	16	26.136	poly-crystalline silicon	250	4000
56	Clifton Terrace Model School #2	Wellington City	20º East of N	15	1.65	0.99	1.6335	16	26.136	Yingli YL250P-29b	250	4000
57	Clyde Quay School	Wellington City	22º East of N	23	1.65	0.99	1.6335	16	26.136	Yingli YL250P-29b	250	4000
58	Hampton Hill School	Wellington City	10º East of N	12	1.65	0.99	1.6335	16	26.136	Polycyrstalline Silicon	250	4000
59	Miramar North Primary School	Wellington City	25º East of N	26	1.65	0.99	1.6335	16	26.136	Polycrystalline silicon	250	4000
60	Newlands Intermediate	Wellington City	10º East of N	14	1.65	0.99	1.6335	16	26.136	Polycrystalline silicon	250	4000
61	Northland Primary School	Wellington City	3º West of N	23	1.65	0.99	1.6335	16	26.136	Polycrystalline silicon	250	4000
62	Paparangi School	Wellington City	N	10	1.65	0.99	1.6335	16	26.136	Yingli YL250P-29b	250	4000
63	Ridgeway Primary School	Wellington City	19º East of N	20	1.65	0.99	1.6335	16	26.136	Polycrystalline silicon	250	4000
64	Te Aro Primary School	Wellington City	45º East of N	25	1.65	0.99	1.6335	16	26.136	Polycrystalline silicon	250	4000
65	Thorndon Primary School	Wellington City	68º East of N	30	1.65	0.99	1.6335	16	26.136	Polycrystalline silicon	250	4000
66	Temuka Primary School	Temuka	17º East of N	13	1.65	0.99	1.6335	16	26.136	Polycrystalline silicon	250	4000

5.2.2 Digitising School Building with Roof-Mounted PV Panels

It was necessary to manually digitised rooftop of school buildings in this study due to the lack of available automated existing building plans. At this stage, the Google aerial imagery was utilised as a base map display of the school's geographical location for roof pattern and building layout. The aerial image was exported and scaled with 2D-CAD to provide for a correct dimension of building footprint and rooftop surface. The PV-located building block was outlined and each panel was drawn over the building rooftop to scale.

The diagrams of the building rooftop with the PV layout were used to construct a 3D model of each school building using 3D-CAD. The geometric 3D information was obtained from Google Street View. The assumptions on a classroom height were made where not available. The remaining parameters required for 3D digitising including the pitch of the roof and the PV mounted angle were listed in the Schoolgen website. The 3D dimensions of PV panels on the rooftop were digitised at the highest possible precision in order to perform

accurate simulation of incoming solar radiation on the defined surface. Examples of digitised models are displayed in Figure 5-8.

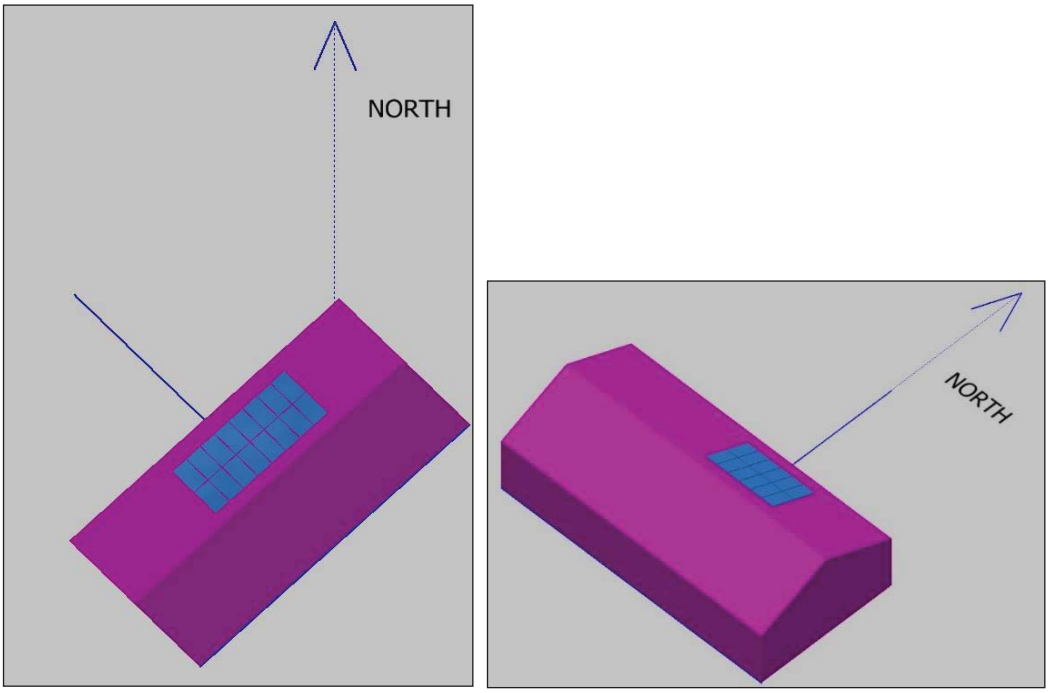

Figure 5-8: Examples of 3D-modeled school building with roof-mounted PV panels digitized in 3D-CAD software (#55 Amesbury School – Wellington City and #34 Aokautere School – Palmerston North)

5.2.3 Solar access analysis

Autodesk Ecotect uses the hourly record of direct and diffuse radiation from the selected weather station data file for solar access calculation. The latitude and longitude provided on the Schoolgen website enabled the closest NIWA weather station to be located. The remaining conditions required were each building's height and PV panel dimensions, degree of panel orientation towards north, and PV mounted angles. Using these inputs, the solar access analysis function calculated the amount of solar radiation incident on the located PV panels over the specified time period of the year.

Ecotect software required options to set up a realistic environment in the analysis field. For the type of sky setting, Ecotect only offers two sky conditions

either overcast or uniform sky model. Based on the overall New Zealand weather conditions concerning high cloud cover, the overcast sky was selected for every school sites. The overshadowing effect was also expected to be minimal due to the classroom layout appropriate for Schoolgen PV installations. Table 5-2 displays the input parameters selected in the software options for solar analysis.

Table 5-2: Summary of input parameters for Schoolgen solar access analysis settings in Ecotect

Input	Description	Value
Terrain	Ground surface elevation geometry	Default horizontal flat surface of analysis plane
Building geometry	Import digitized school building model	Digitized input parameters
Orientation	Aspect of building surfaces in relative site context direction toward the sun.	Specified direction of the roof
Latitude Longitude	Geographic location of the school	As specified for each school
Weather data	Solar radiation data file downloaded in Ecotect	Nearest NIWA weather station identified for each site
Calculation period	Time period selected for calculating solar radiation	Whole year – Last 12 months
Sky type	Choices of sky model representing the sky conditions used to calculate the distribution of incoming diffuse radiation to the surface.	Overcast sky
Surface subdivisions	Resolution size of each surface plane to be analyzed e.g. size of tiles across the surfaces.	Default
Azimuth Divisions	Size of sky segments subdivisions of sky dome to be calculated for each zenith angle. The lower degree (minimum value 2°) increases the accuracy given a more refined shading mask.	5°
Altitude Divisions	Sizes of sky segments subdivisions of sky dome. Each altitude band has certain number of azimuth segments.	5°
Overshadowing Accuracy	Adjustment for the calculation of overshadowing masks level of precision, the higher settings the more rays are generated.	High
Diffuse proportion	The solar exposure component with the choice of ground reflection or direct light only which ignoring all diffuse and reflected radiation.	Ground Reflection – default value
Calculated data	The option of how the analysis values will be totaled up from the choice of cumulative, average daily or peak values.	Cumulative values

Figure 5-9a displays an example of incoming solar radiation calculated for roof-mounted PV panels of Amesbury School over a one-year period. As this

study targeted on the solar quantity that is available on the panels, therefore only PV objects in the model were selected to perform the analysis. The annual average amount of radiation reaching the location of PV panels was shown in yellow indicating the solar value in a maximum range. Figure 5-9b displays the object attributes data with total solar radiation of 1,481,415 Wh/m² (1,481 kWh/m²) in this school.

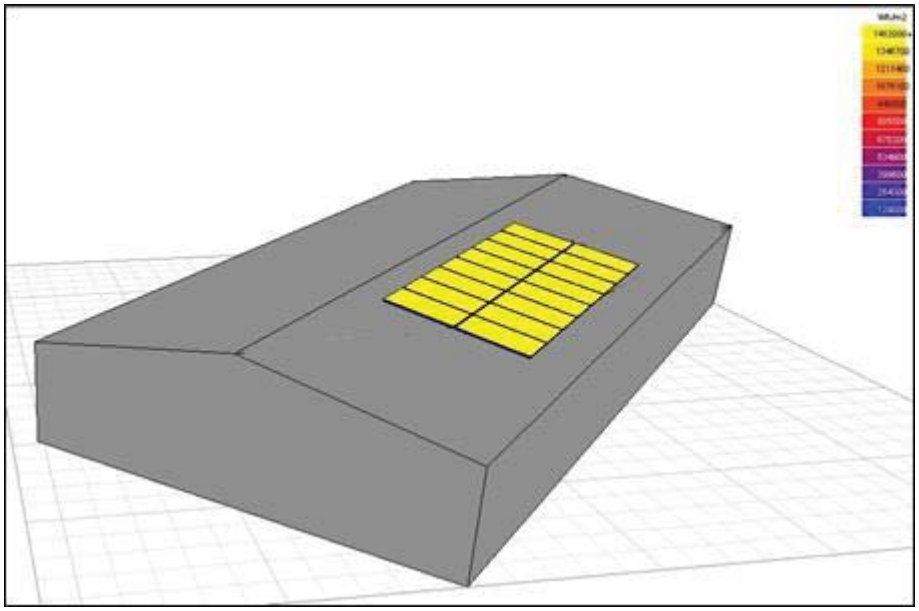

Figure 5-9a: Display of Ecotect analysis for incoming solar radiation on PV panels (#55 Amesbury School – Wellington City)

Report: Object Attributes - Selected							
Description: Lists attributes of objects in model							
Model:							
Object Attributes							
Objects	Object	Orient.	Tilt	Area	Total Radiation	Total Direct Radiation	Total Diffuse Radiation
ID	Type	(°)	(º)	(m²)	(Wh/m²)	(Wh/m²)	(Wh/m²)
0	Wall	46	0	0.082	210358.906	111220	99138.898
1	Wall	136	10	0.049	401839.188	137876.078	263963.125
2	Wall	-134	0	0.082	129214.305	30075.342	99138.961
3	Wall	-44	-10	0.049	599295.812	379228.344	220067.469
4	Ceiling	-44	80	1.633	1481415.375	897359.938	584055.438
5	Wall	46	0	0.082	210358.906	111220	99138.898
6	Wall	136	10	0.049	396007.875	137876.078	258131.812
7	Wall	-134	0	0.082	129214.258	30075.342	99138.914
8	Wall	-44	-10	0.049	597375.75	377307.688	220068.094
9	Ceiling	-44	80	1.633	1481415.375	897359.938	584055.438

Figure 5-9b: Microsoft Excel numerical list of individual object area and total radiation received on each surface (solar panels shown as ceiling in the object type list due to the software default setting) (Example from #55 Amesbury School – Wellington City)

5.2.4 Global Formula for Calculating PV Potential

The key determinant of PV output potential is the amount of solar radiation reaching the PV surface. The basis for calculating solar PV electricity also requires other considerations to be taken into account the module efficiency and other system losses from factors discussed in the literature reviews. Equation 3 (Global PV formula - Photovoltaic-software, 2014) described the first strand of the research (Section 3.2.4) was adopted for this evaluation as it integrates the measures required in assessing PV potential.

E = Pr x r x H x A ..... Equation 3

Where E is the energy output (kWh/year); Pr is the Performance Ratio that considers coefficient for system losses (Default value = 0.75); A is the total area of PV panel (m2) which can be obtained from the size of single panel multiplied by the number of panels installed on Schoolgen rooftop; H is an annual average solar radiation (kWh/m²/year) obtained from Ecotect analysis; r is the module efficiency (%) from output capacity of a single panel (kW) divided by single panel area (Photovoltaic-software, 2014).

The module efficiency was obtained from the rated capacity of PV technology of a single panel divided by each panel area. The calculation process of module efficiency was completed by Microsoft Excel function using the essential data from school system profile. The PV output potential for each school dataset was calculated by applying the modelling result of annual average solar radiation on Schoolgen PV panels to other variables in Equation 3.

5.2.5 Data Analysis

5.2.5.1 Comparison of Modelled Findings with Actual Generation

The key analysis focus for this part of research is to assess the validity of the PV analysis model into predicting the amount of energy generation from a PV system. From the analysis model developed, the anticipated result from the model's predicted PV generation was analysed against actual generation data recorded by each Schoolgen system. The available data of PV generated outputs was displayed in conjunction to the total amount of solar radiation of the site. The solar radiation data measured from the nearest NIWA weather station was used as a basis to analyse the modelled incoming solar radiation outcome from Ecotect simulation to examine the effects of inclination and orientation variability. The availability of the solar radiation was the key factor influencing the performance of PV systems installed at different schools.

The PV generation data can be accessed and downloaded in Microsoft Excel file over the choice of last 7 days, last 30 days or last 12 months. In this method, the PV production quantity for one-year period was obtained from the last 12 months (June 2014 – May 2015). The total PV generation amount was compared with the modelled prediction on the annual basis to find the difference between two values. The percentage error calculated from the difference between the estimate and actual values using percentage error formula was the key indicator for evaluating the reliability of model prediction.

$$\textbf{Percentage error} = \frac{\textbf{Appproximate value} - \textbf{Exact value}}{\textbf{Exact value}}\ \boldsymbol{x}\ \mathbf{100\%}$$

..... Equation 6

5.2.5.2 Comparing Schoolgen System Performance

The study aims to examine the Schoolgen solar generation data to analyse the generation outputs and performance capacity of Schoolgen PV systems. In order

to do this, the net capacity factor was used to provide an indication for comparing the performance variability between Schoolgen schools. The capacity factor was calculated by dividing the actual PV generation output produced over a defined time period (one year basis in this study) by the maximum possible output of installed capacity rated for the system.

$$\textbf{Capacity factor} = \frac{\textbf{Amount of PV output in one year period}}{\left(\frac{\textbf{24hours}}{\textbf{day}}\right)\textbf{x 365 days x total installed capacity}} \; \boldsymbol{x}\; \textbf{100}\%$$

..... Equation 7

When it comes to solar energy as a renewable energy source, the capacity factor is generally observed in the range of around 15% when compared to other forms of generation. This is directly corresponding to the resource limitation of sunshine hours available for energy generation during the year. The capacity factor can be quite varied depending on the PV technology and locations. In this phase of the research, different types of PV technology were compared to determine the impact of influencing factors and operating conditions that affect the amount of energy generated by the PV systems in different locations of Schoolgen schools.

CHAPTER 6: MODEL VALIDATION RESULTS

This chapter shows the results obtained from the model validation methods. The modelling outcomes from Rooftop PVGen model for Schoolgen application were compared to the actual generation data. The performance prediction and analysis assessed the amount of PV generated by Schoolgen PV systems and the factors that affect the outputs. The analyses results are reported and discussed here in details.

6.1 Solar Modelling Results

The key modelling outcomes obtained from Rooftop PVGen model for Schoolgen application were the amount of annual average solar radiation incident (kWh/m²) on PV panels installed on each Schoolgen school's rooftop. This amount was obtained from the modelling output reports by performing solar simulation on PV-installed rooftop models using Ecotect solar access analysis described in section 5.2.3 (an example of results shown in Figure 5-9a and Figure 5-9b). This is a key variable used for applying into PV equation along with the distribution of panel area, performance ratio and module efficiency to calculate PV potential generation for the system. Table 6-1a and Table 6-1b display the summary of annual average solar radiation from total 66 modelling outputs in comparison to the solar radiation data supplied from the nearest NIWA weather station in similar timeframe.

Table 6-1a: Summary of solar modelling results of Schoolgen schools (2kW capacity installations)

	School	Location	Nearest NIWA station for solar data	Monitored data from NIWA Solar radiation kWh/m2/year (June2014-May2015)	Ecotect Modeling Results Annual average solar radiation on tilted plane kWh/m2/yr
1	Mangakahia Area School	Mangakahia	Whangarei	1550	**1441**
2	Wangarei Heads Primary School	Whangarei	Whangarei	1550	**1510**
3	Westlake Girls High School	North Shore	Mangere EWS	1550	**1627**
4	Northcote Collge	North Shore	Mangere EWS	1550	**1528**
5	Greenhithe Primary School	North Shore	North Shore	1551	**1550**
6	Glendowie College	Orakei	Mangere EWS	1551	**1501**
7	Pakuranga College	Horwick	Mangere EWS	1550	**1634**
8	Henderson Valley Primary School	Waitakere	Mangere EWS	1551	**1575**
9	Tirimoana Primary School	Waitakere	Mangere EWS	1550	**1542**
10	Silverdale Primary School	Albany	Mangere EWS	1550	**1550**
11	Hamilton Girls High School	Hamilton	Ruakura 2 EWS	1508	**1474**
12	Maeroa Intermediate School	Hamilton City	Ruakura 2 EWS	1507	**1534**
13	Fairfield College	Hamilton	Ruakura 2 EWS	1507	**1507**
14	Forest Lake Primary School	Hamilton	Ruakura 2 EWS	1507	**1486**
15	Matamata Primary School	Hamilton	Ruakura 2 EWS	1507	**1474**
16	St Pauls Collegiate	Hamilton	Ruakura 2 EWS	1507	**1449**
17	St Peter Chanel Catholic School	Hamilton	Ruakura 2 EWS	1507	**1486**
18	Vardon Primary School	Hamilton	Ruakura 2 EWS	1507	**1474**
19	Te Kowhai School	Te Kowhai	Ruakura 2 EWS	1507	**1474**
20	Mercury Bay Area School	Whitianga	Ruakura 2 EWS	1550	**1547**
21	Raglan Area School	Raglan	Ruakura 2 EWS	1507	**1474**
22	Taupo-nui-a-Tia College	Taupo	Ruakura 2 EWS	1507	**1488**
23	James Street School	Whakatane	Whakatane	No data	**1622**
24	Whakatane Intermediate School	Whakatane	Whakatane	No data	**1618**
25	Te Kura O Waikaremoana School	Hawkes Bay	Gisborne AWS	No data	**1632**
26	Napier Intermediate School	Napier	Napier Aero AWS	1598	**1547**
27	Pukehou School	Hastings	Napier Aero AWS	1598	**1513**
28	Hastings Intermediate School	Hastings	Napier Aero AWS	1621	**1568**
29	St Johns Hill Primary School	Wanganui	Palmerston North EWS	1406	**1567**
30	Wanganui Intermediate	Wanganui	Palmerston North EWS	1406	**1583**
31	Awahou School	Manawatu	Palmerston North EWS	1407	**1375**
32	Kimbolton School	Manawatu	Palmerston North EWS	1407	**1377**
33	Mount Bigg School	Manawatu	Palmerston North EWS	1406	**1362**
34	Aokautere School	Palmerston North	Palmerston North EWS	1406	**1383**
35	Hokowhitu School	Palmerston North	Palmerston North EWS	1407	**1377**
36	Newbury School	Palmerston North	Palmerston North EWS	1407	**1362**
37	St Anthony's Primary	Pahiatua	Palmerston North EWS	1406	**1479**
38	Paraparaumu Collge	Kapiti Coast	Wallaceville EWS	1840	**1393**
39	Douglas Park School	Masterton	Wallaceville EWS	1810	**1498**
40	Paremata School	Porirua	Wallaceville EWS	1840	**1495**
41	Plateau Primary School	Upper Hutt	Wallaceville EWS	1840	**1493**
42	Clifton Terrace Model School #1	Welllington City	Wallaceville EWS	1810	**1557**
43	Wadestown School	Welllington City	Wallaceville EWS	1840	**1493**
44	Eastern Hutt School	Lower Hutt	Wallaceville EWS	1810	**1489**
45	Muritai School	Lower Hutt	Wallaceville EWS	1810	**1467**
46	Raphael House	Lower Hutt	Wallaceville EWS	1840	**1493**
47	Bank Avenue School	Christchurch	Christchurch	1494	**1497**
48	Middleton Grange School	Christchurch	Christchurch	1494	**1490**
49	Sumner Primary School	Christchurch	Christchurch	1494	**1436**
50	Lake Tekapo School	Mackenzie	Tekapo	1687	**1583**

Table 6-1b: Summary of solar modelling results of Schoolgen schools (4kW capacity installations)

	School	Location	Nearest station for solar data	Monitored data from NIWA Solar radiation kWh/m2/year (June2014-May2015)	Ecotect Modeling Results Annual average solar radiation on tilted plane kWh/m2/yr
51	Bayswater Primary School	North Shore	Mangere EWS	1538	**1543**
52	Stanley Primary Bay School	North Shore	Mangere EWS	1550	**1559**
53	Takapuna Normal Intermediate	North Shore	Mangere EWS	1550	**1575**
54	May Road Primary School	Auckland	Mangere EWS	1542	**1597**
55	Amesbury School	Wellington City	Wallaceville EWS	1808	**1481**
56	Clifton Terrace Model School #2	Wellington City	Wallaceville EWS	1810	**1529**
57	Clyde Quay School	Wellington City	Wallaceville EWS	1810	**1536**
58	Hampton Hill School	Wellington City	Wallaceville EWS	1843	**1552**
59	Miramar North Primary School	Wellington City	Wallaceville EWS	1840	**1548**
60	Newlands Intermediate	Wellington City	Wallaceville EWS	1840	**1558**
61	Northland Primary School	Wellington City	Wallaceville EWS	1840	**1574**
62	Paparangi School	Wellington City	Wallaceville EWS	No data	**1438**
63	Ridgeway Primary School	Wellington City	Wallaceville EWS	1840	**1544**
64	Te Aro Primary School	Wellington City	Wallaceville EWS	1840	**1529**
65	Thorndon Primary School	Wellington City	Wallaceville EWS	1840	**1407**
66	Temuka Primary School	Temuka	Tekapo	1685	**1491**

The amount of annual average solar radiation calculated by Ecotect analyses showed different results to the solar radiation data from the NIWA weather station. While some values agreed well, the variations shown in the schools located around Kapiti Coast down to Lower Hutt (School #38 - School #46 for 2kW installation), and the Wellington City (school #55 - School #65 for 4kW installation). The modelling results were presented with relatively much lower amount than the supplied NIWA data from Wallaceville EWS station in Wellington City.

The reason for this discrepancy was the difference between the source of weather data used by Ecotect from various New Zealand climate stations (Figure 6-1) and the actual weather data used by Schoolgen. Ecotect software runs the solar simulations depending on the input parameters of location latitude and longitude to determine the solar radiation measured from the nearest site. This means Schoolgen and Ecotect could have the solar radiation amount calculated by weather data from different climate zones for some locations. In this case, Ecotect utilised the solar data from Manawatu (MW as shown in Figure 6-1) weather station which locates within closer range to the schools from Kapiti Coast to Lower Hutt area, rather than Wallaceville EWS station as used by Schoolgen.

While schools in Northshore area (school #3, #4, #51- #53) have Mangere EWS which is a long way away from Northshore recorded as the nearest weather station in the Schoolgen system. However, there was no discrepancy between two results for these Northshore schools because Ecotect also used Auckland weather data (AK in Figure 6-1) which is the same Mangere EWS as used by Schoolgen schools in Auckland.

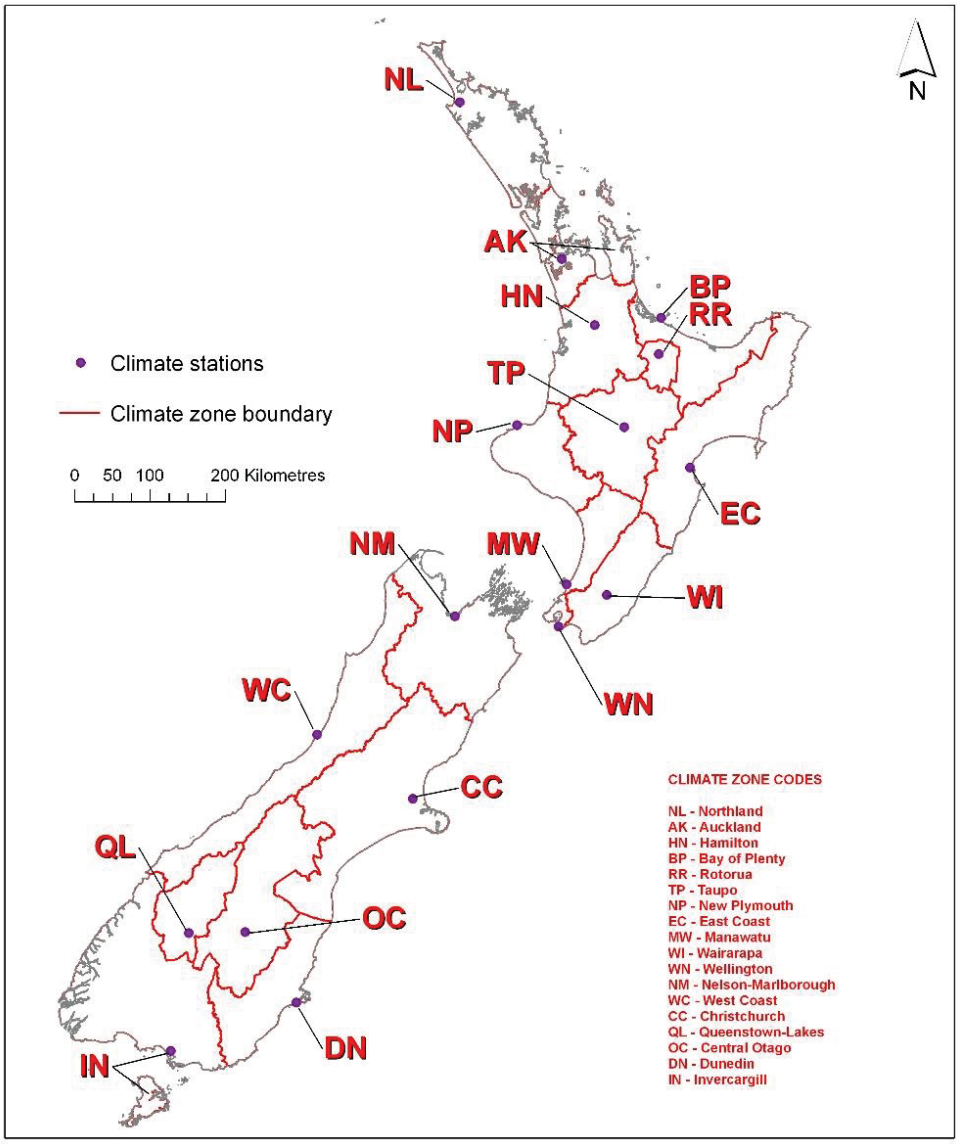

Figure 6-1: Map of New Zealand NIWA climate zones and weather stations utilized by the solar analysis function of Ecotect software (Source: Autodesk Ecotect Software)

The average solar radiation of schools positioned in similar climate zones is corresponding to the inclination and orientation of each individual system. These differed between schools. Schools had their PV panels installed parallel to the

existing roof pitch, which means there were variations in panel tilt angles between each site. The theoretically optimum tilt angle of a PV panel is the site's latitude facing north in order to capture most sun on the whole year basis. Therefore the optimum solar efficiency varies by the latitudinal influences of each location, and resulting in a variation of effectiveness when comparing solar radiation amount on panels installed at different Schoolgen sites.

6.2 Calculating Schoolgen PV Potential Generation

The calculation of PV potential generation for each Schoolgen system was obtained by applying the solar modelling results to Equation 3. The variables include the distribution of total panel area (m^2), and the module efficiency ratio, which was determined from the output capacity of a single panel (either 2kW or 4kW), divided by the area from the given dimension of each panel type. The calculated module efficiency and PV energy output result for each sample set is presented in Table 6-2a and Table 6-2b.

When examining each parameter obtained for PV potential calculation, the ratio of module efficiencies was varied by different manufacturers and types of material used. Because the panels come in various sizes, the distribution of the higher output capacity per surface area means more efficiency of the panel. When comparing the efficiency within types, the highest output panel was found to be the polycrystalline 'CSUN250-60P' model contained in four Schoolgen schools (school #1, #2, #23, #24) with 15.40% efficiency. Another polycrystalline type of 'Yingli YL250P-29b' model (installed in school #25, and all of the 4kW installations shown in Table 6-2b) also presented with a consistent efficiency yielding at 15.30% respectively. Other polycrystalline modules used in the majority of Schoolgen schools are 'Schott ASE-165-GT-FT/MCI 170W' model with relatively lower efficiency of 12.96%. While the 'Sharp NT-R5E3E polycrystalline' model installed at five Auckland schools (school #4, #5, #7, #9, #10) was comparable in the range of Schott model with a close 12.87% yield.

Table 6-2a (List of 2kW capacity installations): Calculation of PV generation potential by the proposed equation: Energy output (E) = Total panel area (A) x modelled annual average solar radiation (H) x Module Efficiency (r) x Performance Ratio (Pr)

	School	Location	Ecotect Modeling Results	Total PV panel area	Module efficiency	Performance Ratio	PV Energy output
			Annual average solar	(Size of a single panel	(Output capacity of a single	(Coefficient for system	(A x H x r x Pr)
			radiation on tilted plane	times total number of panels)	panel divided by single	losses, default value)	
					panel area)		
			kWh/m2/yr	m2	%		kWh/yr
			H	A	r	Pr	E
1	Mangakahia Area School	Mangakahia	1441	12.9888	15.40%	0.75	**2162**
2	Wangarei Heads Primary School	Whangarei	1510	12.9888	15.40%	0.75	**2264**
3	Westlake Girls High School	North Shore	1627	15.7464	12.96%	0.75	**2490**
4	Northcote Collge	North Shore	1528	16.3200	12.87%	0.75	**2407**
5	Greenhithe Primary School	North Shore	1550	16.3200	12.87%	0.75	**2441**
6	Glendowie College	Orakei	1501	15.7464	12.96%	0.75	**2297**
7	Pakuranga College	Horwick	1634	16.3200	12.87%	0.75	**2574**
8	Henderson Valley Primary School	Waitakere	1575	15.7464	12.96%	0.75	**2409**
9	Tirimoana Primary School	Waitakere	1542	16.3200	12.87%	0.75	**2429**
10	Silverdale Primary School	Albany	1550	16.3200	12.87%	0.75	**2441**
11	Hamilton Girls High School	Hamilton	1474	15.7464	12.96%	0.75	**2255**
12	Maeroa Intermediate School	Hamilton City	1534	15.7464	12.96%	0.75	**2347**
13	Fairfield College	Hamilton	1507	15.7464	12.96%	0.75	**2306**
14	Forest Lake Primary School	Hamilton	1486	15.7464	12.96%	0.75	**2273**
15	Matamata Primary School	Hamilton	1474	15.7464	12.96%	0.75	**2255**
16	St Pauls Collegiate	Hamilton	1449	15.7464	12.96%	0.75	**2217**
17	St Peter Chanel Catholic School	Hamilton	1486	15.7464	12.96%	0.75	**2273**
18	Vardon Primary School	Hamilton	1474	15.7464	12.96%	0.75	**2255**
19	Te Kowhai School	Te Kowhai	1474	15.7464	12.96%	0.75	**2255**
20	Mercury Bay Area School	Whitianga	1547	15.7464	12.96%	0.75	**2367**
21	Raglan Area School	Raglan	1474	15.7464	12.96%	0.75	**2255**
22	Taupo-nui-a-Tia College	Taupo	1488	15.7464	12.96%	0.75	**2277**
23	James Street School	Whakatane	1622	12.9888	15.40%	0.75	**2433**
24	Whakatane Intermediate School	Whakatane	1618	12.9888	15.40%	0.75	**2427**
25	Te Kura O Waikaremoana School	Hawkes Bay	1632	13.0680	15.30%	0.75	**2447**
26	Napier Intermediate School	Napier	1547	15.7464	12.96%	0.75	**2367**
27	Pukehou School	Hastings	1513	15.7464	12.96%	0.75	**2316**
28	Hastings Intermediate School	Hastings	1568	15.7464	12.96%	0.75	**2399**
29	St Johns Hill Primary School	Wanganui	1567	15.7464	12.96%	0.75	**2398**
30	Wanganui Intermediate	Wanganui	1583	15.7464	12.96%	0.75	**2421**
31	Awahou School	Manawatu	1375	15.7464	12.96%	0.75	**2103**
32	Kimbolton School	Manawatu	1377	15.7464	12.96%	0.75	**2106**
33	Mount Bigg School	Manawatu	1362	15.7464	12.96%	0.75	**2084**
34	Aokautere School	Palmerston North	1383	15.7464	12.96%	0.75	**2115**
35	Hokowhitu School	Palmerston North	1377	15.7464	12.96%	0.75	**2106**
36	Newbury School	Palmerston North	1362	15.7464	12.96%	0.75	**2084**
37	St Anthony's Primary	Pahiatua	1479	15.7464	12.96%	0.75	**2263**
38	Paraparaumu Collge	Kapiti Coast	1393	15.7464	12.96%	0.75	**2132**
39	Douglas Park School	Masterton	1498	15.7464	12.96%	0.75	**2292**
40	Paremata School	Porirua	1495	15.7464	12.96%	0.75	**2287**
41	Plateau Primary School	Upper Hutt	1493	15.7464	12.96%	0.75	**2285**
42	Clifton Terrace Model School #1	Welllington City	1557	15.7464	12.96%	0.75	**2382**
43	Wadestown School	Welllington City	1493	15.7464	12.96%	0.75	**2285**
44	Eastern Hutt School	Lower Hutt	1489	15.7464	12.96%	0.75	**2279**
45	Muritai School	Lower Hutt	1467	15.7464	12.96%	0.75	**2245**
46	Raphael House	Lower Hutt	1493	15.7464	12.96%	0.75	**2285**
47	Bank Avenue School	Christchurch	1497	22.8800	8.74%	0.75	**2246**
48	Middleton Grange School	Christchurch	1490	22.8800	8.74%	0.75	**2235**
49	Sumner Primary School	Christchurch	1436	22.8800	8.74%	0.75	**2154**
50	Lake Tekapo School	Mackenzie	1583	22.8800	8.74%	0.75	**2374**

Table 6-2b (List of 4kW capacity installations): Calculation of PV generation potential by the proposed equation: Energy output (E) = Total panel area (A) x modelled annual average solar radiation (H) x Module Efficiency (r) x Performance Ratio (Pr)

	School	Location	Ecotect Modeling Results	Total PV panel area	Module efficiency	Performance Ratio	PV Energy output
			Annual average solar	(Size of a single panel	(Output capacity of a single	(Coefficient for system	(A x H x r x Pr)
			radiation on tilted plane	times total number of panels)	panel divided by single	losses, default value)	
					panel area)		
			kWh/m2/yr	m2	%		kWh/yr
			H	A	r	Pr	E
51	Bayswater Primary School	North Shore	1543	26.136	15.30%	0.75	**4630**
52	Stanley Primary Bay School	North Shore	1559	26.136	15.30%	0.75	**4678**
53	Takapuna Normal Intermediate	North Shore	1575	26.136	15.30%	0.75	**4725**
54	May Road Primary School	Auckland	1597	26.136	15.30%	0.75	**4792**
55	Amesbury School	Wellington City	1481	26.136	15.30%	0.75	**4444**
56	Clifton Terrace Model School #2	Wellington City	1529	26.136	15.30%	0.75	**4588**
57	Clyde Quay School	Wellington City	1536	26.136	15.30%	0.75	**4607**
58	Hampton Hill School	Wellington City	1552	26.136	15.30%	0.75	**4655**
59	Miramar North Primary School	Wellington City	1548	26.136	15.30%	0.75	**4644**
60	Newlands Intermediate	Wellington City	1558	26.136	15.30%	0.75	**4673**
61	Northland Primary School	Wellington City	1574	26.136	15.30%	0.75	**4723**
62	Paparangi School	Wellington City	1438	26.136	15.30%	0.75	**4314**
63	Ridgeway Primary School	Wellington City	1544	26.136	15.30%	0.75	**4632**
64	Te Aro Primary School	Wellington City	1529	26.136	15.30%	0.75	**4587**
65	Thorndon Primary School	Wellington City	1407	26.136	15.30%	0.75	**4222**
66	Temuka Primary School	Temuka	1491	26.136	15.30%	0.75	**4474**

The least efficient panels presented among Schoolgen installations was the 'Auria M125000' model made of thin-film silicon material used in four South Island locations (school #47 - #50). The panel only yielded 8.74% efficiency which was almost half the output capacity of the highest efficiency type. As mention earlier in Section 5.1.2 for the description of Schoolgen PV systems, this thin-film silicon called micromorph was specifically designed to be more efficient than a traditional thin-film material. The intended purpose of the micromorph installation was to trial the performance of this technology in term of its efficiency, reliability and cost-effectiveness, in comparison to the conventional crystalline type (Schoolgen and NZ Power Company Genesis Energy, 2006-2015).

However, the efficiency of thin-film per m^2 was lower than the crystalline silicon type due to a much thinner layer of reduced material. Consequently a larger area was required to produce the same amount of power. The calculated PV

energy output showed that the schools with thin-film panels (school #47-#50) had consistent potential comparing to other schools that have the same amount of solar radiation. This resulted from the contribution of more area for panels installed. It was necessary to assess the actual generation data in order to determine the efficiency of micromorph technology by the performance of the system.

6.3 Comparison of Modelled Findings with Actual Generation

To assess the validity of the model, each modelled estimate (Table 6-2a and Table 6-2b) was compared to the generation output of Schoolgen data in 12 month period (from June 2014 – May 2015). The degree of accuracy was obtained by calculating the percentage error from the difference between the estimate and actual values (Math is Fun, 2014). The results are displayed in Table 6-3a and Table 6-3b.

A percentage error to zero means a higher of accuracy. Since the error value of measurement was obtained by subtracting the estimate from the actual value, a measure of quantity difference could be either a negative or positive integer. A negative error means an underestimation (when the estimate is too low, less than actual value), while a positive error indicates an overestimation (when the estimate is too high, more than actual value).

Table 6-3a Comparison of the modelled prediction with actual PV generation from Schoolgen data for 2kW capacity installations

	School	Location	Calculated amount of PV potential by modeled prediction kWh/yr (Estimate value)	Recorded amount of actual PV generation in one-year period (June 2014 - May 2015) kWh/yr (Actual value)	Difference between Estimate and actual value (Estimate - Actual)	Percentage Error (Estimate - Actual) x 100% Actual
1	Mangakahia Area School	Mangakahia	2162	2658	-496	**-18.66%**
2	Wangarei Heads Primary School	Whangarei	2264	2271	-7	**-0.29%**
3	Westlake Girls High School	North Shore	2490	2495	-5	**-0.22%**
4	Northcote Collge	North Shore	2407	2493	-86	**-3.45%**
5	Greenhithe Primary School	North Shore	2441	2592	-151	**-5.82%**
6	Glendowie College	Orakei	2297	2498	-201	**-8.05%**
7	Pakuranga College	Horwick	2574	2618	-44	**-1.69%**
8	Henderson Valley Primary School	Waitakere	2409	2429	-20	**-0.80%**
9	Tirimoana Primary School	Waitakere	2429	2567	-138	**-5.39%**
10	Silverdale Primary School	Albany	2441	2398	43	**1.80%**
11	Hamilton Girls High School	Hamilton	2255	2398	-143	**-5.97%**
12	Maeroa Intermediate School	Hamilton City	2347	2617	-270	**-10.30%**
13	Fairfield College	Hamilton	2306	2403	-97	**-4.04%**
14	Forest Lake Primary School	Hamilton	2273	2300	-27	**-1.18%**
15	Matamata Primary School	Hamilton	2255	2467	-212	**-8.60%**
16	St Pauls Collegiate	Hamilton	2217	2437	-220	**-9.01%**
17	St Peter Chanel Catholic School	Hamilton	2273	2521	-248	**-9.84%**
18	Vardon Primary School	Hamilton	2255	2435	-180	**-7.40%**
19	Te Kowhai School	Te Kowhai	2255	2340	-85	**-3.64%**
20	Mercury Bay Area School	Whitianga	2367	2703	-336	**-12.41%**
21	Raglan Area School	Raglan	2255	2760	-505	**-18.30%**
22	Taupo-nui-a-Tia College	Taupo	2277	2558	-281	**-10.98%**
23	James Street School	Whakatane	2433	2818	-385	**-13.66%**
24	Whakatane Intermediate School	Whakatane	2427	2999	-572	**-19.09%**
25	Te Kura O Waikaremoana School	Hawkes Bay	2447	2695	-248	**-9.19%**
26	Napier Intermediate School	Napier	2367	2911	-544	**-18.69%**
27	Pukehou School	Hastings	2316	2659	-343	**-12.92%**
28	Hastings Intermediate School	Hastings	2399	2134	265	**12.40%**
29	St Johns Hill Primary School	Wanganui	2398	2399	-1	**-0.05%**
30	Wanganui Intermediate	Wanganui	2421	2568	-147	**-5.71%**
31	Awahou School	Manawatu	2103	1994	109	**5.48%**
32	Kimbolton School	Manawatu	2106	2244	-138	**-6.14%**
33	Mount Bigg School	Manawatu	2084	2539	-455	**-17.91%**
34	Aokautere School	Palmerston North	2115	1472	643	**43.70%**
35	Hokowhitu School	Palmerston North	2106	2404	-298	**-12.39%**
36	Newbury School	Palmerston North	2084	2516	-432	**-17.16%**
37	St Anthony's Primary	Pahiatua	2263	2230	33	**1.50%**
38	Paraparaumu Collge	Kapiti Coast	2132	2438	-306	**-12.57%**
39	Douglas Park School	Masterton	2292	2106	186	**8.85%**
40	Paremata School	Porirua	2287	2563	-276	**-10.76%**
41	Plateau Primary School	Upper Hutt	2285	2414	-129	**-5.36%**
42	Clifton Terrace Model School #1	Welllington City	2382	2478	-96	**-3.88%**
43	Wadestown School	Welllington City	2285	2567	-282	**-11.00%**
44	Eastern Hutt School	Lower Hutt	2279	2199	80	**3.63%**
45	Muritai School	Lower Hutt	2245	2190	55	**2.52%**
46	Raphael House	Lower Hutt	2285	2514	-229	**-9.12%**
47	Bank Avenue School	Christchurch	2246	1704	542	**31.81%**
48	Middleton Grange School	Christchurch	2235	1602	633	**39.51%**
49	Sumner Primary School	Christchurch	2154	2069	85	**4.13%**
50	Lake Tekapo School	Mackenzie	2374	2428	-54	**-2.21%**

Table 6-3b: Comparison of the modelled prediction with actual PV generation from Schoolgen data for 4kW capacity installations

	School	Location	Calculated amount of PV potential by modeled prediction kWh/yr (Estimate value)	Recorded amount of actual PV generation in one-year period (June 2014 - May 2015) kWh/yr (Actual value)	Difference between Estimate and actual value (Estimate - Actual)	Percentage Error (Estimate - Actual) x 100% Actual
51	Bayswater Primary School	North Shore	4630	5764	-1134	**-19.68%**
52	Stanley Primary Bay School	North Shore	4678	4870	-192	**-3.95%**
53	Takapuna Normal Intermediate	North Shore	4725	5663	-938	**-16.57%**
54	May Road Primary School	Auckland	4792	4311	481	**11.16%**
55	Amesbury School	Wellington City	4444	5036	-592	**-11.75%**
56	Clifton Terrace Model School #2	Wellington City	4588	5280	-692	**-13.11%**
57	Clyde Quay School	Wellington City	4607	5046	-439	**-8.69%**
58	Hampton Hill School	Wellington City	4655	4551	104	**2.28%**
59	Miramar North Primary School	Wellington City	4644	5284	-640	**-12.12%**
60	Newlands Intermediate	Wellington City	4673	5431	-758	**-13.96%**
61	Northland Primary School	Wellington City	4723	5022	-299	**-5.96%**
62	Paparangi School	Wellington City	4314	5296	-982	**-18.55%**
63	Ridgeway Primary School	Wellington City	4632	5377	-745	**-13.85%**
64	Te Aro Primary School	Wellington City	4587	5280	-693	**-13.12%**
65	Thorndon Primary School	Wellington City	4222	4646	-424	**-9.12%**
66	Temuka Primary School	Temuka	4474	4910	-436	**-8.89%**

The percentage errors in Table 6-3a and Table 6-3b, shows that modelled calculated values were underestimated the actual generation amounts. The percentage errors ranged from -0.05% to 43.7%. The lowest error of -0.05% obtained for school #29 (only 1 kWh difference from the true value), which considered a very high accuracy of a modelled estimation. The largest underestimation was seen in school #51 with -19.68% (by 1,134 kWh difference). While the overestimation ranged from 1.5% to 43.7%. Of the 66 datasets, 25 estimations were measured with accuracy within the range of $\pm$6% percentage error and another 17 counts fall between $\pm$6.01% - $\pm$12% interval. This reflected the majority of small percentage errors obtaining from a relatively sufficient degree of precision in modelled estimations. The following graph summarises the frequency of occurrences that fall within each interval size of percentage error in absolute values (ignore minus sign).

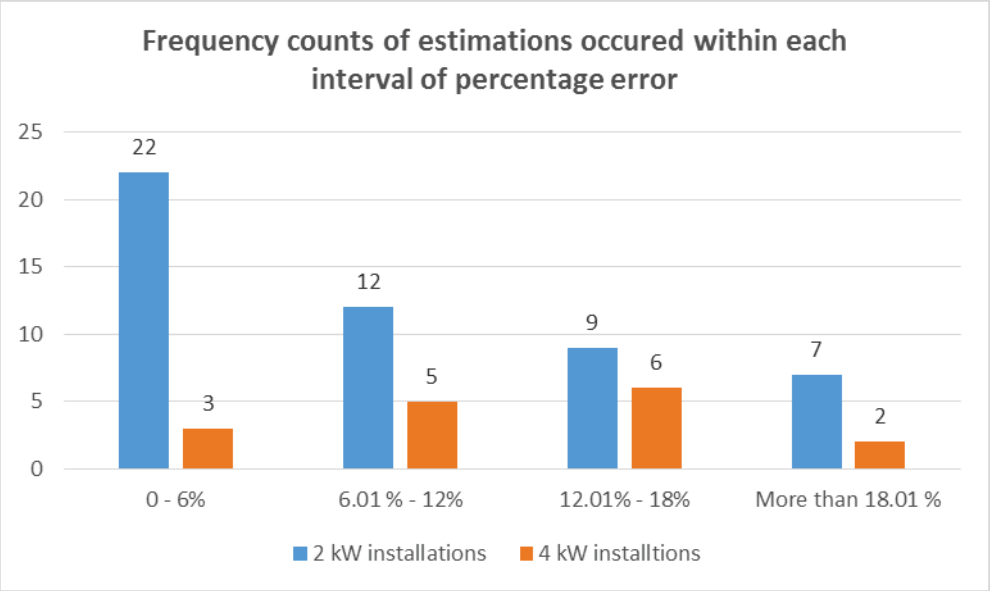

Figure 6-2: Frequency counts of occurrences by the number of estimations that fell within each interval size of percentage errors

From Table 6-3a and 6-3b, it can be noticed that among the 66 schools data set, 9 out of 50 from the list of 2kW installations and 2 out of 16 from the list of 4kW installations were positive errors which represented values of overestimation. However, some values had very large errors. This particularly appeared in school #34 in Palmerston North showing a highest overestimation error with 43.70%. Together with school #47 and #48 in Christchurch that indicated a relatively large error of 31.81% and 39.51% respectively.

In order to identify the possibilities for these unusually large errors, the study examined the actual generation data associated with these schools in comparison to other schools in similar climate zone. It was found that school #34 has actually produced significantly lower outputs comparing to the other two schools in Palmerston North (such as school #35, #36), which have the same type of panel installed in similar direction and inclination (Schott ASE-165-GT-FT/MCI 170W panels all installed north facing with 16º pitch for school #34, comparing to 15º and 12º pitch for school #35 and #36 respectively).

The main reason for these unusually low production amounts observed in the data can be explained by the outages related to electrical network issues or a disruption of schools underground network cable occurring at some point of system operation (Merz, 2009). Thus the periods that the Schoolgen systems have the performance affected by these operational issues were likely to be generated low production or registered with null values in Schoolgen database. While the cases of school #47 and #48 could be additionally affected by the low-efficiency type of thin-film micromorph panel used. However, the other two schools (#49 and #50) installed with similar technology were not observed with similarly high rate of prediction errors in the data. This discrepancy was addressed in more details through the analyses of each technology type.

6.4 Comparing Schoolgen Systems by Capacity Factor

The capacity factor of each school system was calculated to provide an indication of performance in its operating condition as a method for comparison between systems and the evaluations of the system themselves. The capacity factor is the ratio of an actual energy output over a given period to the maximum possible outputs if operated at full capacity for that entire period of time. Since there are several factors affecting the performance and energy generation outputs of a PV system, including the efficiency by the type of technology, seasonal variations, geographical location as well as orientation and inclination of the panels. In most cases, the capacity factors can vary greatly between systems due to these effects of variation in performance parameters. The capacity factor for the last 12 months period of Schoolgen data obtained in this study are displayed in Table 6-4a and 6-4b.

Table 6-4a: Capacity factor calculated for each Schoolgen schools for 2kW capacity installations

	School	Location	Direction of the roof Degree	Roof Pitch/ Panel Pitch Degree	Module efficiency (Output capacity of a single panel divided by single panel area)	Total installed capacity	Recorded amount of actual PV generation in one-year period (June 2014 - May 2015)	Capacity factor Actual generation Maximum Capacity (24 hours/day x 365 days x total installed capacity)
					%	W	kWh/yr	%
1	Mangakahia Area School	Mangakahia	N	15	15.40%	2000	2658	15.17%
2	Wangarei Heads Primary School	Whangarei	NE	20	15.40%	2000	2271	12.96%
3	Westlake Girls High School	North Shore	16º East of N	12	12.96%	2040	2495	13.96%
4	Northcote Collge	North Shore	5º West of N	12	12.87%	2100	2493	13.55%
5	Greenhithe Primary School	North Shore	N	27	12.87%	2100	2592	14.09%
6	Glendowie College	Orakei	25º West of N	45	12.96%	2040	2498	13.98%
7	Pakuranga College	Horwick	15º West of N	15	12.87%	2100	2618	14.23%
8	Henderson Valley Primary School	Waitakere	N	15	12.96%	2040	2429	13.59%
9	Tirimoana Primary School	Waitakere	5º East of N	15	12.87%	2100	2567	13.95%
10	Silverdale Primary School	Albany	N	15_27	12.87%	2100	2398	13.04%
11	Hamilton Girls High School	Hamilton	N	15	12.96%	2040	2398	13.42%
12	Maeroa Intermediate School	Hamilton City	N	15	12.96%	2040	2617	14.64%
13	Fairfield College	Hamilton	N	40	12.96%	2040	2403	13.45%
14	Forest Lake Primary School	Hamilton	N	20	12.96%	2040	2300	12.87%
15	Matamata Primary School	Hamilton	N	15	12.96%	2040	2467	13.80%
16	St Pauls Collegiate	Hamilton	N	10	12.96%	2040	2437	13.64%
17	St Peter Chanel Catholic School	Hamilton	N	20	12.96%	2040	2521	14.11%
18	Vardon Primary School	Hamilton	N	15	12.96%	2040	2435	13.63%
19	Te Kowhai School	Te Kowhai	N	15	12.96%	2040	2340	13.09%
20	Mercury Bay Area School	Whitianga	N	20	12.96%	2040	2703	15.13%
21	Raglan Area School	Raglan	N	15	12.96%	2040	2760	15.44%
22	Taupo-nui-a-Tia College	Taupo	5º East of N	45	12.96%	2040	2558	14.31%
23	James Street School	Whakatane	N	20	15.40%	2000	2818	16.08%
24	Whakatane Intermediate School	Whakatane	South	10_30	15.40%	2000	2999	17.12%
25	Te Kura O Waikaremoana School	Hawkes Bay	35º East of N	27	15.30%	2000	2695	15.38%
26	Napier Intermediate School	Napier	N	15	12.96%	2040	2911	16.29%
27	Pukehou School	Hastings	N	10	12.96%	2040	2659	14.88%
28	Hastings Intermediate School	Hastings	N	20	12.96%	2040	2134	11.94%
29	St Johns Hill Primary School	Wanganui	N	12	12.96%	2040	2399	13.42%
30	Wanganui Intermediate	Wanganui	N	15	12.96%	2040	2568	14.37%
31	Awahou School	Manawatu	N	15	12.96%	2040	1994	11.16%
32	Kimbolton School	Manawatu	N	15	12.96%	2040	2244	12.56%
33	Mount Bigg School	Manawatu	N	12	12.96%	2040	2539	14.21%
34	Aokautere School	Palmerston North	N	16	12.96%	2040	1472	8.24%
35	Hokowhitu School	Palmerston North	N	15	12.96%	2040	2404	13.45%
36	Newbury School	Palmerston North	N	12	12.96%	2040	2516	14.08%
37	St Anthony's Primary	Pahiatua	N	15	12.96%	2040	2230	12.48%
38	Paraparaumu Collge	Kapiti Coast	N	20	12.96%	2040	2438	13.64%
39	Douglas Park School	Masterton	N	25	12.96%	2040	2106	11.78%
40	Paremata School	Porirua	N	25	12.96%	2040	2563	14.34%
41	Plateau Primary School	Upper Hutt	N	30	12.96%	2040	2414	13.51%
42	Clifton Terrace Model School #1	Welllington City	20º East of N	15	12.96%	2040	2478	13.87%
43	Wadestown School	Welllington City	N	30	12.96%	2040	2567	14.36%
44	Eastern Hutt School	Lower Hutt	N	25	12.96%	2040	2199	12.31%
45	Muritai School	Lower Hutt	N	15	12.96%	2040	2190	12.25%
46	Raphael House	Lower Hutt	N	30	12.96%	2040	2514	14.07%
47	Bank Avenue School	Christchurch	N	20	8.74%	2000	1704	9.73%
48	Middleton Grange School	Christchurch	10º West of N	20	8.74%	2000	1602	9.14%
49	Sumner Primary School	Christchurch	NE	20	8.74%	2000	2069	11.81%
50	Lake Tekapo School	Mackenzie	N	25	8.74%	2000	2428	13.86%

Table 6-4b: Capacity factor calculated for each Schoolgen schools for 4kW capacity installations

	School	Location	Direction of the roof Degree	Roof Pitch/ Panel Pitch Degree	Module efficiency (Output capacity of a single panel divided by single panel area)	Total installed capacity	Recorded amount of actual PV generation in one-year period (June 2014 - May 2015)	Capacity factor Actual generation / Maximum Capacity (24 hours/day x 365 days x total installed capacity)
					%	W	kWh/yr	%
51	Bayswater Primary School	North Shore	N	20	15.30%	4000	**5764**	**16.45%**
52	Stanley Primary Bay School	North Shore	22º East of N	35	15.30%	4000	**4870**	**13.90%**
53	Takapuna Normal Intermediate	North Shore	30º East of N	15	15.30%	4000	**5663**	**16.16%**
54	May Road Primary School	Auckland	17º East of N	15	15.30%	4000	**4311**	**12.30%**
55	Amesbury School	Wellington City	44º West of N	10	15.30%	4000	**5036**	**14.37%**
56	Clifton Terrace Model School #2	Wellington City	20º East of N	15	15.30%	4000	**5280**	**15.07%**
57	Clyde Quay School	Wellington City	22º East of N	23	15.30%	4000	**5046**	**14.40%**
58	Hampton Hill School	Wellington City	10º East of N	12	15.30%	4000	**4551**	**12.99%**
59	Miramar North Primary School	Wellington City	25º East of N	26	15.30%	4000	**5284**	**15.08%**
60	Newlands Intermediate	Wellington City	10º East of N	14	15.30%	4000	**5431**	**15.50%**
61	Northland Primary School	Wellington City	3º West of N	23	15.30%	4000	**5022**	**14.33%**
62	Paparangi School	Wellington City	N	10	15.30%	4000	**5296**	**15.11%**
63	Ridgeway Primary School	Wellington City	19º East of N	20	15.30%	4000	**5377**	**15.35%**
64	Te Aro Primary School	Wellington City	45º East of N	25	15.30%	4000	**5280**	**15.07%**
65	Thorndon Primary School	Wellington City	68º East of N	30	15.30%	4000	**4646**	**13.26%**
66	Temuka Primary School	Temuka	17º East of N	13	15.30%	4000	**4910**	**14.01%**

In examining the performance of systems to identify any relationship between the variables of location and the efficiency by PV technology type, the capacity factors of systems with the same technology installed were compared to find the output characteristics influenced by the operating conditions within the same region. While most values of capacity factor for Schoolgen systems obtained in this study were in the range between 11.16% - 17.12%, which was comparable to the expected measures of current technology efficiency. One school had an unusually low production of only 8.24% capacity factor (school #34). When comparing to other schools with similar type of panel technology and climate location, this is presumably due to the related outages from operational issues discussed in previous section. For another reported cases of low capacity factor in school #47 and #48 with 9.73% and 9.14% respectively, these schools were investigated in relation to school #49 for having similarly low efficiency type of thin-film micromorph panels installed within the same Christchurch location. It was found that school #49 also performed at relatively low capacity with only a slightly higher production than the other two (11.81%). While another micromorph thin-film installed at school #50 in Mackenzie (Lake Tekapo district

location) tends to perform better with a capacity factor obtained in the range consistent to other high performance technology type. Therefore, it can be concluded that this thin-film micromorph panels are not very effective in Christchurch climate condition.

As expected, the most efficient type of polycrystalline panels of 'CSUN250-60P' model by 15.40% efficiency rate used in school #1, #2, #23, #24 generally performed better. This was evident in school #24 which achieved the highest capacity factor of 17.12% out of all Schoolgen schools over the last 12 months period. Moreover, the same panel located in Whakatane (16.08% and 17.12%) appears to perform slightly better compared the ones in the upper area of North Island (Whangarei with 12.96% and 15.17%). However, when comparing between 'Yingli YL250P-29b' models of 15.30% module rated efficiency, the results showed a consistency in capacity factor values in the range of 12.99% - 15.50% for schools in Wellington City, Hawkes Bay and Temuka in South Island. While schools in North Shore/Auckland show slightly more variation by 12.30% -16.45% range, providing with higher capacity factors achieved in two North Shore schools suggesting that the systems in this area of North Island tends to perform slightly better than schools in southern locations by this type of panel.

The majority of Schoolgen schools have 'Schott ASE-165-GT-FT/MCI 170W' model of polycrystalline panels installed with efficiency of 12.96%. These systems show consistency in capacity factor values ranging from 12.87% - 14.64% between schools located in the northern part of New Zealand from North Shore to Hamilton down to Te Kowhai and Taupo. However, two schools (school #20 in Whitianga and school #21 in Raglan) have achieved the capacity factors of 15.13% and 15.44% respectively which is relatively higher than other schools with similar panel type. While five schools using slightly lower efficiency panels with 12.87% rating by 'Sharp NT-R5E3E polycrystalline' model in North Shore down to Albany locations have also presented with a consistent range of 13.04% - 14.23% to 'Schott ASE-165-GT-FT/MCI 170W' model panels in similar locations.

There were more variations in the southern parts of North Island schools with 12.96% efficiency type of 'Schott ASE-165-GT-FT/MCI 170W' panels. While school #26 in Napier has a significantly high capacity factor of 16.29%, this level was comparable to the capacity factors generated by the high efficiency type of panels. Considering the zoning from Hastings to Wanganui with capacity factors ranging from 11.94% - 14.88% to the lower area of Manawatu, Palmerston North and Pahiatua with 11.16% - 14.21% (excluding exceptionally low production in school #34) and down to Kapiti Coast, Masterton, Wellington and Lower Hutt with 11.78% - 14.36%, it can be seen that these systems perform at a relatively consistent rate of productions, and have little influence by locations to the capacity factor values.

6.5 Schoolgen PV Analysis - Findings and Discussion

This section discusses the findings of the results as well as the outcomes in relation to the research objectives**.** From the second strand of the research, the study proposes Rooftop PVGen model by merging computer-simulation techniques and PV modelling, combining mathematical equations (Equation 5) for calculating the potential generation of rooftop PV systems. In order to test the reliability of the modelling outcomes, the second case used existing energy generation data of the PV systems installed for schools around New Zealand within Schoolgen programme. The accuracy of the model was evaluated by the comparison of the modelled output potential against the actual generation recorded by the Schoolgen data, to determine the capabilities of the analysis tools being used into predicting the amount of PV energy output. The capacity factor based on the actual generation data of each system was calculated to provide an indication of performance and the better understanding of operating conditions that affect the amount of energy generation of these PV systems.

6.5.1 Modelling Solar Radiation

Based on the operational characteristics of a PV system that are highly dependent on the solar radiation amount available on the panel surface, the study

focused on the impact of solar radiation as the indication of viability of the system. The device structure and installation parameters of each Schoolgen system were used for digitizing a PV rooftop model which was applied through a range of solar access analysis functionalities of computer-simulation to calculate solar radiation under the operating conditions in the context of selected location and environment.

The task of creating the total of 66 Schoolgen PV rooftop models was a time-consuming process in this study. As Ecotect solar simulation uses the geographical information to integrate with the building height, panel tilt in relation to roof angle, and orientation which vary among systems. Therefore each rooftop model needed to be manually digitised according to this variation which greatly contributed to the processing time required to generate every Schoolgen rooftop sample.

The output from each model analyses was an annual average amount of solar radiation in Watt-hours per square meter area which was converted into kilowatts-hours in order to allow the comparison to Schoolgen unit. The simulation performance of the model was compared with the solar radiation data supplied from the nearest NIWA weather station. The results showed that the predictions agree well with the monitored data in most PV locations. The modelling output variations between systems can be explained by the effects of location and installation parameters that clearly influenced the incoming radiation amount of the site. While the differences derived from the weather data sources used by the software for the selected location and the NIWA station used in the Schoolgen database. The Schoolgen data only provides an indicative figure of solar radiation supplied for the whole region rather than monitoring the solar radiation amount retrieved by the PV panels themselves.

6.5.2 PV Performance Prediction

In order to analyses to assess and compare the modelled findings with the actual generation amount, the modelled averaged solar radiation was used to predict the annual averaged amount of PV output potential along with other variables required by the mathematical equation proposed in this study. The system parameters including size, panel type and efficiency were included into analysis. While there are two main types of PV panels installed at various Schoolgen schools - the polycrystalline silicon and the micromorph thin-film panels, there are also three variations of PV manufacturers which presented a significant difference in panel efficiency among Schoolgen systems.

The PV output potential estimated in this study based on the modelled average solar radiation and the efficiency of the module technology installed for each school, together with the distribution of panel area and the performance ratio which were taken into account the different type of losses associated with the system's ability to deliver performance. The analysis assumed the performance ratio to a default value of 0.75 as the coefficient for system losses associated for Schoolgen systems. The calculations of PV potential reveal varied results between locations and types of PV technology. The key findings of model accuracy by the measure of percentage error showed that the modelled calculated PV energy significantly underestimate the actual production recorded by most Schoolgen systems. Of all the 66 samples, 55 were underestimates with the size of errors varied from the value as accurate as -0.05% to a large error of -19.68%. 25 out of 66 estimations showed percentage errors within $\pm$6% which demonstrated high accuracy of the model. Among the overestimated calculations, 3 Schoolgen schools have been found to be producing at significantly less than overall expectations. These unusually low productions incurred in the data were determined to be the period when the systems were affected from the outages related to network issues and consequently disrupting PV production.

6.5.3 Performance Ratio

When taking the difference between modelled estimates and the actual production into account, it is important to remember that the calculation assumed the performance ratio of 0.75. This default value chosen was found to significantly reduce the estimate output and consequently underestimate the actual performance. Since the performance ratio of a PV installation is the ratio of the actual energy yields which includes the coefficient for losses that may arise from the state of operation. In this study, the performance ratio value used in the formula into calculating the PV output potential was a default value typically used in many related studies and industry professionals based on the assumption of potential losses associated with PV production. However, as it was observed that the majority of modelled estimates were lower than the actual productions. This indicated that most Schoolgen PV systems were operating at higher capacities than predicted by this level of system losses. In order to test the model accuracy in comparison to Schoolgen production, the performance ratio was calculated to see the level in which Schoolgen systems were operating. The following Table 6-5a and 6-5b provides some indications of performance ratio calculated from the modelled average solar radiation to meet the actual production level of the last 12 months by Schoolgen systems.

Table 6-5a: The calculation to determine the value of the performance ratio on the basis of modelled solar radiation to meet the actual production level of Schoolgen systems for 2kW installations

	School	Location	Recorded amount of actual PV generation in one-year period (June 2014 - May 2015)	Ecotect Modeling Results Annual average solar radiation on tilted plane	Total PV panel area (Size of a single panel mes total number of panels	Module efficiency (Output capacity of a single panel divided by single panel area)	Calculated Performance Ratio ((E/H)/A)/r
			kWh/yr	kWh/m2/yr	m2	%	
			E	H	A	r	Pr
1	Mangakahia Area School	Mangakahia	**2658**	1441	12.9888	15.40%	**0.92**
2	Wangarei Heads Primary School	Whangarei	**2271**	1510	12.9888	15.40%	**0.75**
3	Westlake Girls High School	North Shore	**2495**	1627	15.7464	12.96%	**0.75**
4	Northcote Collge	North Shore	**2493**	1528	16.3200	12.87%	**0.78**
5	Greenhithe Primary School	North Shore	**2592**	1550	16.3200	12.87%	**0.80**
6	Glendowie College	Orakei	**2498**	1501	15.7464	12.96%	**0.82**
7	Pakuranga College	Horwick	**2618**	1634	16.3200	12.87%	**0.76**
8	Henderson Valley Primary School	Waitakere	**2429**	1575	15.7464	12.96%	**0.76**
9	Tirimoana Primary School	Waitakere	**2567**	1542	16.3200	12.87%	**0.79**
10	Silverdale Primary School	Albany	**2398**	1550	16.3200	12.87%	**0.74**
11	Hamilton Girls High School	Hamilton	**2398**	1474	15.7464	12.96%	**0.80**
12	Maeroa Intermediate School	Hamilton City	**2617**	1534	15.7464	12.96%	**0.84**
13	Fairfield College	Hamilton	**2403**	1507	15.7464	12.96%	**0.78**
14	Forest Lake Primary School	Hamilton	**2300**	1486	15.7464	12.96%	**0.76**
15	Matamata Primary School	Hamilton	**2467**	1474	15.7464	12.96%	**0.82**
16	St Pauls Collegiate	Hamilton	**2437**	1449	15.7464	12.96%	**0.82**
17	St Peter Chanel Catholic School	Hamilton	**2521**	1486	15.7464	12.96%	**0.83**
18	Vardon Primary School	Hamilton	**2435**	1474	15.7464	12.96%	**0.81**
19	Te Kowhai School	Te Kowhai	**2340**	1474	15.7464	12.96%	**0.78**
20	Mercury Bay Area School	Whitianga	**2703**	1547	15.7464	12.96%	**0.86**
21	Raglan Area School	Raglan	**2760**	1474	15.7464	12.96%	**0.92**
22	Taupo-nui-a-Tia College	Taupo	**2558**	1488	15.7464	12.96%	**0.84**
23	James Street School	Whakatane	**2818**	1622	12.9888	15.40%	**0.87**
24	Whakatane Intermediate School	Whakatane	**2999**	1618	12.9888	15.40%	**0.93**
25	Te Kura O Waikaremoana School	Hawkes Bay	**2695**	1632	13.0680	15.30%	**0.83**
26	Napier Intermediate School	Napier	**2911**	1547	15.7464	12.96%	**0.92**
27	Pukehou School	Hastings	**2659**	1513	15.7464	12.96%	**0.86**
28	Hastings Intermediate School	Hastings	**2134**	1568	15.7464	12.96%	**0.67**
29	St Johns Hill Primary School	Wanganui	**2399**	1567	15.7464	12.96%	**0.75**
30	Wanganui Intermediate	Wanganui	**2568**	1583	15.7464	12.96%	**0.80**
31	Awahou School	Manawatu	**1994**	1375	15.7464	12.96%	**0.71**
32	Kimbolton School	Manawatu	**2244**	1377	15.7464	12.96%	**0.80**
33	Mount Bigg School	Manawatu	**2539**	1362	15.7464	12.96%	**0.91**
34	Aokautere School	Palmerston North	**1472**	1383	15.7464	12.96%	**0.52**
35	Hokowhitu School	Palmerston North	**2404**	1377	15.7464	12.96%	**0.86**
36	Newbury School	Palmerston North	**2516**	1362	15.7464	12.96%	**0.91**
37	St Anthony's Primary	Pahiatua	**2230**	1479	15.7464	12.96%	**0.74**
38	Paraparaumu Collge	Kapiti Coast	**2438**	1393	15.7464	12.96%	**0.86**
39	Douglas Park School	Masterton	**2106**	1498	15.7464	12.96%	**0.69**
40	Paremata School	Porirua	**2563**	1495	15.7464	12.96%	**0.84**
41	Plateau Primary School	Upper Hutt	**2414**	1493	15.7464	12.96%	**0.79**
42	Clifton Terrace Model School #1	Welllington City	**2478**	1557	15.7464	12.96%	**0.78**
43	Wadestown School	Welllington City	**2567**	1493	15.7464	12.96%	**0.84**
44	Eastern Hutt School	Lower Hutt	**2199**	1489	15.7464	12.96%	**0.72**
45	Muritai School	Lower Hutt	**2190**	1467	15.7464	12.96%	**0.73**
46	Raphael House	Lower Hutt	**2514**	1493	15.7464	12.96%	**0.83**
47	Bank Avenue School	Christchurch	**1704**	1497	22.8800	8.74%	**0.57**
48	Middleton Grange School	Christchurch	**1602**	1490	22.8800	8.74%	**0.54**
49	Sumner Primary School	Christchurch	**2069**	1436	22.8800	8.74%	**0.72**
50	Lake Tekapo School	Mackenzie	**2428**	1583	22.8800	8.74%	**0.77**

Table 6-5b: The calculation to determine the value of the performance ratio on the basis of modeled solar radiation to meet the actual production level of Schoolgen systems for 4kW installations

	School	Location	Recorded amount of actual PV generation in one-year period (June 2014 - May 2015)	Ecotect Modeling Results Annual average solar radiation on tilted plane	Total PV panel area (Size of a single panel imes total number of panels	Module efficiency Output capacity of a single panel divided by single panel area)	Calculated Performance Ratio ((E/H)/A)/r
			kWh/yr	kWh/m2/yr	m2	%	
			E	H	A	r	Pr
51	Bayswater Primary School	North Shore	**5764**	1543	26.136	15.30%	**0.93**
52	Stanley Primary Bay School	North Shore	**4870**	1559	26.136	15.30%	**0.78**
53	Takapuna Normal Intermediate	North Shore	**5663**	1575	26.136	15.30%	**0.90**
54	May Road Primary School	Auckland	**4311**	1597	26.136	15.30%	**0.67**
55	Amesbury School	Wellington City	**5036**	1481	26.136	15.30%	**0.85**
56	Clifton Terrace Model School #2	Wellington City	**5280**	1529	26.136	15.30%	**0.86**
57	Clyde Quay School	Wellington City	**5046**	1536	26.136	15.30%	**0.82**
58	Hampton Hill School	Wellington City	**4551**	1552	26.136	15.30%	**0.73**
59	Miramar North Primary School	Wellington City	**5284**	1548	26.136	15.30%	**0.85**
60	Newlands Intermediate	Wellington City	**5431**	1558	26.136	15.30%	**0.87**
61	Northland Primary School	Wellington City	**5022**	1574	26.136	15.30%	**0.80**
62	Paparangi School	Wellington City	**5296**	1438	26.136	15.30%	**0.92**
63	Ridgeway Primary School	Wellington City	**5377**	1544	26.136	15.30%	**0.87**
64	Te Aro Primary School	Wellington City	**5280**	1529	26.136	15.30%	**0.86**
65	Thorndon Primary School	Wellington City	**4646**	1407	26.136	15.30%	**0.83**
66	Temuka Primary School	Temuka	**4910**	1491	26.136	15.30%	**0.82**

It can be seen from the tables that the Schoolgen systems were operating in the range between 0.52 – 0.93 level of performance ratio. When assessing the performance ratio according to each type of panel to determine the range in which each specific type of panel was operating, the performance ratio of the polycrystalline 'CSUN250-60P' model contained in four Schoolgen schools (school #1, #2, #23, #24) with 15.40% efficiency was found to be in the highest range between 0.75 – 0.93. While another polycrystalline type of 'Yingli YL250P-29b' model (installed in school #25, and all of the 4kW installations shown in Table 6-2b) with 15.30% efficiency had the majority of systems operating between 0.78 – 0.93, and only 2 out of 17 systems were operating at lower than 0.75 (school #54 and #58 at 0.67 and 0.73 respectively). Another polycrystalline modules 'Schott ASE-165-GT-FT/MCI 170W' model with lower efficiency of 12.96% was operating within 0.75 – 0.92 with 7 out of 36 schools were operating at lower than 0.75 (0.67 – 0.74). While the 'Sharp NT-R5E3E polycrystalline' model installed at five Auckland schools (school #4, #5, #7, #9, #10) with 12.87% yield was in 0.74 – 0.80 range. The least efficient panels 'Auria

M125000' model made of thin-film silicon material used in four South Island locations (school #47 - #50) was found operating at the lowest 0.54– 0.77 range.

As the study assumed the performance ratio of 0.75 for calculating PV potential in Section 6.2 as shown in Table 6-2a and 6-2b, thus indicating the reason why the majority of Schoolgen systems operating at over 0.75 performance ratio were found to be underestimated by the modelled estimations. In order to improve the model accuracy, the performance ratio could be adjusted according to each type of panel efficiency. The ability to set a more accurate performance ratio according to each system type will minimise prediction errors and improve the reliability of the modelling outcome.

6.5.4 Schoolgen Performance Indication from Capacity Factor

The efficiency of a PV system depends on its ability to generate expected amounts of output according to the potential rated capacity. In this case, the capacity factor from the actual generation was calculated to evaluate and compare the performance between each Schoolgen system over the one-year period operations. This method of comparison was chosen due to the availability of the data appropriate for the calculation, to providing for an indication of performance by the generated output against the maximum capacity measured by the number of hours in the specified time-period.

Set against this background, the capacity factor was generally low when it comes to solar technology due to the unused capacity from the limitation of sunshine hours. Other reasons for reduced capacity factors were related to the variability of solar radiation available during the peak sunshine periods. In this case, Schoolgen performance results represented capacity factor values in the range between 11.16% - 17.12%. The correlation between the panel efficiency and the capacity factor can be seen where the higher efficiency type of module tends to perform better in certain location. Most Schoolgen systems have consistency in capacity factors ranged more or less within $\pm$2% of their module

efficiency. The higher capacity factors were achieved in schools in northern locations These PV systems performed better than schools in southern locations with the same type of panel.

CHAPTER 7: CONCLUSIONS

This chapter concludes the research study with the key findings and the overall outcomes in relation to the research objectives. It provides the summary of the analytical approaches used into developing Rooftop PVGen model. The chapter highlights the key contributions of the corresponding methods employed for model validation and data comparison in this study. The conclusion is outlined with the recommendations for the area of improvements and the indications to the future analysis opportunities in this area.

7.1 Case Study 1 - Solar Harvesting Potential from Roofs of Invercargill Homes

The first strand of the research investigated the solar harvesting potential that can be made available for photovoltaic (PV) system on existing residential rooftops of a city in New Zealand. Using Invercargill as a case study, the study evaluated the opportunities in the existing housing stock, and explored the potential capacity of large-scale PV deployments to inform the way to achieve the energy sustainability by the residential sector.

From this purpose, the study developed Rooftop PVGen model for predicting solar harvesting potential of residential rooftops that is applicable for large-scale analysis. The work provided a high level overview and a collation of activities required for obtaining rooftop data of a whole city. The method involved merging computer-simulation of solar energy produced from PV modelling and mapping incoming solar radiation data from north facing residential rooftop area. The work utilised New Zealand statistical census map of population and dwelling data, as well as digital aerial map to quantify the efficient roof surface area available for PV installations. The solar PV potential was calculated using existing formulas to investigate the contribution of roof area to the solar PV potential in buildings using roof area and population relationship.

The study compared the potential of large-scale solar PV production of all the residential sites in the study area with the total energy consumption in the residential sector. The amount of solar PV potential of 82,947,315 kWh per year was estimated from the total solar efficient roof surfaces of 740,504 m^2. This equates to approximately 60.8% of the residential electricity used in Invercargill's urban area, based on the 7,700 kWh typical annual electricity consumptions per household. The result represents an immense opportunity to harvest sustainable energy from Invercargill's residential rooftops.

The study provided a structured approach to meet the research objectives. The presented methodology served as a repository of information for a set of principle techniques and analysis tools, to guide the assessment of solar harvesting potential and the application of rooftop PV system. The development of Rooftop PVGen model based on the use of indicative criteria and relevant database information enables the estimation of roof area for a large-scale PV potential from current capabilities of the resource available in the public domain. The model can be customised for predicting this potential from rooftops in different geographical locations by applying the information specific to the analysis area. Base on the size of this study area, an understanding of the large-scale distribution of roof area for PV potential have implications on urban form and energy access of the region. This will also inform future research in the development of distributed generation by solar PV from geographical potential across New Zealand.

7.2 Case Study 2 – Model Validation using Existing Data from PV Generation on Selected New Zealand Schools

The second strand of the research focused on the validation of the model and the analysis tools proposed in Case Study 1. The work undertaken involved the calculation of rooftop PV potential from grid-connected solar photovoltaic (PV) systems that are installed in New Zealand schools under the Schoolgen programme. Access to Schoolgen database allowed the analysis of electricity

generation and performance capacity of each PV system in the actual state of operations. The accuracy of the modelling outcomes was evaluated by the comparison of the modelled output potential against the actual generation recorded by the Schoolgen data using the measure of percentage error. The capacity factor based on the actual generation data of each system was calculated to provide for an indication of performance and the better understanding of operating conditions that affect the amount of energy generated by the PV systems.

A step-by-step procedure of Rooftop PVGen Model was applied to calculate the potential PV generation of Schoolgen PV systems. The total of 66 Schoolgen PV rooftop models was incorporated in the analysis. The modelled averaged solar radiation was conducted to predict the annual averaged amount of PV output potential by using the variables of the relevant equation. At this stage, the actual system parameters including size, panel type and efficiency were also included in the analysis.

A comparison of the predicted outputs with the actual outputs showed that the model significantly underestimate the actual production recorded by most Schoolgen systems. Of all the 66 samples, 55 were underestimates with the size of errors vary from a value as accurate as -0.05% to a large error of -19.68%. The total 25 estimations were measured with accuracy within the range of $\pm$6% percentage error, and another 17 counts fall between $\pm$6.01% - $\pm$12% interval. This reflected the majority of small percentage errors which demonstrated the high accuracy of modelled estimations. The majority of Schoolgen systems operating at over 0.75 performance ratio were found to be underestimated. This indicated that most Schoolgen PV systems were operating at higher capacities than predicted by this level of system losses.

The research also focused on the analysis of PV performance based on the variables of system specifications to identify the baseline for current progress as

well as potential barriers in the implementation. The results have provided some key indications of the system parameters that affect performance. The analysis showed the effects of PV technology type, site orientation, direction and tilted angle of the panels on the ability to generate expected amount of potential capacity. Understanding the variations of energy output based on solar resource availability in different site scenarios was particularly helpful in identifying the strengths and weaknesses of each system deployment. This in turn has provided more in depth analysis of the research and served to expand the area for improvements in the design of the model.

7.3 Recommendations for Future Work

As the Rooftop PVGen Model was designed to overcome the lack of available data, the findings were obtained from the methodology based on simplifications of the overall performance of the system design and other associated component factors adopted in the proposed equation for the practicability of the analysis. In this case, a number of opportunities have surfaced throughout the analytical process in the area for improvements to reduce the uncertainties that inherent in the process. Particularly the effects of the default value of the 0.75 performance ratio which was found to significantly reduce the estimate output and consequently underestimate the actual performance. With an appropriate method to identify the input parameters, it will be possible to optimise the overall quality of the results. The future analysis of the solar harvesting potential throughout a city should move beyond the assumption of performance ratio and module capacity, to the use of data based on the actual size, panel type and efficiency according site-specific access to resources. The influence of topography and system temperature could also be taken into account. The ability to do this will overcome the inconclusive point of data and minimise prediction errors for future PV analysis.

Due to a need for a site-specific PV analysis model to identify the potential savings and financial returns on investment to assist in decision-making process, the economic implication of the grid-connected PV system should also be

assessed more specifically on the quantity of power output that is used on-site to offset the purchased energy and the quantity that is injected to the grid. As the proposition of the PV system varies according to the system type and application in the contribution of energy use, the operational issues related to the nature of daytime energy usage pattern and domestic loads should be investigated to add into the basis of energy demand predictions. Future research can take into consideration the indicative factors that affect performance and energy production pattern to inform the economic aspect of the analysis. This would allow the incorporation of significant variables in the development of a more appropriate energy prediction model and a decision-support system to evaluate the technical and economic viability that a PV system can contribute towards the electricity savings in the future.

REFERENCES

Adaramola, M. S. (2014). The effects of solar panel temperature on the power output efficiency Calabar, Nigeria. *Journal of Association of Radiographers of Nigeria*, 23(2009), 16-22.

Amado, M. & Poggi, F. (2014). Solar urban planning: a parametric approach. *Energy Procedia*, 48, 1539-1548.

Araya-Munoz et al. (2014). Araya-Munoz, D., Carvajal, D., Saez-Careeno, A., Bensaid, S., Soto-Marquez, E. Assessing the solar potential of roofs in Valparaiso (Chile). *Energy and Buildings*, 69, 62-73.

Armstrong, M. & Ryan, V. (2009). Matching renewable technology to local resources and the household and neighbourhood level. Report EN6590/4 for Beacon Pathway Limited.

Arnette, A. (2013). Integrating rooftop solar into a multi-source energy planning optimization model. *Applied Energy*, 111, 456-467.

Australian Government (n.d.). National Solar School Program. Department of Industry and Science. Retrieved April, 2015 from http://www.industry.gov.au/ENERGY/PROGRAMMES/SOLARSCHOOLSPROGRAM/Pages/default.aspx

Ayompe et al. (2010). Ayompe, L., Duffy, A., McCormack, S., & Conlon, M. Projected costs of a grid connected domestic PV system under different scenarios in Ireland, using measured data from a trial installation. *Energy Policy*, 38, 3731-3743.

Baker et al. (2013). Baker, E., Fowlie, M., Lemoine, D., Reynolds, S. The economics of solar electricity. Retrieved March, 2015 from https://ei.haas.berkeley.edu/research/papers/WP240.pdf

Branker et al. (2011). Branker, K., Pathak, M., Pearce, J.M. A review of solar photovoltaic levelized cost of electricity. *Renewable and Sustainable Energy Reviews*, 15, 4470-4482.

BRANZ (2010). Study Report: Energy use in New Zealand Households: Final Report on the Household Energy End-use Project (HEEP). Retrieved March, 2015 from http://www.branz.co.nz/cms_show_download.php?id=a9f5f2812c5d7d3d53fdaba15f2c14d591749353

Bruckner et al. (2005). Bruckner, T., Morrison, R., Wittmann, T. Public policy modelling of distributed energy technologies: strategies, attributes and challenges. *Ecological Economics*, 54, 328-345.

Byrd et al. (2013). Byrd, H., Ho, A., Sharp, B., Kumar-Nair, N. Measuring the solar potential of a city and its implications for energy policy. *Energy Policy*, 61 (2013), 944-952.

Byrd, H. (2013). The solar potential of Auckland. Transforming Cities: Innovations for Sustainable Futures is a Thematic Research Initiative (TRI). School of Architecture and Planning, University of Auckland, New Zealand.

Carl, C. (2014). Calculating solar photovoltaic potential on residential rooftops in Kailua Kona, Hawaii. Master of Science, Geographic Information Science and Technology, Thesis. University of Southern California, Los Angeles, CA, United States.

Chaurey et al. (2004). Chaurey, A., Ranganathan, M, Mohanty, P. Electricity access for geographically disadvantaged rural communities – technology and policy insights. *Energy policy*, 32, 1693-1705.

Corson, J. (2010). Urban Design Strategy: South Invercargill. Invercargill City Council. Retrieved August 1, 2014 from file:///C:/Documents%20and%20Settings/Sam/My%20Documents/Downloads/South%20Invercargill%20Urban%20Design%20Strategy%20(1).pdf

Coughlin, J. & Kandt, A. (2011). Solar school assessment and implementation project: Financing options for solar installations on K-12 schools. Technical Report, NREL/TP- 7A40-51815. National Renewable Energy Laboratory, U.S. Department of Energy, Colorado.

Davis, G. (2015, September 21). Invercargill health suffers from state housing neglect. *The Southland Times*. Retrieved September, 2015 from http://www.stuff.co.nz/southland-times/opinion/72201642/invercargill-health-suffers-from-state-housing-neglect--letter

EECA [Energy Efficiency and Conservation Authority] (2001). Solar energy use and potential in New Zealand. Report by the Energy Efficiency and Conservation Authority, Wellington.

EECA (2010). Domestic-scale distributed generation: Guidance for local government. Retrieved March, 2015 from http://www.eeca.govt.nz/sites/all/files/dg-guidance-for-local-govt-may-2010.pdf

EECA (2014a). Solar water heating. Retrieved July 29, 2014 from http://www.energywise.govt.nz/products-and-appliances/water-heating/solar

EECA (2014b). Solar electricity generation (photovoltaic). Retrieved July 29, 2014 from http://www.energywise.govt.nz/how-to-be-energy-efficient/generating-renewable-energy-at-home/solar-electricity-generation

EECA (2014c). Solar. Retrieved July 29, 2014 from http://www.eeca.govt.nz/efficient-and-renewable-energy/renewable-energy/solar-energy-in-nz

Eltayeb, S. (2013). Renewable energy in New Zealand – by the numbers. Master of Science in Mathematics, Thesis. Massey University, Manawatu, New Zealand.

Environment Southland (n.d.). Southland Regional Policy Statement, Urban Issues and Options Paper. Retrieved August 6, 2014 from http://www.es.govt.nz/media/12529/urban-issues-and-options-paper.pdf

Environment Southland (June 2014). Invercargill air quality breaches national standards. Retrieved August 6, 2014 from http://www.es.govt.nz/your-council/news/2014/invercargill%E2%80%99s-air-quality-breaches-national-standards/

EPIA (European Photovoltaic Industry Association) (2014). Global market outlook for photovoltaic 2014-2018. Retrieved March, 2015 from http://www.epia.org/fileadmin/user_upload/Publications/EPIA_Global_Market_Outlook_for_Photovoltaics_2014-2018_-_Medium_Res.pdf

Ettah et al. (2009). Ettah, E.B., Eno, E.E., Udoimuk, A.B. The effects of solar panel temperature on the power output efficiency Calabar, Nigeria. *Journal of Association of Radiographers of Nigeria*, 23(2009), 16-22.

Fitgerald et al. (2011). Fitgerald, W., Fahmy, M., Smith, I., Carruthers, M., Carson, B., Sun, Z., Bassett, M. An assessment of roof space solar gains in a temperate maritime climate. *Energy and Buildings*, 43, 1580-1588.

Ford et al (2014). Ford, R., Stephenson, J., Scott, M., Williams, J., Wooliscroft, B., King, G., & Miller, A. PV in New Zealand: The story so far. Centre for Sustainability, University of Otago. Retrieved September 1, 2015 from http://www.whatpowercrisis.co.nz/site/whatpowercrisis/files/pdfs/PV%20Uptake%20in%20NZ%20The%20story%20so%20far%20140917.pdf

Fu, P. & Rich, P. M. (1999). Design and Implementation of the Solar Analyst: An ArcView extension for modelling solar radiation at landscape scales. Retrieved September 1, 2014 from http://proceedings.esri.com/library/userconf/proc99/proceed/papers/pap867/p867.htm#method

Genesis Energy (n.d.). Solar Energy FAQs. Retrieved on August 10, 2014 from http://www.schoolgen.co.nz/students/solar-energy-faqs

Ghosh, S. & Vale, R. (2006). The potential for solar energy use in New Zealand residential neighbourhood: A case study considering the effect on CO2 emissions and the possible benefits of changing roof form. *Australasian Journal of Environmental Management*, 13(4), 216-225.

Ghosh, S. & Vale, R. (2009). Linking residential densities, dwelling typologies and possible provisions for localized energy infrastructure in retrofitting urban forms. Retrieved July 27, 2014 from http://soac.fbe.unsw.edu.au/2009/PDF/Ghosh%20Sumita_Vale%20Robert.pdf

Gifford, A. (2014, 2 July). Can solar fit into the energy mix? *The New Zealand Herald.* Retrieved March, 2015 from http://www.nzherald.co.nz/element-magazine/news/article.cfm?c_id=1503340&objectid=11285518

Gipe, P. (2013, 3 April). 100% renewables and higher: The new trend in energy targets. *Renew Economy*. Retrieved on March, 2015 from http://reneweconomy.com.au/2013/100-renewables-and-higher-the-new-trend-in-energy-targets-55116

Gulliver, A. (2014, 2 November). Green calls for power buyback umpire. *Stuff.co.nz.* Retrieved March, 2015 from http://www.stuff.co.nz/national/politics/10692224/Greens-call-for-power-buyback-umpire

Hofierka, J. & Kanuk, J. (2009). Assessment of photovoltaic potential in urban areas using open source radiation tools. *Renewable Energy*, 34, 2206-2214.

IEA (International Energy Agency) (2013a). Tracking clean energy progress 2013. Retrieved March, 2015 from http://www.iea.org/publications/tcep_web.pdf

IEA (2013b). Renewable energy: Medium-term market report 2013. Retrieved March, 2015 from http://www.iea.org/textbase/npsum/mtrenew2013sum.pdf

IEA (2014). Tracking clean energy progress 2014. Retrieved March, 2015 from http://www.iea.org/publications/freepublications/publication/Tracking_clean_energy_progress_2014.pdf

Invercargill City Council. (2014). Invercargill City Council Xplorer. Retrieved September 1, 2014 from http://apps.geocirrus.co.nz/Viewer.html?Viewer=ICC-Public

IRENA (International Renewable Energy Agency) (2013). Renewable energy generation costs in 2012: An overview. Retrieved March, 2015 from http://www.irena.org/DocumentDownloads/Publications/Overview_Renewable%20Power%20Generation%20Costs%20in%202012.pdf

Isaacs et al. (2010). Isaacs, N., Saville-Smith, K., Camilleri, M., Burrough, L. Energy in New Zealand houses: comfort, physics and consumption. *Building Research and Information*, 38:5, 470-480.

Izquierdo et al. (2008). Izquierdo, S., Rodrigues, M., Fueyo, N. A method for estimating the geographical distribution of the available roof surface area for large-scale photovoltaic energy-potential evaluations. *Solar Energy*, 82, 929-939.

Jagemann et al (2013). Jagemann, C., Hagspiel, S., Lindenberger, D. The economic inefficiency of grid parity: The case of German photovoltaics. EWI Working Paper No.13/19. Institue of Energy Economics at the University of Cologne (EWI). ISSN: 1862-3808. Retrieved Aril 2015, from http://www.ewi.uni-koeln.de/fileadmin/user_upload/Publikationen/Working_Paper/EWI_WP_13-19_The_economic_inefficiency_of_grid_parity.pdf

Jakubiec, J. A. & Reinhart, C.F. (2013). A method for predicting city-wide electricity gains from photovoltaic panels based on LiDAR and GIS data combined with hourly Daysim simulations. *Submission to Solar Energy*. Building Technology Program, Massachusetts Institute of Technology, Cambridge, MA.

Jonsson et al. (2012). Review of solar modelling in the urban environment. Retrieved September 1, 2014 from http://www.wspgroup.com/upload/upload/sebe_state_of_the%20art_120323.pdf

Kalogirou, S. (2009). Solar Energy Engineering: processes and systems: chapter 9. *Academic Press*; 2009, p. 469-517. Retrieved May, 2015 from http://books.google.co.nz/books?id=B_E33NK7-YkC&pg=PA469&source=gbs_toc_r&cad=4#v=onepage&q&f=false

Kanters et al. (2014). Kanters, J., Wall, M., Kjellsson, E. The solar map as a knowledge base for solar energy use. *Energy Procedia*, 48, 1597-1606.

Karteris et al. (2013). Karteris, Slini, Th., Papadopoulos, M.A. Urban solar energy potential in Greece: A statistical calculation model of suitable built roof areas for photovoltaic. *Energy and Buildings*, 62, 459-468.

Kassner et al. (2008). Kassner, R. Koppe, W., Schuttenberg, T., Bareth, G. Analysis of the solar potential of roofs by using official LIDAR data. *The International Archives of the Photogrammetry, Remote Sensing and Spatial Information Science*, Vol. XXXVII. Part B4, 399-403.

Kensek, K. & Suk, J.Y. (2011). Daylighting factor (overcast sky) versus daylight availability (clear sky) in computer-based daylighting simulations. *Journal of Creative Sustainable Architecture & Built Environment*, CSABE, Vol. 1.

Kim et al. (2009). Kim , J.Y., Jeon, G.Y., Hong, W.H. The performance and economic analysis of grid-connected photovoltaic systems in Daegu, Korea. *Applied Energy*, 86, 265-272.

King, K. (2014, 17 February). Solar energy the future for NZ schools?. *3News.* Retrieved March, 2015 from http://www.3news.co.nz/tvshows/campbelllive/solar-energy-the-future-for-nz-schools-2014021716#axzz3ZYtysT36

Kovach, A. & Schmid, J. (1996). Determination of energy output losses due to shading of building-integrated photovoltaic arrays using a raytracing technique. *Solar Energy*, 57(2), 117-124.

Levinson et al. (2009). Levinson, R., Akbari, H., Pomerantz, M., Gupta, S. Solar access of residential rooftops in four California Cities. *Solar Energy*, 83, 2120-2135.

Lindberg, F. (2007). Modelling the urban climate using a local governmental geo-database. *Meteorological Applications*, 14, 263-273.

Ma et al. (2014). Ma, T., Yang, H., Lu, L. Solar photovoltaic system modelling and performance prediction. *Renewable and Sustainable Energy Reviews*, 36 (2014), 304-315.

Mackay, D. JC. (2009). Sustainable Energy – Without the Hot Air. *UIT Cambridge Ltd., England*. Retrieved May 2015 from http://www.withouthotair.com/c6/page_38.shtml

Mardaljevic, J. & Ryaltt, M. (2003). Irradiation mapping of complex urban environments: An image-based approach. *Energy and Buildings*, 35, 27-35.

Math is Fun (2014). Percentage Error: The difference between approximate and exact values as a percentage of the exact value. Retrieved May, 2015 from http://www.mathsisfun.com/numbers/percentage-error.html

MBIE (Ministry of Business, Innovation and Employment) (2013). 2012 Calendar Year Edition: Energy Greenhouse Gas Emissions. New Zealand Energy Greenhouse Gas Emissions Report 2013. Retrieved March, 2015 from http://www.med.govt.nz/sectors-industries/energy/energy-modelling/publications/energy-greenhouse-gas-emissions/energy-greenhouse-gas-emissions-2014.pdf

MBIE (2014a). 2013 Calendar Year Edition: Energy Greenhouse Gas Emissions. New Zealand Energy Greenhouse Gas Emissions Report 2013. Retrieved March, 2015 from http://www.med.govt.nz/sectors-industries/energy/energy-modelling/publications/energy-greenhouse-gas-emissions/energy-greenhouse-gas-emissions-2014.pdf

MBIE (2014b). Energy in New Zealand 2014. Retrieved March, 2015 from http://www.med.govt.nz/sectors-industries/energy/energy-modelling/publications/energy-in-new-zealand/Energy-in-New-Zealand-2014.pdf

MED (Ministry of Economic Development) (2011). New Zealand Energy Strategy 2011-2021 and New Zealand Energy Efficiency and Conservation Strategy 2011-2016. Retrieved July 29, 2014 from http://www.med.govt.nz/sectors-industries/energy/pdf-docs-library/energy-strategies/nz-energy-strategy-lr.pdf

Meral, M. E. & Dincer, F. (2011). A review of the factors affecting operation and efficiency of photovoltaic based electricity generation systems. *Renewable and Sustainable Energy Reviews*, 15 (2011), 2176-2184.

Merz, S. K. (2009). Micro-generation performance data project. Final Report. Retrieved May, 2015 from http://knowledge.neri.org.nz/assets/uploads/files/3dd70-SKM---Microgeneration-performance-data-project-Jun-2009.pdf

MfE (Ministry for the Environment) (2009). New Zealand's 2020 Emissions Target. Retrieved July 25, 2014 from http://www.mfe.govt.nz/publications/climate/nz-2020-emissions-target/nz-2020-emissions-target.pdf

MfE (2011). Emissions Trading Scheme Review 2011: Issues statement and call for written submission. Emissions Trading Scheme Review Panel. Wellington: Ministry for the Environment.

MfE (2013). Emission factors and methods 2007. Retrieved May, 2015 from http://www.mfe.govt.nz/publications/climate-change/guidance-voluntary-corporate-greenhouse-gas-reporting-data-and-methods-7

MfE (2014). International Climate Change Policy. Retrieved July 25, 2014 from http://www.mfe.govt.nz/issues/climate/international/policy.html#unfccc

Miklanek, P. & Meszaros (1993). The estimation of energy income in grid points over the basin using simple digital elevation model. *Ann. Geophysicae Suppl.* II, 11: 296.

Miller et al. (2014). Miller, A., Williams, J., Wood, A., Santos-Martin, D., Lemon, S., Watson, N., Pandey, S. Photovoltaic solar power uptake in New Zealand. EEA Conference & Exhibition 2014, 18-20 June, Auckland. Retrieved March, 2015 from http://www.epecentre.ac.nz/docs/media/EEA_2014_Paper_PV_Uptake_Miller_Williams_Wood_Santos_Watson_Lemon_Pandey-r11.pdf

Miller et al. (2015). Miller, A., Hwang, M., Grant Read, E., Wood, A. Economics of photovoltaic solar power and uptake in New Zealand. EEA Conference & Exhibition 2015, 24-26 June, Wellington. Retrieved August, 2015 from https://ir.canterbury.ac.nz/bitstream/handle/10092/11137/12654719_EEA_Paper_2015_PV%20Economics%20and%20Uptake-r12.pdf?sequence=1&isAllowed=y

Murray, P. E. (2005). Designing sustainable distributed generation systems for rural communities: An application of optimization modelling and decision analysis to include sustainability concepts and uncertainty into design optimality. Doctor of Philosophy in Agricultural Engineering (Renewable Energy) Thesis. Massey University, Palmerston North, New Zealand.

My Solar Quotes Limited (2015). The price of a solar power system. Retrieved March, 2015 from https://www.mysolarquotes.co.nz/about-solar-power/residential/how-much-does-a-solar-power-system-cost/

National Institute of Building Sciences (2015). Photovoltaics. U.S. Department of Energy Federal Energy Management Program (FEMP). Retrieved April, 2015 from http://www.wbdg.org/resources/photovoltaics.php?r=retro_sustperf#app

Natural frequency (1994 - 2015). Ecotect Tutorials/Solar Radiation. Wiki.naturalfrequency.com, Ecotect help. Archive site for Autodesk Ecotect educational resources, notes and tutorials. Retrieved September, 2014 from http://wiki.naturalfrequency.com/wiki/Ecotect_Tutorials, http://wiki.naturalfrequency.com/wiki/Solar_Radiation_Analysis

NIWA (2005). Energy resources – Solar energy. *Water & Atmosphere*, 13(4), 2005. Retrieved August 5, 2014 from http://www.niwa.co.nz/sites/niwa.co.nz/files/import/attachments/solar.pdf

NIWA (2013). Climate Data and Activities. Retrieved August 5, 2014 from http://www.niwa.co.nz/education-and-training/schools/resources/climate

NIWA (2014). SolarView. Retrieved August 5, 2014 from https://www.niwa.co.nz/our-services/online-services/solarview

NREL (2011). Solar Resource Information. U.S. Department of Energy, Office of Energy Efficiency and Renewable Energy. Retrieved April, 2015 from http://www.nrel.gov/rredc/solar_resource.html

NZ HEW (New Zealand Home Energy Web) (2008). Energy@Home. Retrieved July 30, 2014 from http://www.physics.otago.ac.nz/eman/hew/ehome/energyuse.html

Nguyen & Pearce (2012). Incorporating shading losses in solar photovoltaic potential assessment at the municipal scale. *Solar Energy*, 86 (5), 1245-1260.

Observ'ER (2013a). Electricity production in the world: general forecasts, *worldwide electricity production from renewable energy sources. Fifteen Inventory - Edition 2013*. Retrieved March, 2015 from http://www.energies-renouvelables.org/observ-er/html/inventaire/pdf/15e-inventaire-Chap01-Eng.pdf

Observ'ER (2013b). Conclusion, *Worldwide electricity production from renewable energy sources. Fifteen Inventory - Edition 2013*. Retrieved March, 2015 from http://www.energies-renouvelables.org/observ-er/html/inventaire/Eng/conclusion.asp

Ordonez et al. (2010). Ordonez, J., Jadraque, E., Alegre, J., Martinez, G. Analysis of the photovoltaic solar energy capacity of residential rooftops in Andalusia (Spain). *Renewable and Sustainable Energy Reviews*, 14, 2122-2130.

Perez et al. (1987). Perez, R. & Seals, R., Ineichen, P., Stewart, R., Menicucci, D. A new simplified version of the diffuse irradiance model for the tilted surface. *Solar Energy*, 39(3), 221-231.

Photovoltaic-software (2014). How to calculate the annual solar energy output of a photovoltaic system. Retrieved October 30, 2014 from http://photovoltaic-software.com/PV-solar-energy-calculation.php

Pillai, I. R. & Banerjee. (2007). Methodology for estimation of potential for solar water heating in a target area. *Solar Energy*, 81(2), 162-172.

Pollard, A. & Amitrano, L. (2009). Solar water heating in the Waitakere and Rotorua NOW Homes and in three Papakowhai Renovation homes. Report HR2420/8 for Beacon Pathway Limited

QV New Zealand (2011). Average house size by area. Retrieved October 30, 2014 from http://www.qv.co.nz/resources/news/article?blogId=61

Redweik et al. (2013). Redweik, P., Catita, C.M., Brito, M.C. Solar energy potential on roofs and facades in an urban landscape. *Solar Energy*, 97, 332-341.

Reinhart, C. (2012). Daylight simulations. MIT open course ware. Retrieved September 30, 2014 from http://ocw.mit.edu/courses/architecture/4-430-daylighting-spring-2012/lecture-notes/MIT4_430S12_lec09.pdf

Ren et al. (2009). Ren, H., Gao, W., Ruan, Y. Economic optimization and sensitivity analysis of photovoltaic system in residential buildings. *Renewable Energy*, 34, 883-889.

REN 21 (Renewable energy policy network for the 21st century) (2012). Renewable 2012 Global Status Report. Retrieved March, 2015 from http://www.ren21.net/Portals/0/documents/Resources/GSR2012_low%20res_FINAL.pdf

REN 21 (2013). Renewable 2013 Global Status Report. Retrieved May, 2015 from http://www.ren21.net/Portals/0/documents/Resources/GSR/2013/GSR2013_lowres.pdf

REN 21 (2014). Renewable 2014 Global Status Report. Retrieved June, 2015 from http://www.ren21.net/Portals/0/documents/Resources/GSR/2014/GSR2014_full%20report_low%20res.pdf

Renewable Energy World (4 May 2015). Photovoltaic (solar cell) Systems. Retrieved May 4, 2015 from http://www.renewableenergyworld.com/rea/tech/solar-energy/solarpv

Robinson, D. & Stone, A. (2004). Solar radiation modelling in the urban context. *Solar Energy*, 77(3), 295-309.

Robinson, D. (2006). Urban morphology and indicators of radiation availability. *Solar Energy*, 80(12), 1643-1648.

Ruiz-Arias et al. (2009). Ruiz-Arias, J.A., Tovar-Pescador, J., Pozo-Vazquez-D., Alsamamra, H. A comparative analysis of DEM-based models to estimate the solar radiation in mountainous terrain. *International Journal of Geographical Information Science*, 23:8, 1049-1076.

Ryan et al. (2008). Ryan, V. Burgess, G., Easton, L. New Zealand House Typologies to inform energy retrofits. Report EN6570/9 for Beacon Pathway Limited.

Schoolgen and NZ Power Company Genesis Energy (2006-2015). Genesis Energy/ Schoolgen Programme. Retrieved March, 2015 from http://www.schoolgen.co.nz/

Schoolgen and NZ Power Company Genesis Energy (2006-2015). Solar Energy FAQs. Retrieved on August 10, 2014 from http://www.schoolgen.co.nz/students/solar-energy-faqs

SEIA (Solar Energy Industries Association) (2015). A Study on Solar in U.S. Schools Report. Retrieved June, 2015 from http://www.seia.org/research-resources/brighter-future-study-solar-us-schools-report

SHC IEA (2011). International survey about digital tools used by architects for solar design. Task 41- Solar Energy and Architecture, Subtask B – Methods and Tools for Solar Design (T.41.B.1). Retrieved September 1, 2014 from http://archive.ieashc.org/publications/downloads/International_Survey_About_Digital_Tools_Used_by_Architects_for_Solar_Design.pdf

Sills, B. (2011, 29 August). Solar may produce most of world's power by 2060, IEA says. *Bloomberg*. Retrieved on March, 2015 from http://www.bloomberg.com/news/articles/2011-08-29/solar-may-produce-most-of-world-s-power-by-2060-iea-says

Solar Energy Technologies Programme (2005). Balance of system. Retrieved April, 2015 from http://web.archive.org/web/20080504001534/http://www1.eere.energy.gov/solar/bos.html

Solar Association of New Zealand (2014). Energy Performance. Retrieved July 30, 2014 from http://www.solarassociation.org.nz/content/energy-performance

Souza, L. & Rodrigues, D. (n.d.). A 3D-GIS extension for sky view factor assessment in urban environment. Retrieved August 6, 2014 from http://repositorium.sdum.uminho.pt/bitstream/1822/2299/1/9a2.pdf

Statistics New Zealand (2013a). 2013 QuickStats about a place: Invercargill City. Retrieved August 6, 2014 from http://www.stats.govt.nz/Census/2013-census/profile-and-summary-reports/quickstats-about-a-place.aspx?request_value=15162&tabname=#15162

Statistics New Zealand (2013b). 2013 Census Map – Population and dwelling map. Retrieved August 6, 2014 from http://www.stats.govt.nz/StatsMaps/Home/Maps/2013-census-population-dwelling-map.aspx

Statistics New Zealand (2014). Projections Overview – National family and household projection. Retrieved November 1, 2014 from http://www.stats.govt.nz/browse_for_stats/population/estimates_and_projections/projections-overview/nat-family-hhold-proj.aspx

Suri, M. & Hofierka, J. (2004). A new GIS–based solar radiation model and its application to photovoltaic assessments. *Transactions in GIS*, 8, 175-190.

SUN-AREA. (2012). Automatic solar potential roof cadastre – location analysis for solar power systems in existing buildings. Retrieved August 6, 2014 from http://www.sun-area.net

Svensson, M. K. (2004). Sky view factor analysis – Implications for urban air temperature differences. *Meteorological Applications*, 11, 201-211.

The Press (2013, October 26). Are solar energy worth the cost? *The Press*. Retrieved September 6, 2014 from http://www.stuff.co.nz/the-press/business/the-rebuild/9329703/Are-solar-energy-systems-worth-the-cost

Thompson, J. (2011). Accuracy of daylight assessment. *Build*, 124, 73-74. BRANZ paper. Retrieved September 6, 2014 from http://www.branz.co.nz/cms_show_download.php?id=b8e3f5d337b561eda0c14bcb6ad4e9ab3068c5f9

Tovar-Pescador et al. (2016). Tovar-Pescador, J., Pozo-Vazquez, D., Ruiz-Arias, J.A., Luis Bosch, J. On the use of the digital elevation model to estimate the solar radiation in areas of complex topography. *Meteorol. Appl.*, 13, 279-287.

Urge-Vorsatz et al. (2007). Urge-Vorsatz, D., Danny Harvey, L.D., Mirasgedis, S., Levine, M.D. Mitigating CO2 emissions from energy use in the world's building. *Building Research and Information*, 35(4), 379-398.

U.S. Department of Energy (2013). Photovoltaic cell conversion efficiency basics. Retrieved April, 2015 from http://energy.gov/eere/energybasics/articles/photovoltaic-cell-conversion-efficiency-basics

U.S. Energy Information Administration (2013). Most states have Renewable Portfolio Standards. Retrieved April, 2015 from http://www.eia.gov/todayinenergy/detail.cfm?id=4850

Wang, Y. (2015). Creating a healthier environment in New Zealand primary schools using a solar roof collector in winter. Confirmation Report. School of Engineering and Advanced Technology, Massey University, New Zealand.

Watt, M. (2009). Assessment of the future costs and performance of solar photovoltaic technologies in New Zealand. IT Power (Australia) Pty Ltd. Australia.

Wiginton et al. (2010). Wiginton, L.K., Nguyen, H.T., Pearce, J.M. Quantifying rooftop solar photovoltaic potential for regional renewable energy policy. *Computers, Environment and Urban Systems*, 34, 345-357.

Wikipedia (2015a). Solar cell. Retrieved April, 2015 from http://en.wikipedia.org/wiki/Solar_cell

Wilson, J. P. & Gallant J. C. (2000). *Terrain Analysis: Principles and Applications*. New York: John Wiley & Sons.

Wood et al. (2013). Wood, A., Miller, A., Claridge, N. Moving to the sunny side of the street: Growing residential solar electricity in New Zealand. EEA Conference &Exhibition 2013, 19-21 June, Auckland. Retrieved March, 2015 from http://www.epecentre.ac.nz/docs/media/Wood_EEA_2013_PV.pdf

World Energy Council (2014, December). The $48 trillion question. *World Energy Focus*, 6, 1-2. Retrieved March, 2015 from http://worldenergyfocus.org/wp-content/uploads/2014/12/worldenergyfocus_06_201412.pdf

World Weather and Climate Information (2013). Average weather in Invercargill, New Zealand. Retrieved August 1, 2014 from http://www.weather-and-climate.com/average-monthly-Rainfall-Temperature-Sunshine,Invercargill,New-Zealand

Yamaguchi et al. (2003). Yamaguchi T, Kawakami M, Kitano K, Nakagawa S, Tokoro T, Nakano T. Data analysis on performance of PV system installed in south and north direction. *3rd World Conference on Photovoltaic Energy Conversion*, May 11-18, 2003, Osaka, Japan, 2239-2242.